TÉCNICO LISBOA

Modelling and Optimization of Energy Operational Strategies For a Hybrid Renewable Energy System at the Port of Avilés

Toni Xavier Adrover Vidal

Thesis to obtain the Master of Science Degree in

Energy Engineering and Management

Supervisor: Prof. Helena M. Ramos

Examination Committee

Chairperson: Prof. Jorge de Saldanha Gonçalves Matos

Supervisor: Prof. Helena M. Ramos

Members of Committee: Prof. Rodolfo Espina Valdes

October 2025

Declaration

I declare that this document is an original work of my own authorship and that it fulfils all the requirements of the Code of Conduct and Good Practices of the *Universidade de Lisboa*.

Acknowledgements

First and foremost, I would like to sincerely thank my family for their unwavering encouragement and support throughout every decision I have made in my life. Their constant belief in me has motivated me to continue growing, not only as a professional in the field I am most passionate about, energy, but also as a person in all areas of life.

I am also deeply grateful to my friends, both those I have met during the past two years in Sweden and Portugal, and my lifelong friends who are always there whenever I return home. Their readiness to support me in times of need and to share joyful and relaxing moments has been invaluable, reminding me of the importance of balance beyond the professional realm.

Last but certainly not least, I wish to express my heartfelt gratitude to Professor Helena Ramos for introducing me to such a fascinating project, for trusting me with the study of initiatives like HY4RES, and for her continuous guidance throughout this journey, which began in October of last year. I am truly honoured to have had the opportunity to contribute to her research and to be included in her publication *"Optimization and Machine Learning in Modelling Prospective of Hybrid Energy Balance to Improve Ports' Efficiency"* receiving an EU grant for the job done. Working with someone of her knowledge, dedication, and passion has been an inspiring experience that has significantly helped me grow as an engineer, hoping to continue working together for the preparation of another paper with the findings of this thesis.

Abstract

This thesis investigates the implementation of a hybrid renewable energy module at the Port of Avilés, designed to supply the energy needs of selected port infrastructures through the integration of solar, wind, and hydrokinetic sources. The original system design includes a pump-as-turbine storage solution, while additional simulations were conducted using battery storage to broaden the analysis. To evaluate performance under varying conditions, an Excel-based energy management and optimization tool was developed, allowing for the assessment of four operational scenarios and six configuration setups. Two case studies were conducted: the first examined a single hybrid module managing the total demand, comparing pump-as-turbine and battery storage to identify the most effective option; the second explored the deployment of multiple hybrid modules operating in parallel, each assigned an individual demand profile, with a comparison between centralized and distributed storage strategies. Results show that, due to the relatively low energy demands and limited generation capacity of the system, the single hybrid module with batteries as a storage solution was the most viable configuration, achieving an energy coverage of 89.90%. Moreover, the financial analysis demonstrated a positive outcome, with an internal rate of return of 10.88%, confirming the module's feasibility both technically and economically. These findings highlight the potential for small-scale hybrid renewable systems supported by battery storage to contribute meaningfully to decarbonizing port operations and advancing sustainable infrastructure development.

Keywords

Hybrid Renewable Energy Systems; Energy Management; Optimization Strategies; Energy Storage; Economic Assessment; Ports Efficiency.

Resumo

Esta tese investiga a implementação de um módulo híbrido de energias renováveis no Porto de Avilés, projetado para suprir as necessidades energéticas de infraestruturas portuárias seleccionadas, por meio da integração de fontes solar, eólica e hidrocinética. O projeto original do sistema inclui uma solução de armazenamento com bomba funcionando como turbina, enquanto simulações adicionais foram realizadas utilizando armazenamento em baterias para ampliar a análise. Para avaliar o desempenho sob diferentes condições, foi desenvolvido um modelo de gestão e otimização energética em Excel, permitindo a análise de quatro cenários operacionais e seis configurações distintas. Dois estudos de caso foram conduzidos: o primeiro analisou um único módulo híbrido gerindo o consumo total, comparando as soluções de armazenamento com bomba-turbina e com baterias para identificar a opção mais eficaz; o segundo explorou a implantação de múltiplos módulos híbridos operando em paralelo, cada um com um perfil de consumo individual, comparando estratégias de armazenamento centralizado e distribuído. Os resultados mostram que, devido aos consumos energéticos relativamente baixos e à capacidade de geração limitada do sistema, o módulo híbrido único com baterias como solução de armazenamento foi a configuração mais viável, atingindo uma cobertura energética de 89,90%. Além disso, a análise financeira demonstrou um resultado positivo, com uma taxa interna de rentabilidade de 10,88%, confirmando a viabilidade técnica e económica do módulo. Esses resultados destacam o potencial dos sistemas híbridos de pequena escala, apoiados por armazenamento em baterias, para contribuir significativamente para a descarbonização das operações portuárias e o avanço do desenvolvimento de infraestruturas sustentáveis.

Palavras-chave

Sistemas Híbridos de Energias Renováveis; Gestão de Energia; Estratégias de Otimização; Armazenamento de Energia; Avaliação Econômica; Eficiência dos Portos.

Table of Contents

List of Figures

List of Tables

List of Abbreviations

AI	Artificial Intelligence
CP	Power Coefficient
DoD	Depth of Discharge
EU	European Union
HAWT	Horizontal-Axis Wind Turbines
HOPS	Hybrid Operational System
HRS	Hybrid Renewable Systems
IRENA	International Renewable Energy Agency
IRR	Internal Rate of Return
LCOE	Levelized Cost of Energy
NPV	Net Present Value
OPS	On-shore Power Supply
PAT	Pump-as-Turbine
SoC	State of Charge
SR	Stacking Regressors
VAWT	Vertical-Axis Wind Turbine

List of Symbols

$B_{charge,0}$	Energy used to charge the battery in the initial time step (kWh)
$B_{charge,t}$	Energy used to charge the battery at a specific time step (kWh)
$B_{disch,0}$	Energy discharged from the battery in the initial time step (kWh)
$B_{disch,t}$	Energy discharged from the battery at a specific time step (kWh)
B_{max}	Battery maximum capacity (kW)
$DoD_{97\%}$	Maximum depth of discharge at 97% of the maximum capacity
$E_{HYDRO,t}$	Energy generated by the Hydro system at a specific time step (kWh)
$E_{LOAD,t}$	Energy demand at a specific time step (kWh)
$E_{NET,0}$	Net energy balance in the initial time step (kWh)
$E_{NET,t}$	Net energy balance at a specific time step (kWh)
$E_{Net(M1),t}$	Net energy balance for module 1 at a specific time step (kWh)
$E_{Net(M2),t}$	Net energy balance for module 2 at a specific time step (kWh)
$E_{Net(M3),t}$	Net energy balance for module 3 at a specific time step (kWh)
$E_{PV,t}$	Energy generated by the PV system at a specific time step (kWh)
$E_{surplus,t}$	Toal combined energy surplus in the parallel management (kWh)
$E_{WIND,t}$	Energy generated by the Wind system at a specific time step (kWh)
H	Net head (m)
P	Power output of the wind turbine under operational conditions (W)
P_{max}	Maximum power of the battery that can be discharged in one hour (kW)
P_{turb}	Power output of the wind turbine (W)
$SoC_{50\%}$	State of charge of the battery at 50% of the total capacity (kW)
$SoC_{,0}$	State of charge of the battery in the initial time step (kW)
$SoC_{,t}$	State of charge of the battery at a specific time step (kW)
$SoC_{,t-1}$	State of charge of the battery in the previous time step (kW)
V	Water volume assigned to the PAT system (m^3)
$V_{5\%}$	Volume of water equivalent to 5% of the total storage capacity (m^3)
$V_{50\%}$	Volume of water equivalent to 50% of the total storage capacity (m^3)
$V_{disch,0}$	Volume of water to be discharged in the initial time step (m^3)
$V_{disch,t}$	Volume of water to be discharged at a specific time step (m^3)
$V_{fill,0}$	Volume of water assigned to fill the tank in the initial time step (m^3)
$V_{fill,t}$	Volume of water assigned to fill the tank at a specific time step (m^3)
V_{max}	Maximum storage volume of the tank (m^3)

$V_{need,0}$	Volume needs to satisfy the energy deficit in the initial time step (m^3)
$V_{need,t}$	Volume needs to satisfy the energy deficit at a specific time step (m^3)
$V_{rem,0}$	Remaining volume in the tank in the initial time step (m^3)
$V_{rem,t}$	Remaining volume in the tank at a specific time step (m^3)
$V_{rem,t-1}$	Remaining volume in the tank in the previous time step (m^3)
v	Wind velocity (m/s)
g	Gravitational acceleration (m/s^2)
η_{PAT}	PAT system efficiency
ρ	Water density (kg/m^3)

List of Software

EXCEL-Solver	Optimization tool for spreadsheets
MATLAB	MATrix LABoratory
Portus	Spanish seawater resource database
PVGIS	Photovoltaic Geographical Information System
PVsyst	PV design software

Chapter 1

Introduction

This chapter establishes the foundational context of the thesis by presenting the origin of the project and the underlying motivations that have guided its development. It defines the core objectives, technical, economic, and energy-related, that shape the scope and direction of the study. Additionally, it outlines the overall structure of the thesis, providing a concise summary of each subsequent chapter in order to offer a clear understanding of the research framework and methodological approach adopted throughout the work.

1.1 Overview and motivation

In recent years, significant groundwork has been laid globally, and particularly within Europe, to support the energy transition. This has been driven by the implementation of strategic initiatives aimed not only at achieving climate neutrality in line with the 2030 and 2050 targets, but also at enhancing energy autonomy across local, national, and regional scales.

The European Union (EU) is making significant investments to accelerate the transition toward cleaner, more sustainable energy systems. Central to this effort is the widespread adoption of renewable energy sources, supported by advanced storage solutions that ensure a stable, reliable supply of electricity for all users. Achieving this vision requires the deployment of hybrid systems that seamlessly integrate energy generation and storage. These systems are not only crucial for large-scale infrastructure but also play a key role in enabling decentralized energy models and promoting self-consumption.

In line with this objective, initiatives, such as HY4RES, co-financed by the EU Interreg Atlantic Area programme, have been launched to demonstrate the potential of hybrid systems at a micro scale. HY4RES is focused on fostering the adoption of these systems across diverse sectors, including agriculture, aquaculture, port operations, and community settings, supporting a more flexible, resilient, and low-carbon energy future.

The initiative currently comprises four pilot projects across three countries, Spain, Portugal, and Ireland, with a total investment of 3.2 million euros allocated for the design and implementation of hybrid energy systems between 2023 and 2026 **[1]**. One of these pilot projects is located in the Port of Avilés, Spain, where a combination of renewable energy sources, including photovoltaic solar, wind, and hydrokinetic power, is being integrated with a Pump-as-Turbine (PAT) system. This storage system will absorb excess energy when generation exceeds demand and release it when production falls short, ensuring a stable and efficient energy supply for selected infrastructures within the port.

These initiatives demand a multidisciplinary approach that goes beyond technical considerations to include economic and strategic dimensions. The goal is not only to deliver energy benefits to the sites where hybrid modules are deployed, but also to ensure their financial viability and a reasonable return on investment in the medium term. This is the driving motivation behind the project described in this document, which centres on the development of an Excel-based model, incorporating Solver, for testing and optimizing hybrid energy modules, specifically applied to the Port of Avilés. The model enables the simulation of multiple configurations and scenarios, facilitating a comprehensive evaluation of system performance across diverse contexts. Ultimately, it supports informed decision-making on the feasibility of deploying the technology at a given site and helps identify the most effective energy management strategy to maximise both energy output and economic returns.

The current project is conceived as a continuation of an initial study that outlined the technologies incorporated into the hybrid module and provided preliminary estimates of their energy generation. These estimates have been later refined to improve their accuracy and, along with other relevant parameters, now serve as key inputs to the energy and economic management model developed.

1.2 Objectives and structure

This research is founded on a set of clearly defined objectives encompassing two core dimensions: energy and economics. The specific objectives within each dimension are outlined below, providing a strategic framework for analysing the outcomes and assessing the effectiveness and impact of the developed energy model, including the various scenarios and configurations evaluated.

From an energy objectives perspective, the initial goal is to verify that the generation estimates outlined in the existing preliminary document align with the results obtained through more advanced calculation methodologies, beyond the use of simplified ratios. This verification aims to ensure that the renewable units are operating at their maximum feasible output and, consequently, that the model is based on accurate input data.

Following the validation of generation values, the next objective focuses on the development of an energy management model capable of testing multiple scenarios. This model will help identify the operational limits of the hybrid modules proposed for installation at the Port of Avilés. Through scenario simulation and subsequent analysis, the study aims to determine which configurations yield the best performance in terms of demand coverage, not only at the system level but also for individual components such as generation units and storage technologies. Additionally, the analysis will provide insight into the level of dependency on the electrical grid, highlighting specific periods throughout the year when external imports are most needed.

Regarding the economic objectives, the primary aim is to quantify how the system's energy performance can be translated into financial returns. To that end, several profit-generating strategies will be proposed and evaluated using key economic indicators such as Net Present Value (NPV), Internal Rate of Return (IRR), and Payback Period. Additionally, a complementary metric, euros generated per square meter, will be introduced to assess the spatial efficiency and overall effectiveness of each tested configuration in maximizing the use of available area.

Beyond merely measuring and reporting these outcomes, a core objective of the study is to develop an optimized model capable of identifying a balanced configuration that delivers both strong energy performance and favorable financial returns. This integrated approach represents the fundamental purpose of the project: to demonstrate the technical and economic viability of deploying hybrid modules as a sustainable energy solution in the selected location.

This thesis is structured into six chapters, with a brief overview provided, particularly focusing on the chapters that follow this introductory section.

Chapter 2, dedicated to the literature review, offers an overview of the current direction Europe is taking regarding the decarbonization and electrification of ports. In response to these evolving regulations, the chapter highlights the relevance of hybrid energy systems as a key enabler for compliance. Examples of existing hybrid systems implemented in ports around the world are presented, including their main applications and the types of energy storage technologies that currently offer the most promising performance in ensuring stability, especially in systems reliant on intermittent renewable sources.

Additionally, this chapter discusses energy management and optimization tools that enhance the performance and reliability of hybrid systems in port environments.

Chapter 3 marks the beginning of the core technical content of the thesis, focusing on the methodology. This section outlines the approaches used to calculate the individual energy generation from the solar panels, wind turbines, and hydrokinetic turbines that comprise the hybrid module. The calculated results are compared with the data provided in the preliminary design, allowing for the selection of the most efficient calculation method. This chapter, also details the process of selecting demand profiles that best align with the previously calculated generation levels. Finally, it concludes with a comprehensive description and explanation of the operational methodology behind the developed energy management model.

Chapter 4 introduces the first case study, which analyses the performance of the hybrid module when all selected demand profiles are assigned to a single unit. In this section, two scenarios are developed for the comparison of two different storage systems, pump-as-turbine and batteries. Each scenario presents a detailed comparison between the base configuration and its optimized version, highlighting the key differences in performance. In addition to the analysis of results, the chapter includes the specific governing equations for each system, as well as the corresponding optimization processes used to enhance their efficiency.

Chapter 5 presents the second case study, which explores the operation of multiple hybrid modules functioning in parallel. In this section, only the storage technology that delivered the best performance in the previous analysis is considered. The focus shifts to evaluating whether it is more advantageous to implement individual storage systems for each module or to use a centralized storage configuration. Both solutions are compared against the best-performing scenario from Chapter IV to determine the most suitable overall solution.

Finally, Chapter 6 presents the main conclusions drawn from the entire study, along with proposed future work. This includes further research directions and recommendations for enhancing the performance of the hybrid module, not only in port environments but also in other sectors where its application could prove beneficial.

Chapter 2

Literature Review

This chapter sets the stage by outlining the current regulatory trends driving the electrification of ports, with a particular emphasis on developments within Europe. It underscores the growing importance of hybrid energy systems as a mean to meet the increasing energy demands of port infrastructures while aligning with decarbonization goals. The chapter presents real-world case studies where hybrid systems have already been implemented in port settings, demonstrating their practical potential. Furthermore, it highlights the critical role of advanced forecasting, optimization, and energy management techniques in ensuring the efficient and resilient operation of these complex energy systems.

2.1 Future direction of ports energy requirements

Port facilities across the globe serve as critical infrastructures that underpin a wide array of essential activities. They function as strategic nodes for maritime transport, facilitating not only the movement of people but also the secure and efficient delivery of vital goods, including food supplies, with over 80% of the global trade carried by sea **[2]**. Moreover, ports play a pivotal role in the global logistics chain, enabling the distribution of machinery, raw materials, and other industrial commodities. In doing so, they significantly contribute to economic integration and connectivity between cities, regions, and nations worldwide.

To ensure that each of these activities can be carried out safely and efficiently, a reliable power supply is essential, making ports significant hubs of energy demand. Given the substantial consumption associated with such facilities, the implementation of corrective measures aimed at both reducing emissions and providing clean energy for port operations is of critical importance **[3]**. These efforts are particularly relevant in the context of advancing toward the sustainability goals set for 2030, especially within the European Union.

One of the regulations expected to have a significant impact, particularly in terms of emission reduction, is the FuelEU Maritime Regulation (EU 2023/1805). This directive stipulates that, starting in 2030, all container and passenger ships of 5,000 gross tonnage or more must connect to on-shore power supply (OPS) systems while docked. Initially, this requirement will apply to ports within the TEN-T network and will extend, by 2035, to all EU ports equipped with the necessary infrastructure **[4]**. The electrification of these maritime operations will inevitably lead to a substantial increase in electricity demand across port facilities. As a result, it becomes even more critical to ensure that the supporting energy infrastructure is sufficiently robust to prevent any risk of supply shortages. According to studies conducted by the European Union, from 2030 onward, average electricity demand across EU ports is projected to range between 6 and 13 TWh per year, highlighting the scale and impact of the measures being introduced **[5]**.

2.2 Hybrid renewable energy systems in port environments

The growing imperative to ensure a stable and sustainable energy supply from renewable sources, alongside the rising electricity demands driven by regulatory developments, strongly indicates that the future of energy in port operations will rely on hybrid systems **[6]**. A number of pilot projects have already been conducted, yielding reliable and promising outcomes that highlight the viability and resilience of well-optimized infrastructure solutions.

At the Port of Souda in Crete, a case study was proposed to assess the impact of integrating wind turbines, solar panels, and energy storage systems operating together as a hybrid solution. Across the various scenarios analysed, a reduction in the levelized cost of energy (LCOE) of over 50% was observed in the vast majority of cases, with the hybrid system contributing up to nearly 90% of the total energy supply in the most favourable configurations **[7]**.

The highly positive results demonstrated in the previous case study are replicable across numerous other applications where hybrid power generation systems can be employed within port facilities. Additional studies, such as one conducted across four ports in Egypt, have shown that hybrid systems, applied in this instance to water desalination processes, are significantly more cost-effective than relying on renewable sources individually. The relative cost of electricity production was reduced at all ports examined when hybrid systems were implemented, while simultaneously decreasing the number of converters and batteries required compared to scenarios where wind and solar sources operated independently **[8]**.

Further evidence reinforces the conclusion that using renewable energy sources in isolation is significantly less efficient, and therefore less effective in supporting the sustainability of port operations, compared to their integration in hybrid systems. At the Port of Ningbo-Zhoushan, the feasibility of implementing hybrid systems was explored not only to advance electrification but also to support hydrogen production. The study revealed that, over the five-year installation period, the poorest performance occurred in the second year, when only the solar panels were operational, highlighting the limitations of single-source renewable systems **[9]**.

Despite the numerous benefits that hybrid energy systems can offer, one of the main challenges lies in the difficulty of installing a sufficient number of generation units within the limited space available at many ports to achieve full energy self-sufficiency. For this reason, the potential integration of offshore hybrid systems has also been explored, involving the use of floating platforms and structures containing components such as solar panels and wind turbines **[10]**. This approach helps preserve onshore space and avoids disrupting port logistics. However, careful planning is required to ensure these installations are positioned outside the navigational routes of vessels approaching or docking at the port.

Efficient space utilization is a critical factor when deploying renewable energy solutions in port environments, where maintaining seamless operational activities is essential. In this context, integrating compact, high-energy-density storage systems is equally important. Among current technologies, lithium-ion batteries are the most commonly used, particularly for small-scale systems, due to their favourable energy density, typically ranging from 75 to 250 Wh/kg **[11]**. However, energy density should not be the sole determinant when selecting a storage technology. Cost-effectiveness also plays a vital role. Various studies indicate that thermal energy storage, when incorporated into hybrid configurations, can offer greater economic advantages compared to batteries, fuel cells, or pumped storage, especially when combined with solar and wind power sources **[12]**.

Although less commonly implemented, interest in the application of hydrogen storage systems, has increased in recent years. While concrete data on the number of ports located near salt formations is limited, with examples such as Walvis Bay in Namibia **[13]**, recent research identifies salt caverns as promising candidates for the development of underground hydrogen storage infrastructure **[14]**. This concept holds growing potential for hybrid energy systems in ports, primarily due to its minimal surface footprint and the exceptionally high energy density of hydrogen, which far exceeds that of lithium-ion batteries **[11]**.

2.3 Optimization approaches and management strategies for hybrid energy systems

Relying on hybrid systems that depend heavily on intermittent energy sources requires the implementation of advanced management and optimization strategies to ensure their operation is as efficient as possible **[15]**.

One of the key aspects to consider before applying energy management strategies is the availability of reliable climatic and generation data, which is typically achieved through predictive systems. In many cases, individual machine learning algorithms and models are used for such forecasting tasks. While these models can deliver acceptable results, recent studies have shown that the use of ensemble learning techniques, specifically stacking regressors (SR), significantly improves the accuracy of predictions, particularly for variables such as direct solar irradiance and wind speed **[16]**.

Following the prediction of fundamental data used to estimate renewable energy generation, artificial intelligence (AI) plays a key role in the optimization of hybrid renewable systems (HRS). Currently, approximately 36.01% of research efforts focus on the application of AI, particularly for real-time decision-making. Despite the growing interest in AI-based models, metaheuristic approaches continue to dominate the scientific field, accounting for 47.12% of related research **[17]**.

Focusing on the benefits that artificial intelligence can bring to hybrid renewable systems, its applications span a wide range of areas. These include component-by-component system sizing to help reduce the levelized cost of energy, consumption pattern prediction to ensure a more reliable energy supply, critical load detection, and load shifting analysis, among others **[18]**. Effective energy management through the use of artificial intelligence has also proven to have a positive impact on emissions, achieving reductions of up to 11.5% in case studies such as Jeju Island. In this instance, AI not only contributed to lowering emissions but also helped mitigate curtailment issues **[19]**.

In addition to the application of artificial intelligence, complementary methods such as digital twins are increasingly being used, particularly in built environments. Traditional monitoring systems often fail to provide fully reliable results and lack a comprehensive perspective on improving energy management. Depending on the environment and building usage patterns, digital twins can begin delivering meaningful data in a short period of time. In office buildings, for example, a reliability rate of 97% can be achieved in just three days **[20]**. These systems are highly effective in identifying consumption inefficiencies and can also be applied to port facilities.

All these methods enhance the performance of energy systems operating under traditional frameworks. However, in environments with a significant lack of data, it is crucial to develop an initial model that is as optimized as possible. From that point onward, advanced methodologies can be used to continuously refine and improve the model over time and the energy management strategies, when having enough data.

Chapter 3

Methodology

This section presents the methodology used to define the key inputs for the energy management tool developed to evaluate the hybrid module. It begins with a refined estimation of renewable energy generation, comparing these calculations against initial projections to validate accuracy. The process for selecting representative consumption profiles and appropriate electricity tariffs is then outlined, ensuring realistic simulation conditions. These inputs form the foundation for modeling various operational scenarios. Finally, the structure and core functionalities of the energy management tool are described, emphasizing how it processes data and conducts performance simulations.

3.1 Renewable energy generation modelling

In small-scale energy projects or systems designed for self-consumption, it is crucial to maximize the generation of the installed technologies. The more optimized the system, the higher the level of energy coverage and autonomy, which in turn enhances the return on investment and overall system efficiency.

As outlined in previous sections, this project commenced with a preliminary design aimed at defining the individual generation profiles of each renewable energy source using basic parameters. The results were based on general assumptions.

The use of advanced software and calculation methods has become standard in the industry, facilitating a more precise alignment between simulations and actual outcomes. Consequently, this section evaluates whether the generation calculations from the initial project concept align with the results obtained through alternative methods, including the application of advanced software.

3.1.1 Photovoltaic unit

3.1.1.1 Description of the preliminary PV design and results

Photovoltaic solar energy is currently one of the fastest growing and most promising energy sources worldwide. In recent years, this technology has not only seen significant technical advancements but has also experienced a substantial reduction in both installation costs and levelized cost of energy. These developments have driven the increase in projects across both residential and utility-scale sectors. According to data from the International Renewable Energy Agency (IRENA), installation costs decreased by between 46% and 85% from 2010 to 2020, depending on the market and country, with global costs reaching a minimum of 658 USD/kW and 100 USD/kW for battery technology **[21]**.

Over the past decade, Spain has emerged as a key player in the development and adoption of photovoltaic technology. From 2013 to 2020, residential installation costs for photovoltaic panels decreased by approximately 1,507 USD/kW, making the technology increasingly attractive not only to large corporations but also to individual consumers.

Building on the former context and with a focus on the current project, solar energy is anticipated to be a fundamental element within the system's generating units. Before proceeding with new simulations and adjustments for this renewable source, it is crucial to first examine the pre-established conditions and results from the preliminary design. This will define a baseline for comparing the outcomes generated by the simulations.

In line with the technical design specifications, the photovoltaic unit is equipped with two Deepblue 3.0 JA Monocrystalline panels, each with a power rating of 405 W, resulting in a total installed capacity of 810 W. With an estimated operational period of 292 days, or approximately 80% of the year, and an average solar irradiation of 3 kWh/m²/day, the panels are projected to generate around 567.65 kWh annually. While this represents a relatively small generation capacity due to the limited number of

modules, it is expected that they will provide around 43% of the total energy production **[22]**.

Although the results obtained fall within a reasonable range, they overlook important factors such as panel tilt angle, system losses, and the degradation of photovoltaic modules over time. To achieve a more precise and realistic evaluation, it is essential to conduct advanced simulations that account for these variables. For this purpose, PVsyst has been chosen as the tool to design the photovoltaic system and verify whether the generation estimates align with the actual performance of the installation.

3.1.1.2 Redefinition of the photovoltaic unit

When designing and developing a photovoltaic installation, several key parameters must be considered from the outset. One of the most important is the irradiation that the panels will receive throughout the year, as it directly impacts the total energy generation over time.

To optimize solar irradiation capture, factors such as panel orientation and tilt angle must be carefully planned. The ideal orientation for maximum solar exposure depends on the installation's location. In the northern hemisphere, panels should face as far south as possible, while in the southern hemisphere, they should be oriented towards the north to ensure maximum solar incidence.

In the design in question, this is not a constraint, as the panels are mounted on an independent metal structure, providing full flexibility in their orientation. Given that Avilés is located in the northern hemisphere, the panels will be aligned towards the south to optimize solar exposure and maximize energy generation efficiency.

Regarding the tilt angle, it is commonly recommended to set the panels at an angle close to the latitude of the installation site to increase energy capture. While this approach may be suitable in certain conditions, its accuracy diminishes at higher latitudes due to increased standard error **[23]**. To determine the optimal angle for the Port of Avilés, the Photovoltaic Geographical Information System (PVGIS) has been employed. This tool uses the site's coordinates to identify the angle that maximizes solar irradiation incidence, enabling comparisons with alternative angles to assess the variation between the selected and optimal slopes.

This tool provides various functions, including the possibility to export climate data such as the average monthly temperatures throughout the year. This data is crucial for designing the solar installation, as photovoltaic panels are optimized for operation at an ideal temperature, typically around 25°C. Deviations from this temperature necessitate the application of correction factors to the voltage and current, which must be accounted for to ensure the system performs efficiently and reliably.

Based on the results obtained from PVGIS, the optimal tilt angle for the specified location is 36º. However, this angle is not commonly available among standard structure manufacturers, which could lead to additional installation costs if a custom structure is required. Therefore, a comparison has been made with a potential tilt angle of 30º. It is important to note that both tilt angles comply with the regulations outlined in the municipal ordinance governing the installation of photovoltaic panels in Avilés, which specifies that the maximum height from the ground to the top of the panel should not exceed 1.8 meters **[24]**. Table 3.1 presents a comparison between both angles, along with the average temperature

for the selected location.

Table 3.1. Average temperature and comparison between incident irradiation at 36º and 30º.

Month	Irradiation (kWh/m^2/month) (36º)	Irradiation (kWh/m2/month) (30º)	Average Temperature (ºC)
January	90.6	84.8	8.5
February	111.4	106.0	7.4
March	150.7	148.0	11.9
April	175.7	176.4	12.9
May	179.1	183.6	14.4
June	169.9	175.4	18.5
July	177.8	182.9	18.9
August	165.0	167.4	19.5
September	157.8	156.0	18.9
October	109.4	106.0	17.0
November	70.0	66.9	12.6
December	85.5	79.6	9.3
Total	1642.9	1633.0	14.2

The analysis confirms that reducing the panel inclination by 6 degrees has an almost negligible impact on incident irradiation, with a difference of just 0.602%. This validates that adopting the previously mentioned 30º tilt is a reliable choice, as it does not result in significant losses in irradiation capture.

With the orientation and inclination of the panels established, the key components and models of the photovoltaic system are defined, with a particular focus on the panels and the inverter.

To ensure a robust comparison, the panel model from the preliminary design has been retained, ensuring that the simulations are conducted under consistent conditions. As the inverter specification had not been previously determined, this allowed for greater flexibility in its selection. After evaluating the available options, a model with a capacity slightly exceeding the installed photovoltaic power has been chosen. Consequently, the GW1000-XS model from GoodWe has been selected for this installation.

Through the utilization of PVsyst, it has been verified that the panel arrangement in series, and thus within the same string, consistently complies with the inverter's technical specifications. According to the inverter datasheet, a minimum input voltage of 40 V is required. Given that each panel has a maximum power voltage of 31.21 V, arranging them in series results in a total installation voltage derived from the sum of the individual panel voltages. Under standard conditions of 25ºC, the input voltage to the inverter will be 62.42 V.

As previously noted, the voltage is influenced by the ambient temperature to which the panels are exposed. To account for this, tests were conducted using PVsyst under extreme temperatures of -10ºC and 60ºC, applying the voltage correction factors based on temperature as specified in the datasheet. In both cases, the results were favourable, and the inverter’s minimum and maximum voltage limits were

not exceeded. The voltage at -10ºC was calculated to be 81 V, while at 60ºC, it was 55 V. Table 3.2 presents the detailed specifications of both the panels and the inverter.

Table 3.2. Photovoltaic panels and inverter technical specifications.

PV Panels (JAM54S30-405/MR)		**Inverter (GW1000-XS)**	
Parameter	**Value**	**Parameter**	**Value**
Rated maximum power (Pmax) [W]	405	Max. input voltage (V)	500
Open circuit voltage (Voc) [V]	37.23	Mpp. Operating voltage range (V)	40 - 450
Maximum power voltage (Vmp) [V]	31.21	Start-up voltage (V)	40
Short circuit current (Isc) [A]	13.87	Max. Short Circuit Current per MPPT (A)	15.6
Maximum Power Current (Imp) [A]	12.98	Number of MPP Trackers	1
Module efficiency [%]	20.7	Number of Strings per MPPT	1
Temperature coefficient of Isc (α_Isc)	+0.045%/ºC	Nominal output power (W)	1000
Temperature coefficient of Voc (β_Voc)	-0.275%/ºC	Max. AC Active Power (W)	1100
Temperature coefficient of Pmax (γ_Pmp)	-0.350%/ºC	Max. Efficiency	97.2%

To ensure the simulations accurately reflect real-world performance, a series of loss factors have been applied to account for system inefficiencies. Incorporating these factors is essential, as failing to do so could result in overestimated energy generation, leading to discrepancies when comparing simulations to actual performance.

Notably, this analysis does not consider shading losses from nearby objects. Since the installation is designed as an independent structure, the panels will be strategically positioned to prevent any potential obstruction to sunlight. Table 3.3 summarizes the efficiency loss factors integrated into the model.

Table 3.3. Losses applied to the photovoltaic system.

Losses	**Loss factor applied**
Soiling loss factor	1.5%
LID loss factor	0%
Loss due to temperature	3.85%
Degradation loss factor 25 years	13.47%
Mismatch loss	0.5%

After including all relevant factors and constraints, the annual simulation results have been obtained. Unlike the preliminary design, which relied on simplified estimations, this analysis employs advanced professional software to model photovoltaic generation on an hourly basis. By utilizing high-resolution climatic data from the Meteonorm 8.1 database, the accuracy of the results is significantly enhanced.

This refined approach eliminates the reliance on annual average data, instead providing a granular and time-specific assessment of energy production. As a result, the simulation more accurately reflects real-world conditions and system performance. Figure 3.1 illustrates the variation in photovoltaic generation throughout the year, as well as the energy losses incurred during irradiation capture and throughout the different system components.

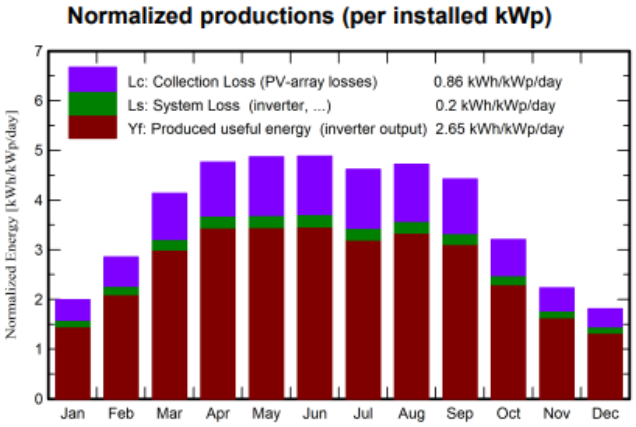

Figure 3.1. Normalized energy generation over the year.

The final generation results demonstrate a significant improvement over the estimates from the preliminary design. By implementing this new methodology, annual photovoltaic production has reached 784.73 kWh, marking a 38.64% increase. Furthermore, the energy generation per installed Watt has risen substantially from 0.70 kWh/W to 0.97 kWh/W. This underscores the importance of applying advanced methodologies when estimating generation, particularly for renewable energy sources, which are inherently variable. Relying on generic data and extrapolating results can sometimes lead to inaccurate or unrepresentative projections.

3.1.2 Wind unit

3.1.2.1 Description of preliminary wind design and results

Similar to the advancements in the photovoltaic sector, wind energy has also seen substantial growth in installed capacity and cost reductions, both in Spain and globally. While small-scale wind systems are less prevalent in residential and industrial settings compared to solar panels, a well-optimized design can enable both technologies to work synergistically. Their complementary nature enhances the efficiency and reliability of hybrid energy systems, such as the one currently under development.

Preliminary forecasts have been made to estimate the contribution of this energy source to overall generation of the hybrid system. However, these projections rely on generic parameters, which, similar to the experience with the photovoltaic unit, may lead to discrepancies between initial predictions and actual performance over time. To address this, it is crucial to implement more refined calculation methods that improve the accuracy of long-term forecasts and minimize the impact of potential mismatches.

From a technical perspective, vertical-axis wind turbines (VAWTs), specifically the SMARAAD 24V model, have been selected for this project. VAWTs offer several advantages over horizontal-axis wind turbines (HAWTs), particularly in urban environments. Unlike HAWTs, VAWTs do not require active alignment with the wind direction, enabling them to capture wind from any angle. They can also operate at lower wind speeds and perform more efficiently in areas with high turbulence. Additionally, VAWTs

facilitate easier maintenance, as critical components such as the gearbox can be more compact and positioned closer to the ground **[25]**. Another notable advantage is their lower noise emissions compared to HAWTs, making them particularly suitable for urban areas with stringent noise regulations.

However, these benefits come with certain trade-offs. In terms of efficiency, HAWTs generally outperform VAWTs. The efficiency of a VAWT depends largely on its design, which can be categorized into three main types: Cup, Savonius, and Darrieus. Cup and Savonius designs operate primarily based on drag forces, resulting in lower efficiencies of approximately 8% and 16%, respectively. In contrast, the Darrieus design utilizes lift-based aerodynamics, allowing it to achieve efficiency levels of up to 40% **[26]**. Modern three-bladed HAWTs, by comparison, can reach efficiencies of approximately 50%, enabling greater power generation for the same swept area. As a result, VAWTs are generally less cost-effective than HAWTs for large-scale applications.

Given the design of a hybrid system for self-consumption and the specified characteristics, the use of the SMARAAD 24V model can be positively endorsed. For this system, each turbine is rated at 800 W, with a total of three turbines to be installed. Similar to the solar section, it is estimated that the turbines will operate for approximately 292 days annually, with a projected generation of 250 W/m² and a swept area of 0.45 m² per turbine.

Considering all the factors outlined above, it is estimated that the wind generation of the hybrid system will total approximately 473.04 kWh by the end of the year. This represents 36% of the total energy contribution of the hybrid module, making wind energy the second most significant source in the system's energy mix.

3.1.2.2 Redefinition of the wind unit

Once the preliminary results have been established, a series of alternative calculations will be conducted to verify that the initial estimates align with methods that incorporate more precise data, such as hourly wind speed.

It is important to acknowledge that modeling wind installations of this scale can be challenging due to the limited availability of commercial software capable of conducting such simulations. As a result, the decision has been made to derive estimates using the power curve in relation to the wind speed supported by the turbines.

For the selected model, the manufacturer's power curve is unavailable, requiring the development of alternative methods for extrapolation. One effective approach involves using the minimum operating speed and the wind velocity at which the turbine reaches its nominal power. By applying these two data points, a polynomial trend line can be generated, enabling the estimation of the power output from the turbine's startup until it reaches its maximum capacity.

Another approach considered is the calculation of the ideal power curve using the power coefficient (CP). Under ideal conditions, where factors such as viscosity are not accounted for, the power coefficient can be determined at the nominal wind speed and applied to lower velocities, enabling the calculation of power at each of these levels. However, a significant challenge with this method is that datasheets

often lack some of the necessary information, such as the chord of the airfoil and the tip speed ratio, requiring assumptions that could potentially skew the accuracy of the calculations.

After evaluating both methodologies, it has been decided to proceed with the first approach, which involves determining the power curve based on the start-up speed and the wind velocity at which nominal power is achieved. Initially, a preliminary trend line has been established to extrapolate the power for intermediate wind speeds. For this particular turbine, the start-up speed is 2 m/s, and the rated wind velocity is 11 m/s. Using these two values, Equation (3.1) has been obtained.

$$P_{turb} = 0.0002 \cdot v^6 - 0.0153 \cdot v^5 + 0.5673 \cdot v^4 - 10.112 \cdot v^3 + 82.934 \cdot v^2 - 185.33 \cdot v + 111.66 \quad (3.1)$$

P_{turb} corresponds to the power output of the turbine in (W) and v to the wind speed in (m/s). After substituting the speed values into the previous formula, a power curve has been derived that closely represents the expected performance of the wind turbine. Once a reliable approximation has been achieved, PVGIS is utilized to obtain wind data for the area, enabling the calculation of hourly energy generation.

To ensure the highest possible accuracy, all calculations have been conducted in Excel, incorporating a series of constraints to maintain the wind turbines within their operational limits. Before detailing these constraints, Table 3.4 presents a summary of key wind data, including the average wind speed for each month of the year and wind directionality, along with a graphical representation of the corresponding power curve.

Table 3.4. Monthly average of wind speed and direction.

Month	Average Wind Speed (m/s)	Average Wind Direction (º)
January	3.05	220.3991935
February	2.50	183.6175595
March	2.82	181.3870968
April	2.31	135.2763889
May	2.61	103.8454301
June	2.47	178.0305556
July	2.92	181.3534946
August	2.39	147.5094086
September	2.67	153.9638889
October	2.58	157.7352151
November	2.92	179.6986111
December	3.37	187.0053763
Total average:	2.72	167.4851849

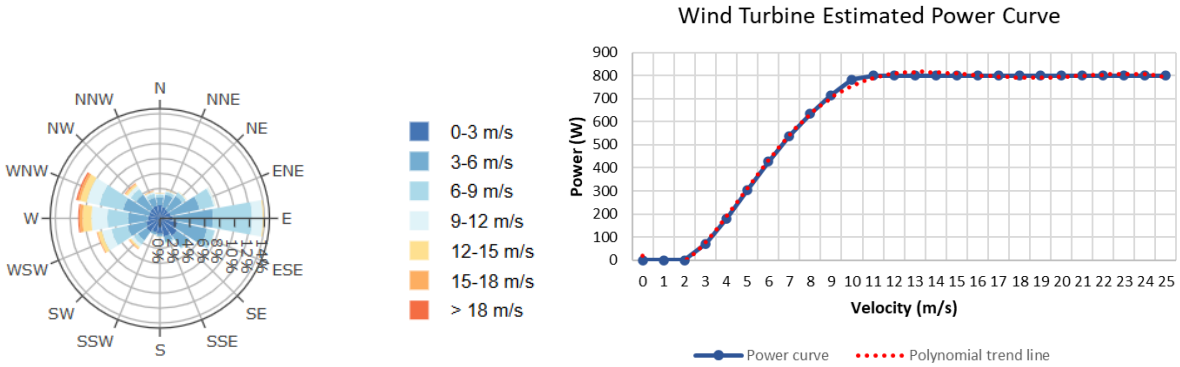

Figure 3.2. Definition of wind direction (50 m) and wind turbine estimated power curve.

After considering all these factors, it is essential to define the operational constraints of the wind turbine, which are necessary to ensure its proper functioning. The turbine has a cut-in speed, marking the point at which it begins generating power, and a rated speed, at which the maximum achievable power is reached and maintained for higher wind speeds. Additionally, a cut-out speed is established, beyond which the turbine ceases operation to ensure safety, protect structural integrity, and minimize wear or potential failures.

For the selected turbine, the manufacturer's datasheet specifies a maximum allowable wind speed of 45 m/s. However, to enhance the system's longevity, a more conservative operational limit of 25 m/s has been set, as illustrated in Figure 3.2. A comprehensive overview of the wind turbine's specifications can be found in the datasheet provided in the Appendix B of this document. All these constraints have been defined with the Equation (3.2);

$$P(v) = \begin{cases} 0 & if\ v < 2 \\ P_{turb}(v) & if\ 2 \leq v < 11 \\ 800 & if\ 11 \leq v \leq 25 \\ 0 & if\ v > 25 \end{cases} \tag{3.2}$$

The parameter $P_{turb}(v)$, corresponds to the turbine power equation between 2 and 11 m/s in function of the wind speed. After defining the climatic wind parameters for the area, along with the wind turbine power curve and the critical wind speeds that determine operational performance, the monthly energy generation data have been analyzed. These calculations, based on hourly wind data, reflect the combined output of the three wind turbines. The results are summarized in Table 3.5 and illustrated in Figure 3.3.

Table 3.5. Monthly wind generation by the three turbines.

Month	Wind Generation (kWh)
January	273.74
February	136.74
March	202.52
April	118.73
May	151.28
June	145.07
July	240.02
August	139.42
September	188.06
October	149.60
November	257.43
December	306.42
Total:	2309.03

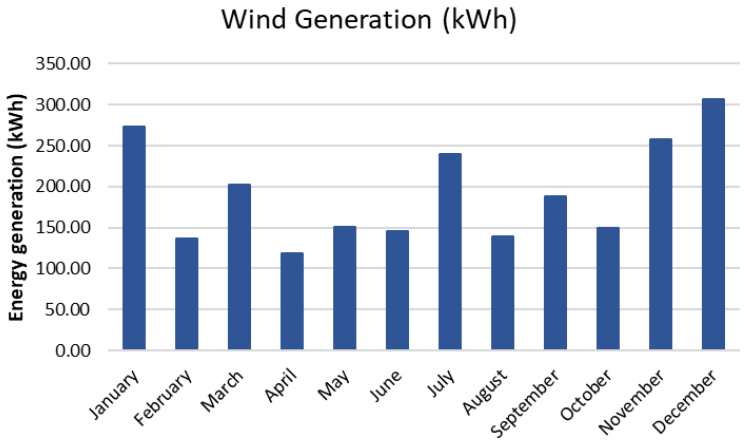

Figure 3.3. Wind generation profile over a calendar year.

The results reveal a substantial divergence from the initial design estimates, with actual energy generation significantly exceeding the projections outlined in the proposal document. This difference is largely due to the inherent variability of wind, which is far less predictable than solar irradiation. While solar energy follows a more stable and cyclical pattern, wind energy is highly dynamic and influenced by atmospheric conditions, resulting in greater fluctuations in the output. The total energy generated by the three wind turbines amounts to 2,309.03 kWh, nearly five times the estimated production based on annualized average parameters. This significant increase in generation fundamentally alters the energy mix of the hybrid module, positioning wind energy as the dominant source while reducing the relative contribution of solar power.

3.1.3 Hydrokinetic unit

3.1.3.1 Description of preliminary hydrokinetic design and results

Hydrokinetic energy is the final power source incorporated into the hybrid module's energy mix, providing a valuable source of supplemental energy. While it is not commonly used for self-consumption or small-scale applications, its integration in this case can be highly positive. The hybrid module is designed for deployment in an estuary designated for port operations, where hydrokinetic energy can enhance efficiency, sustainability, and overall energy resilience.

The original project document provides limited data and technical specifications for this renewable energy source. While it confirms the use of two Savonius vertical-axis turbines, it does not specify the exact model, making it difficult to conduct a precise and detailed comparison between the initial generation estimates and alternative redefined methods of calculation. Key factors considered in estimating the energy output of the hydrokinetic turbines include an average water velocity of 0.7 m/s and a swept area of 0.28 m² per turbine.

Similar to wind energy, vertical-axis turbines come in various types. For this application, the Savonius turbine is the most suitable choice due to its low required start-up speed. Given the low average water velocity, alternative turbine types could significantly reduce the system's efficiency, as they would often remain inactive when the flow speed falls below operational requirements.

According to the established criteria, projections from the base project estimate that the hydrokinetic turbines will produce approximately 135.55 kWh per year, accounting for 10% of the module's total annual energy generation.

3.1.3.2 Redefinition of the hydrokinetic unit

For the redefinition of the hydrokinetic unit's generation data, the marine conditions around the harbour have been reanalysed first, to determine the turbines' actual generation potential more accurately.

For this purpose, prior studies conducted in the area have been utilized alongside current data from the past ten years recorded in the Avilés estuary using the Portus tool, developed by the Spanish Government **[27]**. This information is critical, as the energy potential and current speed vary across different sections of the port. Consequently, selecting the optimal site will be essential to maximizing turbine efficiency.

Based on the velocity profiles shown in Figure 3.4, it has been observed that, as the distance from the estuary mouth increases, current velocities decrease significantly, averaging approximately 0.2 m/s, which is insufficient for effective energy generation. Research is currently focused on developing advanced hydrokinetic turbines that can operate at lower flow velocities, thereby enhancing efficiency and expanding the potential of hydrokinetic energy systems. Among these innovations, experimental three-blade horizontal-axis turbine designs have shown promise, demonstrating functionality at flow speeds as low as 0.14 m/s **[28]**. However, as these models are still in the prototype stage and not yet

commercially available, they cannot currently be incorporated into the hybrid module. At present, most commercially available turbines require a minimum flow velocity of approximately 0.5 m/s, a key parameter that must be considered when estimating the unit's energy output, as it defines the lower operational threshold of the system.

Referring to the information presented in Figure 3.4, it offers a distinct perspective compared to the preliminary design of the project. Initially, the estuary's average velocity was estimated at 0.7 m/s. While this value may apply at certain locations, it cannot be considered representative across the entire area, as the velocity is notably lower in most sections. Consequently, it is concluded that the hybrid module should be positioned as close as possible to the estuary entrance, where current velocities of up to 0.8 m/s can be achieved.

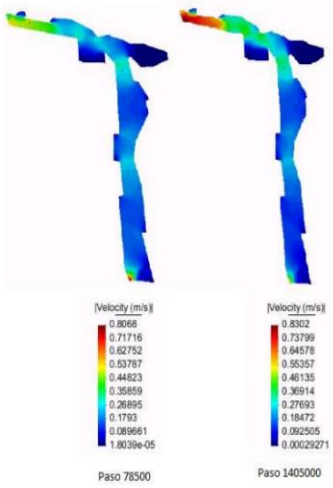

Figure 3.4. Water velocity across Port of Avilés.

Another important factor to consider is the periodicity of the velocity peaks and troughs. Analysis of the historical data has revealed a clear cyclical pattern, with a period of approximately twelve hours between peaks, resulting in 6-hour cycles of increasing and decreasing velocity. This pattern is more clearly illustrated in Figure 3.5. The cyclical variability of the currents will be instrumental in determining the operational periods of the turbines.

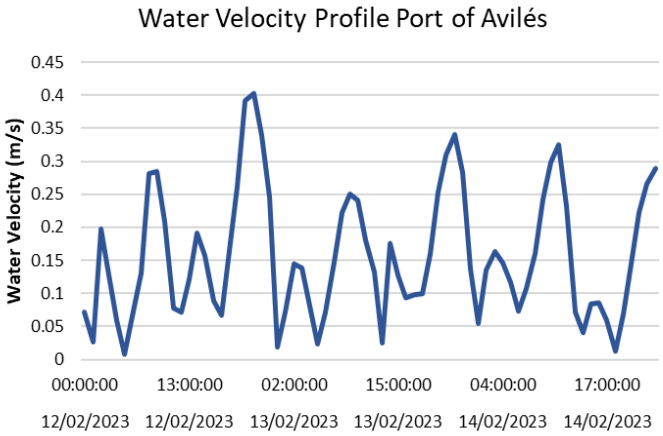

Figure 3.5. Exemplification of a typical water velocity profile in the Port of Avilés.

Scientific studies, primarily based on velocity profiles and other relevant parameters, have been conducted to evaluate the energy potential of the Avilés estuary. In this context, five strategic locations were selected, each defined by its distance from the estuary mouth, and the energy potential per square meter was quantified for each point. The location nearest to the estuary mouth, situated 100 meters way from this reference, was identified as the most optimal for positioning the hybrid module, with an energy potential of 1.59 kWh/m² **[29]**. Given the estuary's considerable width, approximately 164 metres at the proposed site, turbine installation at this location poses substantial technical and logistical challenges,

in addition to the potential disruption of port operations. As a result, the hybrid module is planned for deployment in an auxiliary canal situated roughly 1,000 metres upstream from the estuary mouth, which was also included in the study's surveyed locations. This alternative site offers a significantly narrower span of approximately 19 metres, greatly enhancing the practicality and cost-effectiveness of the installation. Table 3.6 outlines the estimated energy potential at each of the evaluated points.

Table 3.6. Hydrokinetic energy potential from studied reference **[29]**.

Position (m)	**Energy potential (kWh/m^2)**
100	1.59
1000	0.0995
2000	0.0332
3000	0.0545
4000	0.0024

Based on the analysis conducted and the factors previously discussed and considering that the hybrid block will be positioned approximately 1000 meters from the mouth of the estuary, it has been estimated that the hydrokinetic unit will operate in 6-hour generation cycles followed by 6-hour rest periods, in alignment with the natural current patterns of the area. For this specific application, the same swept area of 0.28 m², as defined in the initial project, will be used to ensure a fair and consistent comparison. Under these conditions, the projected annual energy production of the unit is estimated to be 244.05 kWh. This value represents 80.4% increase over the initial estimates, marking a substantial improvement compared to the projections outlined in the original design.

3.1.4 PAT unit

Given the reliance on renewable energy sources, it is essential to implement an effective energy storage solution to ensure system stability and mitigate the fluctuations associated with intermittent generation. To address this challenge, a pump-as-turbine system has been previously selected as the preferred solution. This system enables the storage of excess energy produced during periods of low demand, allowing it to be redeployed when direct generation from the renewable module is insufficient to meet consumption needs. As a result, the PAT system plays a vital role in supporting energy system reliability and ensuring continuous power availability.

While the preliminary design estimates the PAT system's generation capacity at 140.16 kWh, approximately 11% of the total projected output, this value should be considered indicative rather than definitive. The actual performance of the system is influenced by numerous external variables, including the chosen energy management strategy, hourly demand profiles, and specific operating conditions, rather than solely by pump capacity or runtime. Consequently, the effectiveness and utilization of the PAT system may vary significantly. For this reason, no fixed contribution has been assigned in this section; instead, its performance will be assessed individually within each of the simulated scenarios.

From a technical standpoint, the system incorporates a pump capable of operating reversibly as a

turbine. Positioned within the canal designated for the hybrid module, the pump is integrated into a network of pipes and valves that facilitate the transfer of water to an elevated tank, initially set at a height of 3 meters. The system is designed with a nominal power output of 200 W for the pump-as-turbine unit, though this parameter can be tailored to accommodate the specific demands of various operational scenarios.

The hydraulic circuit has been engineered to prioritize operational simplicity and cost-effectiveness, without compromising functionality. The system comprises four valves, two of which are manually operated and positioned near the tank and turbine to ensure ease of access and control. At the core of the system, the main conduit diverges into two distinct branches: the upper branch governs the discharge of water from the tank, while the lower branch facilitates the pumping process to replenish the tank. This dual-path configuration enables efficient flow management and enhances overall system performance. A comprehensive schematic of the complete Pump-as-Turbine system is provided in Figure 3.6.

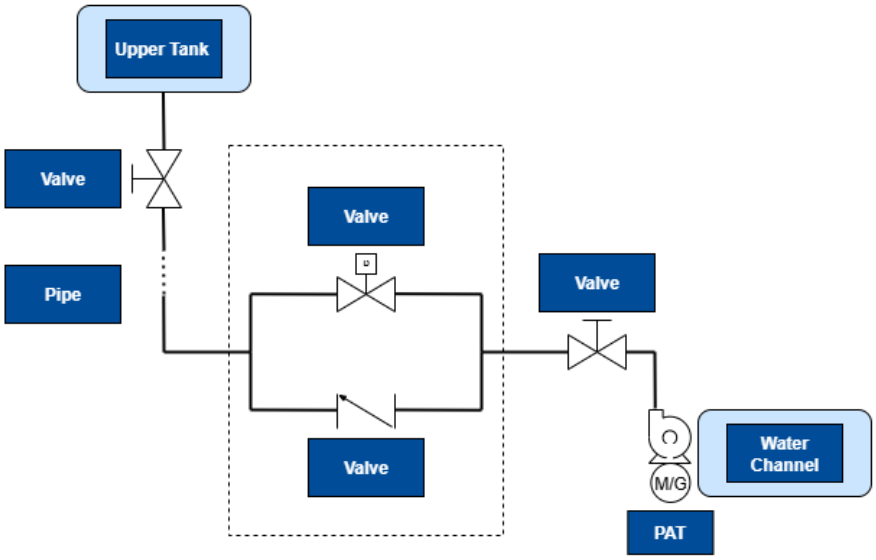

Figure 3.6. Hydraulic scheme of the PAT system.

This system will be maintained throughout the different scenarios tested for the original system design. Additionally, comparative simulations will be conducted to evaluate alternative storage technologies. These simulations aim to identify differences in performance and assess their impact on both energy efficiency and economic viability.

As a result of the individual adjustments made to each energy source, the revised energy mix of the hybrid module reflects a significantly different paradigm compared to the initial estimates presented in the basic project, as shown in Figure 3.7. Moreover, by applying alternative and more refined calculation methods, the system's energy potential has been enhanced by 253%, taking into account that the storage unit contribution has not been considered yet.

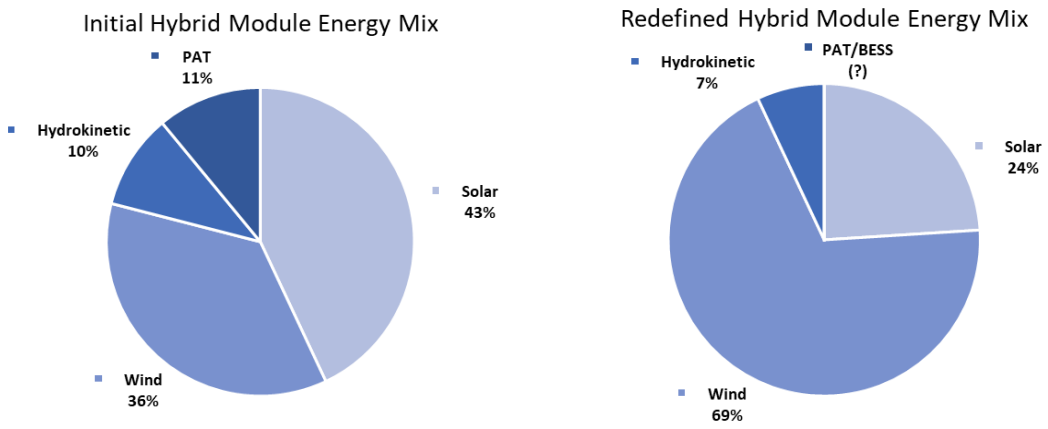

Figure 3.7. Energy mix comparison of the hybrid module before and after the reconfiguration of the generating units.

3.2 Load profile selection

3.2.1 Demand considerations

While accurately estimating the hybrid module's generation capacity is essential for designing effective energy management strategies, the careful selection of target energy demands is equally critical. This choice directly shapes system performance and underpins the methods used to optimise both energy efficiency and economic viability.

According to data recorded at the Port of Avilés, a total of 30 energy supply points have been identified, each corresponding to different infrastructures within the port complex. These facilities support a diverse range of activities, resulting in markedly different energy demand profiles, ranging from minimal consumption to high-intensity usage that generates substantial energy costs over each reporting period.

Considering the variation in energy consumption across the different installations and the generation limitations of the hybrid module, it is crucial to focus on infrastructures with energy demands that closely align with the module's output. This will result in a more balanced system performance, leading to more accurate and reliable conclusions than if the module was used to meet highly diverse profiles.

The energy demands across the port are directly linked to the tariff structures assigned to each infrastructure. Three distinct tariff categories, 2.0 TD, 3.0 TD, and 6.1 TD, are applied, each reflecting the varying energy intensities required by the facilities. A comprehensive understanding of how each tariff structure impacts energy demand costs and the management of the hybrid module is essential, particularly when assessing the economic performance in the development of different scenarios.

3.2.2 Analysis and criteria used for demand profiles selection

Of the 30 supply points registered throughout the port, detailed consumption profiles have been obtained for 23 of them. The collected data have been systematically filtered and categorized based on the

applicable tariff structures and the recorded energy volumes at each meter. As a preliminary step, all supply points operating under the 6.1TD tariff were excluded from further analysis, as their demand levels significantly exceed the operational capacity of the proposed hybrid module.

Subsequent analysis has focused on the consumption profiles associated with the two remaining tariff structures. Among these, three profiles, Vieja Rula, Embarcadero, and Luz Roja, have been identified as particularly suitable. Each is associated with the 2.0 TD tariff and demonstrates a demand pattern that remains consistently within the generation capabilities of the hybrid module throughout the year. This stability is a key advantage, as other profiles, despite being generally compatible, exhibit sporadic demand peaks that disrupt the load profile, potentially compromising the efficiency and reliability of the system.

Beyond the overall scale of demand in relation to the module's generation capacity, the structural characteristics and unique consumption patterns of each profile are of critical importance. A thorough individual analysis is therefore indispensable to ensure optimal management and utilisation of the energy produced by the hybrid module under each of the scenarios considered. This level of granularity allows for more precise adaptation to specific demand behaviours, ultimately enhancing the system's overall efficiency and reliability.

The analysis begins with the consumption profile of Vieja Rula for the year 2023. A detailed examination of its energy requirements and demand trends reveals three distinct behavioural patterns over the study period. These variations will have a direct impact on the management of the hybrid system, particularly in terms of addressing energy deficits and surpluses. The full profile, along with its segmented periods and their specific characteristics, is presented in Figure 3.8.

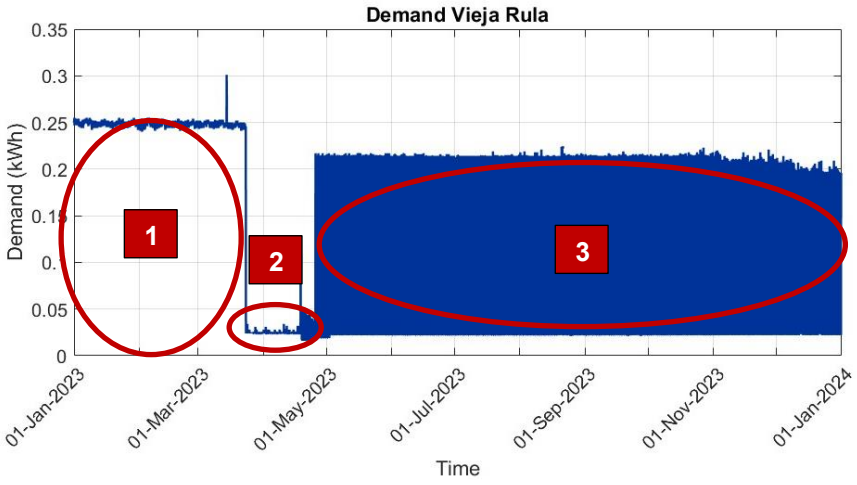

Figure 3.8. Vieja Rula demand profile over 2023.

Region 1 is marked by peak energy demand during this period. However, despite the higher consumption, the energy pattern remains notably stable, with minimal fluctuations between day and night. This stability makes the region highly predictable, facilitating accurate forecasting of when additional grid support will be required and when the hybrid module alone will be sufficient to meet the infrastructure's energy needs.

In reference to the second region, there is a notable decline in consumption, reaching nearly negligible levels over a period of approximately one and a half months. However, due to the absence of historical data on consumption profiles from previous years, it is difficult to ascertain whether this reduction in demand was an isolated event in 2023 or if it reflects a recurring trend in the building's energy requirements.

The third region, which encompasses the majority of the study period, is of particular importance, as it is expected to have the greatest influence on the overall performance of the hybrid energy system. This segment of the consumption profile is distinguished by a key characteristic: energy demand is concentrated during nighttime hours, while daytime consumption remains minimal. Consequently, the design and sizing of the energy storage system become critical. Surplus energy generated during the day must be efficiently stored to meet demand during periods when solar resources are unavailable, shifting the burden of supply to wind and hydrokinetic generation. The total demand of the profile over the year amounts to 1,226.96 kWh.

The second selected consumption profile, associated with Luz Roja, exhibits markedly different energy characteristics compared to the previously analysed infrastructure. In this case, demand remains consistently low and stable throughout the year, with the exception of two isolated peaks observed in March. Given its minimal annual consumption, approximately 6.54 kWh, this profile has been included primarily to complement the other two selected profiles. The storage requirements are virtually negligible, as the low and steady demand would result in frequent energy surpluses if the profile was addressed independently.

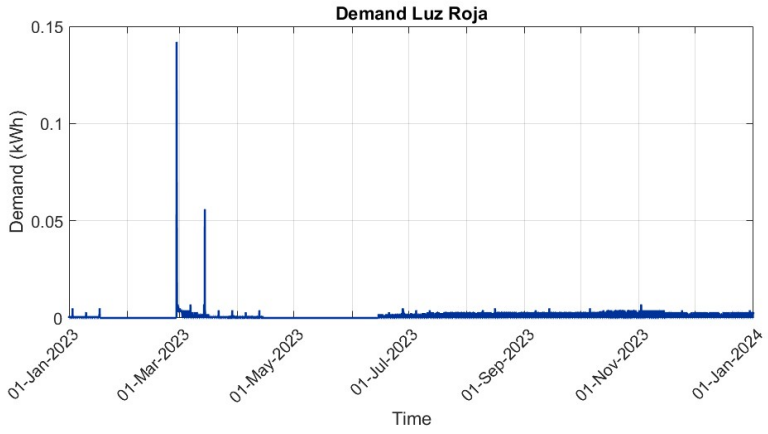

Figure 3.9. Luz Roja demand profile over 2023.

Lastly, regarding the consumption profile of the Embarcadero, identified as the final infrastructure to benefit from the hybrid module’s energy production, this profile accounts for approximately 12% of the total energy demand, equivalent to 171.66 kWh. When compared to the consumption of Vieja Rula, the Embarcadero's demand is significantly lower and also demonstrates a less stable consumption pattern. Although the overall scale of demand remains consistent throughout the year, there is a noticeable variation in energy usage between the first five months and the subsequent seven months, indicating a shift in operational behavior over time.

In the early months of the study period, the Embarcadero’s energy consumption profile remains

consistently stable, showing minimal variation. A modest decline begins in April and extends for approximately six weeks, aligning with a concurrent, though more significant, drop in consumption at Vieja Rula. From June onward, demand returns to the levels observed between January and March. However, the latter half of the year is characterized by recurring consumption peaks. While these fluctuations remain within the operational limits of the hybrid module, they introduce a degree of instability to the profile, contrasting with the steady behaviour exhibited during the first part of the year.

In the absence of historical data on the energy performance of this section of the port, it is difficult to determine whether the consumption peaks observed in the latter half of the year reflect typical operational performance or are anomalies specific to the period under review. Access to such information would be particularly valuable for refining the design of the hybrid module's energy strategies and evaluating the reliability of extrapolating the current profile to future years. Given this uncertainty, the observed pattern will be treated as representative of normal operating conditions, while the proposed energy management model and scenarios will remain adaptable to future revisions as more comprehensive data becomes available.

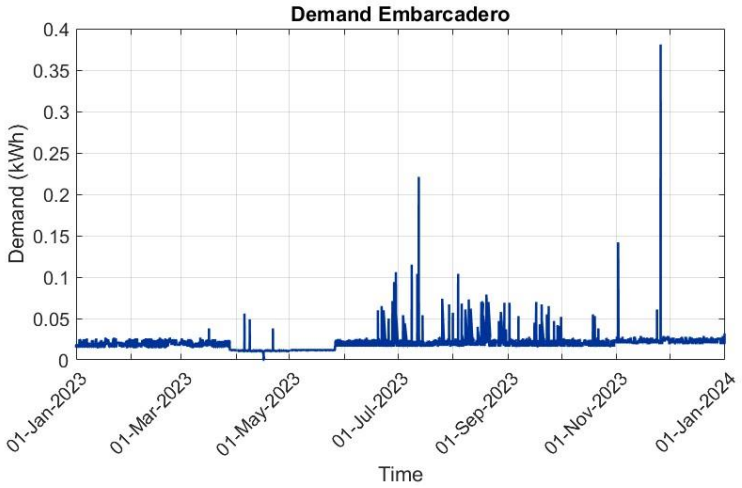

Figure 3.10. Embarcadero demand profile over 2023.

3.3 Tariffs and economic parameters

Upon registering a consumption point, the applicable tariff structure is determined based on the infrastructure type and corresponding energy requirements. These tailored tariffs govern the segmentation of energy consumption across daily and monthly periods for billing purposes. As outlined earlier, three distinct tariff categories are applied throughout the port. While these tariffs may have a limited effect on the evaluation of the module's technical energy performance, they are critical in the financial analysis. This is because the return on investment largely depends on the reduction of grid energy consumption, which directly translates into lower electricity costs and long-term economic savings.

The tariff structures form a critical component of the inputs used in the developed energy analysis model, underscoring the importance of their accurate definition and detailed characterization. Within the port's

operational scope, three distinct tariff types are in effect, 2.0 TD, 3.0 TD, and 6.1 TD, each designed to reflect the specific energy requirements and operational profiles of the infrastructures they serve. A comprehensive overview of these tariff categories and their relevance is provided in Sections 3.3.1 and 3.3.2.

3.3.1 Tariff 2.0 TD

The 2.0 TD tariff in Spain is designed for consumers with a contracted power capacity of up to 15 kW and operates at low voltage. It features a mandatory hourly discrimination structure, divided into three distinct periods: valley, flat, and peak. Since a fixed price is typically applied based on contracted power, regardless of actual consumption, effective management of transmission and distribution tolls assigned to each period becomes a key factor in achieving cost savings. It is essential to emphasize that the assigned prices for this factor do not reflect the final amount to be paid but rather constitute only a portion of the total energy cost.

This tariff is primarily intended for residential use and low-consumption businesses. In many cases, electricity providers may simplify billing by unifying the prices across the different periods. Figure 3.11 illustrates the distribution of daily periods throughout each month of the year.

	JAN	FEB	MAR	APR	MAY	JUN	JUL	AUG	SEP	OCT	NOV	DEC
00:00 - 01:00	P3	P3	P3	P3	P3	P3	P3	P3	P3	P3	P3	P3
01:00 - 02:00	P3	P3	P3	P3	P3	P3	P3	P3	P3	P3	P3	P3
02:00 - 03:00	P3	P3	P3	P3	P3	P3	P3	P3	P3	P3	P3	P3
03:00 - 04:00	P3	P3	P3	P3	P3	P3	P3	P3	P3	P3	P3	P3
04:00 - 05:00	P3	P3	P3	P3	P3	P3	P3	P3	P3	P3	P3	P3
05:00 - 06:00	P3	P3	P3	P3	P3	P3	P3	P3	P3	P3	P3	P3
06:00 - 07:00	P3	P3	P3	P3	P3	P3	P3	P3	P3	P3	P3	P3
07:00 - 08:00	P3	P3	P3	P3	P3	P3	P3	P3	P3	P3	P3	P3
08:00 - 09:00	P2	P2	P2	P2	P2	P2	P2	P2	P2	P2	P2	P2
09:00 - 10:00	P2	P2	P2	P2	P2	P2	P2	P2	P2	P2	P2	P2
10:00 - 11:00	P1	P1	P1	P1	P1	P1	P1	P1	P1	P1	P1	P1
11:00 -12:00	P1	P1	P1	P1	P1	P1	P1	P1	P1	P1	P1	P1
12:00 - 13:00	P1	P1	P1	P1	P1	P1	P1	P1	P1	P1	P1	P1
13:00 -14:00	P1	P1	P1	P1	P1	P1	P1	P1	P1	P1	P1	P1
14:00 - 15:00	P2	P2	P2	P2	P2	P2	P2	P2	P2	P2	P2	P2
15:00 - 16:00	P2	P2	P2	P2	P2	P2	P2	P2	P2	P2	P2	P2
16:00 - 17:00	P2	P2	P2	P2	P2	P2	P2	P2	P2	P2	P2	P2
17:00 - 18:00	P2	P2	P2	P2	P2	P2	P2	P2	P2	P2	P2	P2
18:00 - 19:00	P1	P1	P1	P1	P1	P1	P1	P1	P1	P1	P1	P1
19:00 - 20:00	P1	P1	P1	P1	P1	P1	P1	P1	P1	P1	P1	P1
20:00 - 21:00	P1	P1	P1	P1	P1	P1	P1	P1	P1	P1	P1	P1
21:00 - 22:00	P1	P1	P1	P1	P1	P1	P1	P1	P1	P1	P1	P1
22:00 - 23:00	P2	P2	P2	P2	P2	P2	P2	P2	P2	P2	P2	P2
23:00 - 00:00	P2	P2	P2	P2	P2	P2	P2	P2	P2	P2	P2	P2

Weekends & Festivities
P3
P3
P3
P3
P3
P3
P3
P3
P3
P3
P3
P3
P3
P3
P3
P3
P3
P3
P3
P3
P3
P3
P3
P3
P3

Figure 3.11. 2.0TD tariff structure.

To simplify the economic calculations for the defined scenarios and simulations, unified values and prices have been applied to each period associated with this tariff, as shown in Table 3.7. It is worth to say that all three selected consumption profiles fall under this tariff model, given their classification as low-consumption profiles.

Table 3.7. Transmission and Distribution (T&D) tolls and final energy price for the 2.0TD tariff.

Periods	Transmission and distribution tolls (€/kWh)	Final Energy Price (€/kWh)
P1	0.033081	0.1090
P2	0.019184	0.1090
P3	0.000557	0.1090

3.3.2 Tariff 3.0 TD and 6.1 TD

The 3.0TD and 6.1TD tariff models are addressed together due to their shared period-based structure. However, each tariff has distinct characteristics and is designed to meet the specific needs of different types of infrastructures and usage requirements.

Regarding the 3.0TD tariff, it serves as an intermediate pricing model covering power capacities from approximately 15 to 100 kW. The year is divided into six tariff periods, each assigned a specific price based on the month. This tariff is typically intended for large residences, small to medium-sized businesses, offices, and retail establishments. A key advantage is its flexibility in contracted power, allowing consumers to adjust their allocation, for example, increasing power during off-peak hours and reducing it during peak periods, according to their specific needs.

Similar to the 2.0TD tariff, the costs associated with distribution and transmission tolls vary depending on the tariff period and do not constitute the total final energy price, as additional factors must be considered. In this case, maintaining a uniform price across all periods is uncommon, which increases the impact of these variations when analysing the economic aspects.

Regarding the 6.1TD, this model is designed for large electricity consumers. While the 3.0TD may be optimal for power levels up to 100 kW, it's recommended to opt for the 6.1TD from 50 kW onwards. This option is ideal for customers requiring high voltage, as well as industries such as automotive and metallurgical sectors. In the port area, there are several transformers operating under this tariff model, although they are currently not within the achievable targets for the installation of the hybrid module.

This tariff is also characterized by its division into six tariff periods, following the same structure as the 3.0TD model. It offers flexibility in the power allocation, allowing different power levels to be adopted depending on the period, which helps optimize the overall cost. Figure 3.12 illustrates the distribution of tariff periods throughout the calendar year, taking into account both the time of day and the month.

	JAN	FEB	MAR	APR	MAY	JUN	JUL	AUG	SEP	OCT	NOV	DEC	Weekends & Festivities
00:00 - 01:00	P6	P6	P6	P6	P6	P6	P6	P6	P6	P6	P6	P6	P6
01:00 - 02:00	P6	P6	P6	P6	P6	P6	P6	P6	P6	P6	P6	P6	P6
02:00 - 03:00	P6	P6	P6	P6	P6	P6	P6	P6	P6	P6	P6	P6	P6
03:00 - 04:00	P6	P6	P6	P6	P6	P6	P6	P6	P6	P6	P6	P6	P6
04:00 - 05:00	P6	P6	P6	P6	P6	P6	P6	P6	P6	P6	P6	P6	P6
05:00 - 06:00	P6	P6	P6	P6	P6	P6	P6	P6	P6	P6	P6	P6	P6
06:00 - 07:00	P6	P6	P6	P6	P6	P6	P6	P6	P6	P6	P6	P6	P6
07:00 - 08:00	P6	P6	P6	P6	P6	P6	P6	P6	P6	P6	P6	P6	P6
08:00 - 09:00	P2	P2	P3	P5	P5	P4	P2	P4	P4	P5	P3	P2	P6
09:00 - 10:00	P1	P1	P2	P4	P4	P3	P1	P3	P3	P4	P2	P1	P6
10:00 - 11:00	P1	P1	P2	P4	P4	P3	P1	P3	P3	P4	P2	P1	P6
11:00 -12:00	P1	P1	P2	P4	P4	P3	P1	P3	P3	P4	P2	P1	P6
12:00 - 13:00	P1	P1	P2	P4	P4	P3	P1	P3	P3	P4	P2	P1	P6
13:00 -14:00	P1	P1	P2	P4	P4	P3	P1	P3	P3	P4	P2	P1	P6
14:00 - 15:00	P2	P2	P3	P5	P5	P4	P2	P4	P4	P5	P3	P2	P6
15:00 - 16:00	P2	P2	P3	P5	P5	P4	P2	P4	P4	P5	P3	P2	P6
16:00 - 17:00	P2	P2	P3	P5	P5	P4	P2	P4	P4	P5	P3	P2	P6
17:00 - 18:00	P2	P2	P3	P5	P5	P4	P2	P4	P4	P5	P3	P2	P6
18:00 - 19:00	P1	P1	P2	P4	P4	P3	P1	P3	P3	P4	P2	P1	P6
19:00 - 20:00	P1	P1	P2	P4	P4	P3	P1	P3	P3	P4	P2	P1	P6
20:00 - 21:00	P1	P1	P2	P4	P4	P3	P1	P3	P3	P4	P2	P1	P6
21:00 - 22:00	P1	P1	P2	P4	P4	P3	P1	P3	P3	P4	P2	P1	P6
22:00 - 23:00	P2	P2	P3	P5	P5	P4	P2	P4	P4	P5	P3	P2	P6
23:00 - 00:00	P2	P2	P3	P5	P5	P4	P2	P4	P4	P5	P3	P2	P6

Figure 3.12. 3.0TD and 6.1TD tariff structure.

The pricing of the 3.0TD and 6.1TD tariffs is a critical factor, particularly in surplus management. As will be discussed later, one potential approach involves redirecting excess energy to infrastructures that follow the mentioned tariff models, which are more expensive than the 2.0TD tariff. Table 3.8 represents both the tolls and final energy prices used in the simulations, primarily for the economic viability analysis.

Table 3.8. T&D tolls and final energy price for the 3.0TD and 6.1TD tariffs.

Period	Transmission and distribution tolls (€/kWh)		Energy Final Price (€/kWh)	
	3.0 TD	6.1 TD	3.0 TD	6.1 TD
P1	0.023974	0.021899	0.1928	0.1540
P2	0.012820	0.011675	0.1673	0.1357
P3	0.007573	0.007394	0.1427	0.1133
P4	0.005495	0.005376	0.1229	0.1046
P5	0.000424	0.000406	0.1046	0.0998
P6	0.000234	0.000212	0.1165	0.1048

3.4 Energy management model definition and structure

3.4.1 Overview of the energy management framework

Accurate and well-structured data on energy generation and demand is fundamental to understanding the dynamics between supply and consumption, enabling a more comprehensive analysis of the system's energy balance. To effectively evaluate and manage these parameters, it is essential to develop a robust analytical tool that offers detailed insights into energy usage, its purposes, patterns, and efficiencies. Such a tool would not only support smarter energy management but also enhance economic outcomes and promote environmental sustainability.

To achieve these objectives, an energy management interface has been developed using Microsoft Excel, selected for its broad accessibility and user-friendly features. The interface offers an intuitive, visually streamlined experience, allowing for efficient control of the hybrid energy module. Designed with flexibility in mind, the tool is both scalable and location-independent, making it suitable for a wide range of deployment scenarios. Whether in urban environments like the one studied or in remote rural areas near rivers or other water sources, the tool adapts seamlessly. By enabling effective energy management across diverse settings, it contributes to more sustainable and efficient energy use on a broader scale.

HOPS (Hybrid Operational System) is the platform developed specifically to support the analysis and optimization of the hybrid energy module. It processes a set of key input parameters, such as energy generation profiles, demand patterns, and tariff structures, alongside a detailed inventory of component quantities and their specific costs. These inputs provide the foundational data necessary for conducting comprehensive feasibility studies, directly influencing both the economic viability and energy performance of the proposed solution.

Built to be adaptable, HOPS currently supports the integration of up to five generation sources. As mentioned in previous sections, this study focuses on three primary technologies: photovoltaic, wind, and hydrokinetic power. For energy storage, the tool accommodates either pump-as-turbine systems or battery storage, aligning with the operational scenarios being evaluated. This modular design enables

tailored system configurations while maintaining clarity and control over the modelling process.

To enhance its capabilities and broaden its application, future development of HOPS will involve transitioning from Excel to a more advanced programming environment, such as Python. This evolution will not only support the integration of additional storage technologies and more complex system architectures but will also enable the implementation of advanced analytical features. By strengthening both functionality and scalability, HOPS is positioned to become a versatile decision-support tool for sustainable energy planning across a wide range of contexts.

Figure 3.13. Logo for the Hybrid Operational System.

The underlying logic of the tool is based on the establishment of initial energy balances, which enable the identification of energy surpluses and deficits at any given moment. From this foundation and depending on the available energy resources and storage technologies, the system allows for the simulation of multiple scenarios, whether operating a single module or several in parallel. After evaluating the various configurations supported by the interface, the optimal operational strategy for the module is determined to ensure economic feasibility. In cases where viability cannot be achieved directly, the tool calculates an appropriate energy multiplier ratio to support long-term investment recovery. Figure 3.14 illustrates the interface logic, from the input of initial data to the generation of final results.

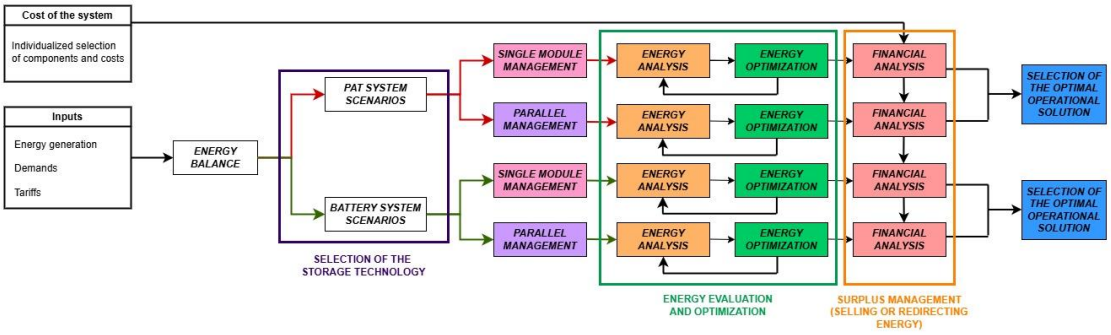

Figure 3.14. HOPS software logic flow diagram.

3.4.2 Utilization methodology based on key parameters

With a clear understanding of the operating logic behind HOPS, it is essential to explore in greater detail the key components that constitute the tool. This includes a thorough analysis of its inputs, the system's cost breakdown, and the outputs it produces. Given their complexity and centrality, all the scenarios will be addressed individually and comprehensively in future sections.

3.4.2.1 Inputs

In any management or computational tool, the quality of the initial inputs is paramount, as they directly influence the accuracy and reliability of the resulting outputs. This principle is particularly relevant in the realm of energy management software, which generally falls into two categories: those that simulate or calculate on-site energy generation in real time, and those that depend on pre-processed generation data, input via a database and typically spanning a defined temporal range.

In this initial version of HOPS, pre-calculated input data has been deliberately chosen to accelerate scenario simulations and conserve computational resources that would otherwise be required for real-time generation modelling from various renewable sources. As a result, Section 3.1 of this document offers a more detailed characterization of generation levels, incorporating advanced methodologies that represent a significant refinement over those used in the preliminary design phase. The data has been annualized and structured with hourly granularity to ensure both accuracy and usability in subsequent analyses.

As previously noted, HOPS has been developed to streamline data processing and facilitate swift, accurate decision-making. To support this objective, the number of required inputs for simulations has been strategically limited to three core categories: energy demand, energy generation, and tariff pricing. The interface also incorporates a navigation bar that allows users to easily access different scenarios and sections, an element present across all Excel tabs for intuitive use. Figure 3.15 provides an overview of the interface, highlighting the section dedicated to data entry for subsequent processing.

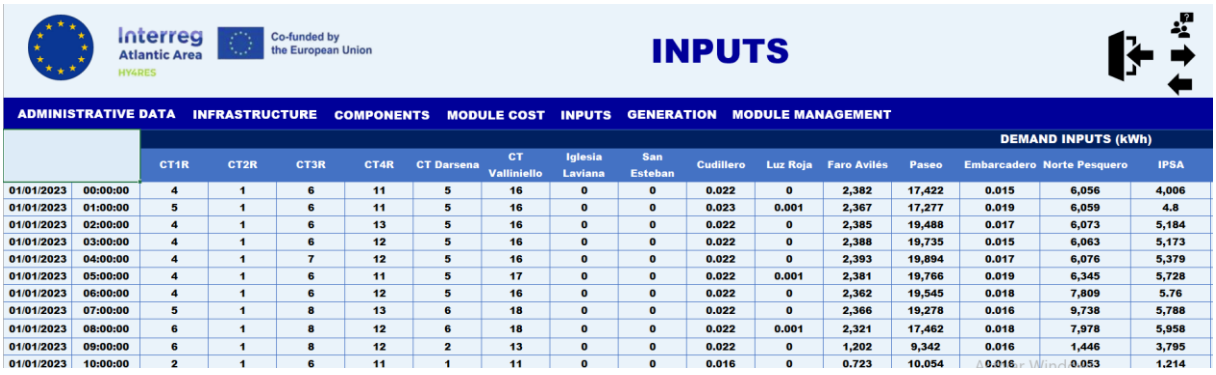

DEMAND INPUTS (kWh)

		CT1R	CT2R	CT3R	CT4R	CT Darsena	CT Valliniello	Iglesia Laviana	San Esteban	Cudillero	Luz Roja	Faro Avilés	Paseo	Embarcadero	Norte Pesquero	IPSA
01/01/2023	00:00:00	4	1	6	11	5	16	0	0	0.022	0	2,382	17,422	0.015	6,056	4,006
01/01/2023	01:00:00	5	1	6	11	5	16	0	0	0.023	0.001	2,367	17,277	0.019	6,059	4.8
01/01/2023	02:00:00	4	1	6	13	5	16	0	0	0.022	0	2,385	19,488	0.017	6,073	5,184
01/01/2023	03:00:00	4	1	6	12	5	16	0	0	0.022	0	2,388	19,735	0.015	6,063	5,173
01/01/2023	04:00:00	4	1	7	12	5	16	0	0	0.022	0	2,393	19,894	0.017	6,076	5,379
01/01/2023	05:00:00	4	1	6	11	5	17	0	0	0.022	0.001	2,381	19,766	0.019	6,345	5,728
01/01/2023	06:00:00	4	1	6	12	5	16	0	0	0.022	0	2,362	19,545	0.018	7,809	5.76
01/01/2023	07:00:00	5	1	8	13	6	18	0	0	0.022	0	2,366	19,278	0.016	9,738	5,788
01/01/2023	08:00:00	6	1	8	12	6	18	0	0	0.022	0.001	2,321	17,462	0.018	7,978	5,958
01/01/2023	09:00:00	6	1	8	12	2	13	0	0	0.022	0	1,202	9,342	0.016	1,446	3,795
01/01/2023	10:00:00	2	1	6	11	1	11	0	0	0.016	0	0.723	10.054	0.016	0.053	1.214

Figure 3.15. Input data entry screen in HOPS.

HOPS currently supports the entry of up to twenty-three demand points, from which users must identify those that could be served by one or more hybrid modules. The criteria for selecting these demand points is thoroughly explained and developed in Section 3.2. From the total of twenty-three consumption points, up to three profiles can be analyzed simultaneously. These profiles can either be grouped together and assigned to a single hybrid module or allocated across three separate modules in parallel configurations. To streamline the process and minimize the need to navigate back to the inputs tab, drop-down menus are available, allowing for efficient selection of the desired profiles, as demonstrated in Figure 3.16.

Figure 3.16. HOPS interface for demand profiles selection.

Furthermore, a dedicated tab is included to graphically display the profiles, allowing users to assess their behaviour, identify usage patterns, and, at an early stage, pinpoint periods during the year when the hybrid module may experience higher demand or when a greater portion of the system's storage capacity might be needed. In addition to the visual representation, the tool provides monthly and annual values for each profile, as well as the percentage contribution of each demand relative to the total consumption of the three selected profiles.

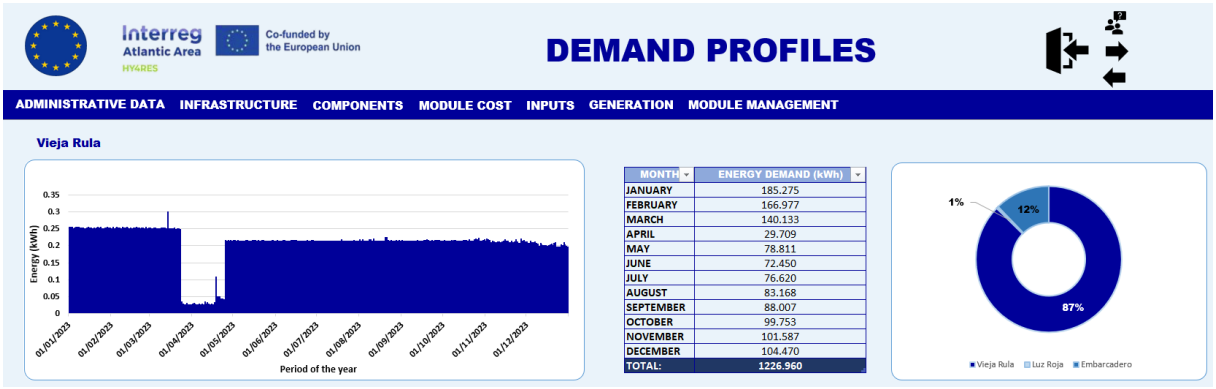

Figure 3.17. HOPS interface for demand profiles visualization.

As with the selected consumption points, the generation units offer a graphical representation of their profiles and the corresponding impact on the total system. The key difference is that, since a maximum of five energy production systems can be entered, there is no need for users to individually select each technology. Instead, all available generation sources are displayed within the interface. If fewer than five sources are utilized, any unfilled columns are automatically interpreted as representing zero production, maintaining the system's flexibility.

Regarding the selection of the tariff model, it is currently aligned with the structure established in Spain, requiring the input of period-specific electricity prices based on utility bills for each infrastructure. In scenarios where multiple consumption points are associated with different electricity providers, resulting in varying rates, either an average tariff must be calculated, or separate simulations should be conducted for each infrastructure. These values are critical, as they significantly influence the economic outputs of the analysis; therefore, their accurate definition is essential to properly assess the overall viability of the system's implementation. The tariff prices have been defined in Section 3.3 of this document.

3.4.2.2 System’s cost breakdown

After defining the inputs, along with their methods of entry, visualization, and interpretation, it becomes essential to focus on one of the key functionalities within HOPS: the ability to conduct a thorough economic breakdown of the hybrid module, providing a precise assessment of the system's actual cost. This breakdown is systematically organized into categories based on the various components, including generation units, energy storage systems, and auxiliary systems like the container structure, ensuring a detailed and transparent cost analysis.

The main objective of this section is to enable the user to define the cost of the hybrid module with the utmost accuracy, a critical factor in assessing the system's financial feasibility. The closer the estimated cost is to the actual value, the more reliable the calculation of return on investment periods will be. While this section is not formally categorized as an input, it essentially functions as one, as it contributes to the initial data necessary for deriving key final results. The reason for entering this data separately is to maintain a clean, user-friendly interface. Moreover, although this value is not directly involved in the energy scenario functionality, it represents an economic figure that must be recovered over the system’s lifetime and, while important, does not influence the analysis of the system's energy operation.

The cost breakdown is not merely intended to establish the final cost of the module, but also to define the system’s key characteristics through concise descriptions of each component, specifying their quantities and unit prices. Two dedicated cost breakdown sheets have been included, outlining the module pricing under two storage configurations: one utilizing the PAT system and the other employing an alternative battery-based storage solution.

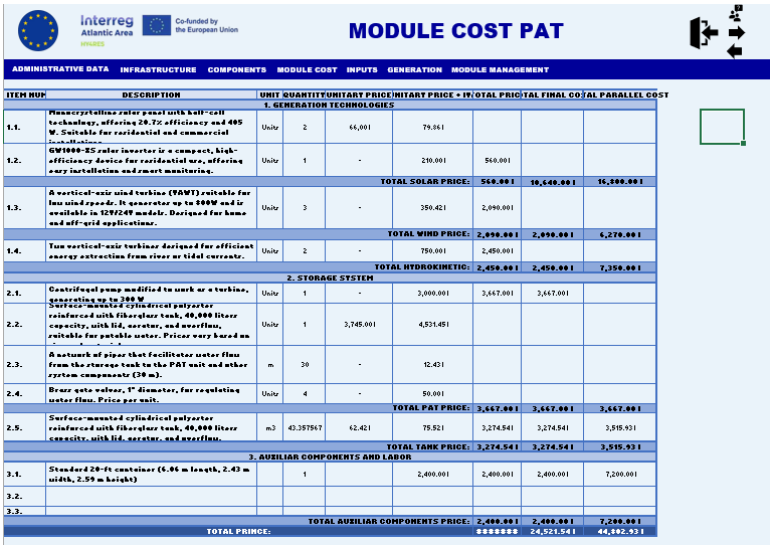

Figure 3.18. Detailed cost entry interface for the hybrid module components.

3.4.2.3 Outputs

After entering all the required parameters, the data must be validated and used to simulate a range of scenarios. Once the simulations are complete, it is crucial to synthesise the key outcomes from two

perspectives: energy performance and economic impact. To ensure the results are easily interpretable, they should be presented as clearly and graphically as possible. Considering that the analysis spans an entire year of hybrid module operation, the visualisation should not be confined to a single, static annual overview. Instead, it should allow for seamless, intuitive navigation across the full time period, enabling a detailed and dynamic exploration of the system's behaviour.

Regarding energy performance, a key initial metric to present, offering a first indication of the system's effectiveness, is the percentage or total amount of energy delivered exclusively by the generating units, without the contribution of any storage systems.

Once this initial ratio is determined, the analysis proceeds to evaluate the impact of the energy strategy when combined with the designed storage system. This evaluation quantifies the additional coverage achieved through storage and identifies the residual energy that must be imported from the grid when the hybrid module alone is insufficient to meet demand. Equally important as understanding the energy shortfall is assessing potential energy surpluses and defining an appropriate management strategy. The method chosen, whether injecting surplus energy into the grid or reallocating it to other infrastructures, will have a significant influence on both the financial performance and the overall sustainability of the system.

Figure 3.19 presents the visualisation of outputs generated by HOPS, offering users the ability to define the analysis period by selecting the start and end dates and times through dedicated input fields. Additionally, users can choose specific components of the hybrid module for display, facilitating a more focused review, particularly useful for detecting and diagnosing anomalies or inconsistencies identified at specific times of the year. Key metrics such as hours of energy coverage, the energy imports profile, and overall energy coverage are also available for display, further enhancing the dashboard's readability.

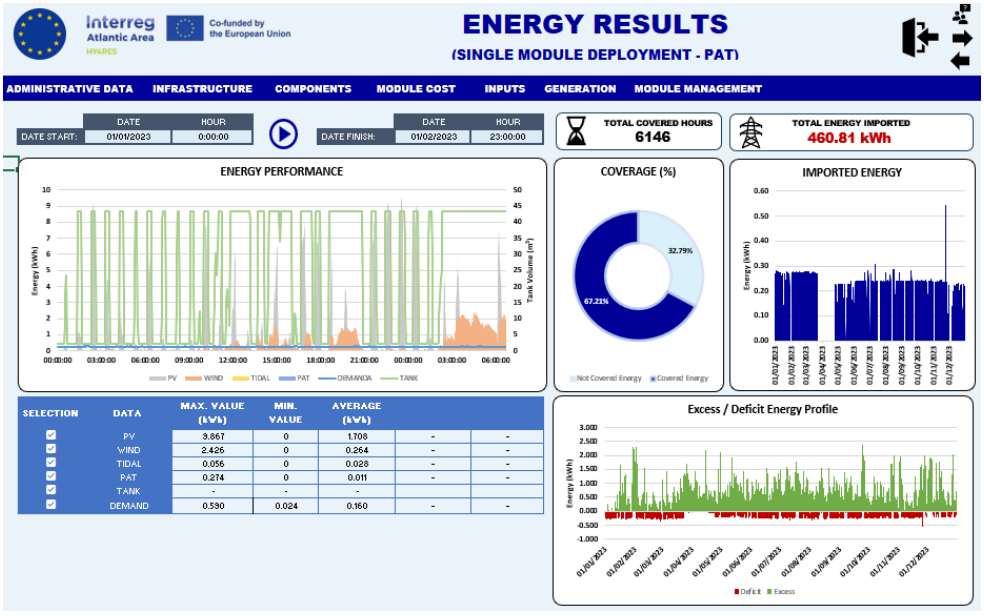

Figure 3.19. Energy results visualization screen.

In the same way that the detailed analysis of the hybrid module's energy performance is a defining feature of the tool, providing a comprehensive assessment of its economic viability is equally critical. To address this, a dedicated dashboard has been developed, displaying the projected economic recovery over a 25-year horizon, along with key financial indicators such as NPV, IRR, and payback period. These metrics are calculated based on annual energy revenues or savings, adjusted according to a discount rate that users can customise to suit the specific financial assumptions of their project. This section also incorporates the impact of the hybrid module's capital cost, which represents the principal investment to be recouped. Figure 3.20 provides an example of how the tool presents the financial performance results. The results shown in the previous figures are not representative; they are provided solely as an example to illustrate the appearance and capabilities of the tool.

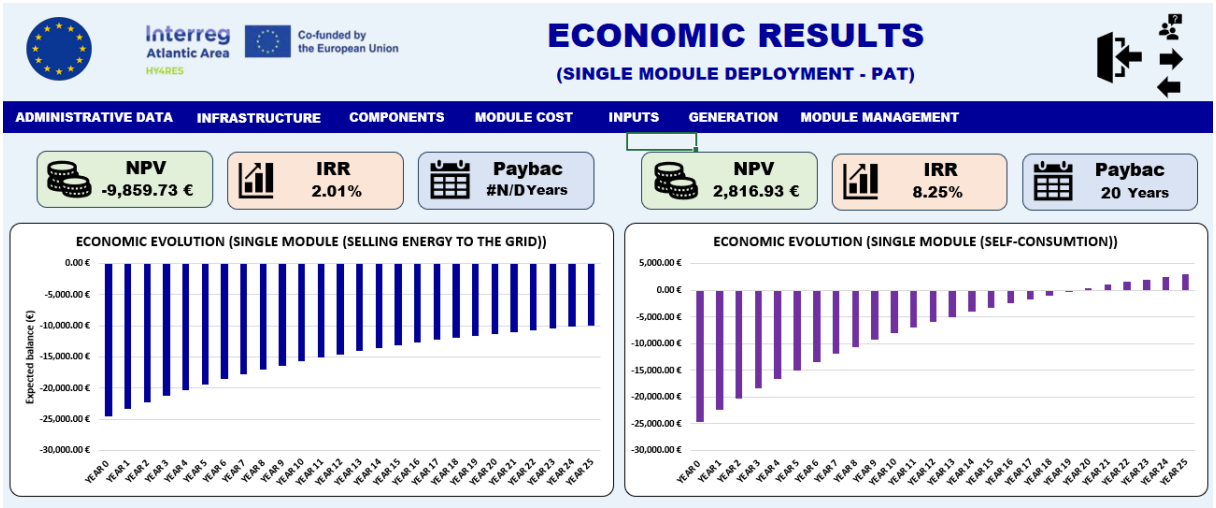

SINGLE MODULE - (SELLING ENERGY TO THE GRID)

YEAR	INVESTMENT	ENERGY COST REDUCTION (€)	ENERGY SELLINGS (€)	TOTAL PROFIT (€)	UPDATED TOTAL PROFIT (€)	ECONOMIC BALANCE END OF THE YEAR (€)
0	14,004.33	-	-	-	-	-14,004.33
1	-	134.57	843.43	977.99	914.01	-13,090.32
2	-	134.57	843.43	977.99	854.22	-12,236.10
3	-	134.57	843.43	977.99	798.33	-11,437.77
4	-	134.57	843.43	977.99	746.11	-10,691.66
5	-	134.57	843.43	977.99	697.29	-9,994.37
6	-	134.57	843.43	977.99	651.68	-9,342.69
7	-	134.57	843.43	977.99	609.04	-8,733.65
8	-	134.57	843.43	977.99	569.20	-8,164.45
9	-	134.57	843.43	977.99	531.96	-7,632.49
10	-	134.57	843.43	977.99	497.16	-7,135.32
11	-	134.57	843.43	977.99	464.64	-6,670.69
12	-	134.57	843.43	977.99	434.24	-6,236.45
13	-	134.57	843.43	977.99	405.83	-5,830.62
14	-	134.57	843.43	977.99	379.28	-5,451.33
15	-	134.57	843.43	977.99	354.47	-5,096.86
16	-	134.57	843.43	977.99	331.28	-4,765.58
17	-	134.57	843.43	977.99	309.61	-4,455.98
18	-	134.57	843.43	977.99	289.35	-4,166.62
19	-	134.57	843.43	977.99	270.42	-3,896.20
20	-	134.57	843.43	977.99	252.73	-3,643.47
21	-	134.57	843.43	977.99	236.20	-3,407.27
22	-	134.57	843.43	977.99	220.75	-3,186.53
23	-	134.57	843.43	977.99	206.30	-2,980.22
24	-	134.57	843.43	977.99	192.81	-2,787.41
25	-	134.57	843.43	977.99	180.19	-2,607.22

SINGLE MODULE - (SELF-CONSUMPTION)

YEAR	INVESTMENT	ENERGY COST REDUCTION (€)	ENERGY REDIRECTED (€)	TOTAL PROFIT (€)	UPDATED TOTAL PROFIT (€)	ECONOMIC BALANCE END OF THE YEAR
0	14,004.33	-	-	-	-	-14,004.33
1	-	134.57	1,639.87	1,774.44	1,658.35	-12,345.98
2	-	134.57	1,639.87	1,774.44	1,549.86	-10,796.12
3	-	134.57	1,639.87	1,774.44	1,448.47	-9,347.65
4	-	134.57	1,639.87	1,774.44	1,353.71	-7,993.94
5	-	134.57	1,639.87	1,774.44	1,265.15	-6,728.79
6	-	134.57	1,639.87	1,774.44	1,182.38	-5,546.41
7	-	134.57	1,639.87	1,774.44	1,105.03	-4,441.38
8	-	134.57	1,639.87	1,774.44	1,032.74	-3,408.64
9	-	134.57	1,639.87	1,774.44	965.18	-2,443.47
10	-	134.57	1,639.87	1,774.44	902.03	-1,541.44
11	-	134.57	1,639.87	1,774.44	843.02	-698.41
12	-	134.57	1,639.87	1,774.44	787.87	89.46
13	-	134.57	1,639.87	1,774.44	736.33	825.78
14	-	134.57	1,639.87	1,774.44	688.16	1,513.94
15	-	134.57	1,639.87	1,774.44	643.14	2,157.08
16	-	134.57	1,639.87	1,774.44	601.06	2,758.14
17	-	134.57	1,639.87	1,774.44	561.74	3,319.88
18	-	134.57	1,639.87	1,774.44	524.99	3,844.87
19	-	134.57	1,639.87	1,774.44	490.65	4,335.52
20	-	134.57	1,639.87	1,774.44	458.55	4,794.07
21	-	134.57	1,639.87	1,774.44	428.55	5,222.62
22	-	134.57	1,639.87	1,774.44	400.51	5,623.13
23	-	134.57	1,639.87	1,774.44	374.31	5,997.44
24	-	134.57	1,639.87	1,774.44	349.82	6,347.27
25	-	134.57	1,639.87	1,774.44	326.94	6,674.20

Figure 3.20. Hybrid module economic results interface.

Chapter 4

Single Module Deployment – Case Study

In this chapter, two distinct scenarios are presented to analyse the performance of a single hybrid module: one utilizing a pump-as-turbine system as the energy storage technology, and the other replacing it with a battery storage system. Each scenario outlines the key equations governing system operation, as well as the optimization strategy employed to maximize overall efficiency. Finally, the resulting outcomes are presented, highlighting which of the two scenarios offers more favourable results from both an energy and economic perspective.

4.1 Scope and objectives of the simulated scenarios

Following the description of the methodology used to define the key input parameters and the development of the simulation tool, the analysis focuses on evaluating the performance of the hybrid module through two case studies: standalone operation and parallel deployment. The first case study investigates the optimal utilisation of resources when the hybrid module operates independently. Various energy storage configurations are assessed, beginning with a pump-as-turbine system and subsequently incorporating battery storage. This analysis aims to determine the most effective configuration to enhance overall system performance, identify the setup that offers the greatest contribution to project feasibility, and define the most optimised version of the hybrid module.

4.2 Scenario 1: single hybrid module with PAT system

4.2.1 Hybrid module operational strategy and energy management

Scenario 1 is developed based on the initial system configuration, which integrates a PAT setup as the designated energy storage solution. As previously described, the analytical framework for all scenarios is structured around an energy balance between the renewable energy generated by the hybrid module and the hourly demand of the selected consumption points. This initial balance enables the identification of the system's energy coverage potential in the absence of storage systems and without the application of energy management strategies. The assessment follows the formulation defined by Equation (4.1), offering a baseline characterisation of energy surpluses and deficits across the system.

$$E_{NET,t} = \left(E_{PV,t} + E_{WIND,t} + E_{HYDRO,t}\right) - E_{LOAD,t} \quad (4.1)$$

$E_{NET,t}$ corresponds to the net energy balance in (kWh) for a specific time period, $E_{PV,t}$, $E_{WIND,t}$ and $E_{HYDRO,t}$ show the energy production for PV, wind and hydrokinetic sources in (kWh), and $E_{LOAD,t}$ corresponds to the demand also in (kWh). This preliminary energy balance is a key step, as it will help to inform the subsequent sizing of the storage system by identifying the magnitude and timing of surplus energy remaining after the net difference between generation and demand is established. For the system to operate efficiently, it is necessary to define a prioritisation strategy that ensures surplus energy is allocated in a structured and optimised manner, aligned with the specific requirements of each scenario. At this stage, two critical components are introduced: the storage systems and the potential contribution of the electrical grid. The grid functions as a secondary source, supplying energy during periods when neither the renewable generation nor the PAT system can fully meet the demand.

The use of pumped storage as an energy buffering solution requires careful consideration of the conversion between electrical energy and hydraulic volume. In this approach, excess electricity is used to elevate water into a storage tank, effectively storing energy as gravitational potential. However, this process entails the physical movement of water through a hydraulic circuit, comprising pumps, pipelines, and valves, during both charging and discharging phases. Due to the mechanical nature of the system,

it is subject to various inefficiencies, including frictional losses, pressure drops, and conversion losses. As a result, only a portion of the surplus energy can be effectively stored and later recovered.

In this context, system efficiency plays a critical role, as higher efficiency enables a greater proportion of surplus energy to be stored and used. This consideration is essential for effective system operation and energy management. Since energy surpluses, $E_{Sur,t}$, are expressed in kWh, the hybrid module's simulation and control model must be capable of translating these values into corresponding volumes of water. To facilitate this, the use of Equation (4.2) is proposed, which establishes a relationship between the energy and key physical parameters such as water volume, V in (m^3), fluid density, ρ in (kg/m^3), gravitational acceleration, g in (m/s^2), and head height, H in (m). This equation is a fundamental component in the design and analysis of pumping systems and has been widely adopted in previous studies **[30] [31]**.

$$E_{Sur,t} = \eta_{PAT} \cdot \rho \cdot g \cdot V \cdot H \tag{4.2}$$

To maintain consistency across the model and ensure clarity in result interpretation, energy values are standardised in kWh. Since Equation (4.2) expresses energy in joules, a unit conversion is necessary to align with this convention. By rearranging the equation to isolate the water volume, a revised formulation is obtained that incorporates the appropriate conversion factor, allowing for accurate translation of energy surpluses or deficits into hydraulic volumes while preserving unit coherence throughout the system, including the PAT system efficiency, η_{PAT}, in the calculation process.

$$V = \frac{E_{Sur,t} \cdot 3.6 \cdot 10^6}{\eta_{PAT} \cdot \rho \cdot g \cdot H} \tag{4.3}$$

Prior to defining the operational methodology of the hybrid module for this scenario, it is essential to establish a set of initial conditions that will serve as the reference point for all subsequent time steps within the analysis period. For the purposes of this study, the system is assumed to commence operation with the storage tank at 50% of its total capacity, irrespective of its final sizing. Moreover, a minimum operational threshold is imposed, whereby the tank must always retain at least 5% of its volume. This constraint is intended to safeguard system components, extend their operational lifespan, and protect the system from hydrodynamic phenomena like cavitation. The available hydraulic head is also predefined, set at 5 metres for this scenario. It is important to emphasise that these parameters can be manually adjusted within the software, allowing users to tailor the model to the specific characteristics and constraints of their system. The values presented here represent the configuration adopted for the present case study.

In light of the aforementioned conditions, energy management in this scenario is divided into four distinct phases: (1) tank charging, (2) energy demand and discharge from the tank, (3) evaluation of the achieved energy coverage, and (4) determination of the final storage state or remaining volume.

4.2.1.1 Tank charging

Determining when the storage tank can be charged begins with referencing the initial energy balance defined in Equation (4.1). This balance serves as the key indicator of whether surplus energy is available

for storage or if a deficit must be covered using the tank's reserves. Within the simulation and optimisation framework, system operation adheres to a core principle: surplus energy shall not be exported unless the storage tank has reached its maximum capacity. This approach reflects the system's overarching objective of maximising energy self-sufficiency and minimising reliance on external sources.

To enable the management model to determine tank charging and surplus energy allocation, a set of governing equations has been defined. These ensure proper operation of the hybrid module according to the available energy at each time step. The formulation differs between the initial hour, which relies on predefined conditions, and subsequent hours, which depend on the preceding system state. Since charging must be interpreted in both energy and volume terms, the conversion in Equation (4.3) is applied.

$$V_{fill,0} = \begin{cases} \left|\frac{E_{NET,0} \cdot 3{,}600{,}000}{\rho \cdot g \cdot H}\right|, & if\ E_{NET,0} > 0\ and\ \left|\frac{E_{NET,0} \cdot 3{,}600{,}000}{\rho \cdot g \cdot H} + V_{max} \cdot \frac{V_{50\%}}{100}\right| < V_{max} \\ 0, & otherwise \end{cases} \quad (4.4)$$

$V_{fill,0}$ denotes the water volume allocated to the tank in the initial time step (m³), V_{max} the maximum tank capacity (m³), $V_{50\%}$ refers to the 50% of tank capacity (m³) and $E_{NET,0}$ corresponds to the net energy balance at the initial time step (kWh). Equation (4.4) specifies that when the initial energy balance is positive and the combined volume of the storable surplus and the initial tank level remains within the tank's maximum capacity, the full surplus volume is stored. If either condition is not met, no energy is allocated to the tank, and storage remains unchanged.

For all subsequent time steps, the same logic applies but is adapted to the system's evolving state. Tank charging depends on the residual volume from the previous hour, and the surplus energy generated in the current hour. However, full utilisation is possible only when the surplus does not exceed the remaining capacity; otherwise, only the storable portion is used, with any excess managed according to the predefined strategy. This charging logic for successive hours is formalised in Equation (4.5).

$$V_{fill,t} = \begin{cases} \left|\frac{E_{NET,t} \cdot 3{,}600{,}000}{\rho \cdot g \cdot H}\right|, & if\ E_{NET,t} > 0\ and\ \left|\frac{E_{NET,t} \cdot 3{,}600{,}000}{\rho \cdot g \cdot H}\right| + V_{rem,t-1} < V_{max} \\ V_{max} - V_{rem,t-1}, & if\ E_{NET,t} > 0\ and\ \left|\frac{E_{NET,t} \cdot 3{,}600{,}000}{\rho \cdot g \cdot H}\right| + V_{rem,t-1} > V_{max} \\ 0, & if\ E_{NET,t} \leq 0 \end{cases} \quad (4.5)$$

In this equation, $V_{fill,t}$ corresponds to the volume of water assigned to fill the tank at a specific time step (m³), $E_{NET,t}$ refers to the net energy balance at that specific time step (kWh) and $V_{rem,t-1}$ indicates the remaining volume in the tank from the previous time step (m³). All other variables retain the definitions provided in the preceding equations.

4.2.1.2 Energy demand and discharge from the tank

While tank loading serves as a cornerstone in defining the energy model, robust deficit management is equally essential to ensure reliable operation of the hybrid system. In periods of insufficient renewable generation, the PAT system must be leveraged to deliver the maximum feasible energy output, all while preserving the technical integrity and economic viability of the overall configuration.

Before assessing the extent to which the storage system can compensate for the energy deficit, it is crucial to first evaluate the actual volume demand, factoring in the inherent inefficiencies of the system. As previously discussed, various loss factors within the PAT system can significantly impact performance. These must be thoroughly accounted for to ensure the accuracy of all estimations and to prevent operational misjudgements that could compromise the reliability of the results.

To accurately reflect system inefficiencies, the efficiency parameter is incorporated into the calculation of the water volume required to cover the energy deficit for a given hour. For instance, if the system operates at 60% efficiency, a proportionally higher volume of water must be discharged from the tank to deliver the required energy output. This efficiency factor, along with other critical parameters such as hydraulic head, is fully configurable by the user, ensuring adaptability to a wide range of system specifications. The quantitative relationship between water volume required, $V_{need,t}$ (m^3), and net energy is formalised through Equation (4.6).

$$V_{need,t} = \begin{cases} \left| \frac{E_{NET,t} \cdot 3{,}600{,}000}{\eta_{PAT} \cdot \rho \cdot g \cdot H} \right|, & E_{NET,t} < 0 \\ 0, & otherwise \end{cases} \quad (4.6)$$

Once the water volume necessary to cover the rest of the demand is defined, the discharge volume, $V_{disch,0}$ (m^3), for the initial time step and, $V_{disch,t}$ (m^3), for subsequent ones, must be determined to generate energy through the turbine. This discharge depends on the storage level at each step and must respect the user-defined minimum threshold, $V_{5\%}$ (m^3). The conversion from energy deficit to water volume remains constant, as it is independent of the tank's state. Moreover, discharge behaviour differs between the first hour and later steps: the initial condition follows user-defined parameters, Equation (4.7), while subsequent discharges depend on the storage level from the preceding hour, Equation (4.8).

$$V_{disch,0} = \begin{cases} V_{need,0} & , \quad if\ V_{max} \cdot \left(\frac{V_{50\%}}{100}\right) \geq V_{need,0}\ and\ V_{max} \cdot \left(\frac{V_{50\%}}{100}\right) - V_{need,0} > V_{max} \cdot \left(\frac{V_{5\%}}{100}\right) \\ V_{max} \cdot \left(\frac{V_{50\%}}{100}\right) - V_{max} \cdot \left(\frac{V_{5\%}}{100}\right), & otherwise \end{cases} \quad (4.7)$$

$$V_{disch,t} = \begin{cases} 0 & , if\ V_{rem,t-1} = V_{max} \cdot \left(\frac{V_{5\%}}{100}\right)\ or\ E_{NET,t} \leq 0 \\ V_{need,t} & , if\ V_{rem,t-1} - V_{max} \cdot \left(\frac{V_{5\%}}{100}\right) \geq V_{need,t} \\ V_{rem,t-1} - V_{max} \cdot \left(\frac{V_{5\%}}{100}\right) & , \ if\ \left(V_{need,t} > V_{rem,t-1}\ or\ V_{rem,t-1} - V_{max} \cdot \left(\frac{V_{5\%}}{100}\right) < V_{need,t}\right) and\ V_{rem,t-1} \geq V_{max} \cdot \left(\frac{V_{5\%}}{100}\right) \end{cases} \quad (4.8)$$

4.2.1.3 Evaluation of the achieved energy coverage

Once the tank's charging and discharging dynamics have been defined, the next step is to assess the system's energy balance following the operation of the PAT system. This evaluation determines whether the energy supplied by the storage system is sufficient to meet the previously identified deficit, or if a residual shortfall must be covered by the electricity grid. The analysis involves comparing the estimated energy demand with the energy equivalent of the volume discharged from the tank. This is achieved through a volume-to-energy conversion, ensuring that the discharged volume corresponds accurately to the initial deficit. The process is formally controlled by Equation (4.9), defining the energy in terms of volume, $V_{cov,t}$ (m^3), that cannot be covered through the storage system.

$$V_{cov,t} = \begin{cases} V_{need,t} - V_{disch,t}, & if\ V_{need,t} > V_{disch,t} \\ 0, & if\ V_{need,t} \leq V_{disch,t} \end{cases} \quad (4.9)$$

4.2.1.4 Determination of the final storage state

Ultimately, defining the final state of the tank after the charging and discharging processes is critical, as each time step is intrinsically linked to the previous one and the available storage at the end of a given hour, $V_{rem,0}$ (m³) for the initial time step, and $V_{rem,t}$ (m³) for the following ones, determines the operational flexibility for the next. Although the model's logic has been presented in a structured sequence, with the final volume determination appearing as the last phase, it is important to recognize that the system functions through continuous, bidirectional interactions. Therefore, the sequence serves more as a conceptual framework than a rigid procedural order. Among all components of the model, the control of the final tank state is the most complex, requiring the greatest number of equations, as it must dynamically account for both energy surpluses and deficits across all time steps, as can be seen in Equations (4.10) and (4.11).

$$V_{rem,0} = \begin{cases} V_{max} \cdot \left(\frac{V_{50\%}}{100}\right) + V_{fill,0} & , if\ V_{fill,0} > 0 \\ V_{max} \cdot \left(\frac{V_{50\%}}{100}\right) - V_{need,0} & , if\ V_{max} \cdot \left(\frac{V_{50\%}}{100}\right) - V_{need,0} \geq V_{max} \cdot \left(\frac{V_{5\%}}{100}\right) \\ V_{max} \cdot \left(\frac{V_{5\%}}{100}\right) & , if\ V_{max} \cdot \left(\frac{V_{50\%}}{100}\right) - V_{need,0} < V_{max} \cdot \left(\frac{V_{5\%}}{100}\right) \\ V_{max} \cdot \left(\frac{V_{50\%}}{100}\right) + V_{fill,0} - V_{need,0} & , if\ V_{max} \cdot \left(\frac{V_{50\%}}{100}\right) + V_{fill,0} - V_{need,0} < V_{max} \\ V_{max} & , if\ V_{max} \cdot \left(\frac{V_{50\%}}{100}\right) + V_{fill,0} - V_{need,0} \geq V_{max} \end{cases} \quad (4.10)$$

$$V_{rem,t} = \begin{cases} V_{max} \cdot \left(\frac{V_{5\%}}{100}\right) & , if\ V_{rem,t-1} + V_{fill,t} - V_{need,t} \leq V_{max} \cdot \left(\frac{V_{5\%}}{100}\right) \\ V_{rem,t-1} + V_{fill,t} - V_{need,t} & , if\ V_{rem,t-1} + V_{fill,t} - V_{need,t} < V_{max} \\ V_{max} & , if\ V_{rem,t-1} + V_{fill,t} - V_{need,t} \geq V_{max} \end{cases} \quad (4.11)$$

4.2.2 Surplus energy management strategies

The operation of the hybrid module may encounter periods when demand exceeds system capacity, requiring grid support to ensure supply, as well as periods of surplus that surpass the tank's storage capacity. In the latter case, alternative management strategies are needed to maximize system benefits beyond cost reduction. Two main approaches are considered: selling the surplus to the grid or redistributing it to other buildings in the port complex. This section examines both strategies as a basis for identifying the option that best aligns with system objectives and delivers the greatest benefit.

4.2.2.1 Grid export

Efficient surplus energy management is critical to optimizing the financial performance of energy projects and shortening the return on investment period. A particularly promising strategy involves selling excess energy, those amounts not captured by the storage system, to the grid. This enables to create an additional revenue stream and enhances overall project profitability.

Surplus energy fed into the grid is typically compensated at rates lower than the retail purchase price. Therefore, selecting an energy off-taker that offers the most favourable compensation rate is essential to maximizing the economic viability of this strategy. In the context of the current case study, the assumed sale price is based on the simplified compensation mechanism applicable to grid-connected self-consumption photovoltaic systems in Spain. This mechanism generally offers compensation in the range of 0.05 €/kWh to 0.10 €/kWh. For modelling purposes, a representative midpoint value of 0.07 €/kWh has been adopted.

To clarify the relationships and energy flows between the various agents involved in this scheme, a flow diagram has been developed and is presented in Figure 4.1.

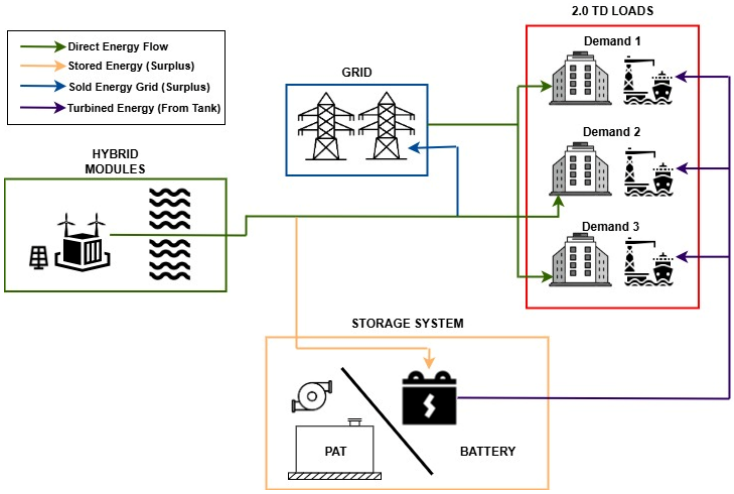

Figure 4.1. Directional energy flow for strategic selling of surplus energy using.

To evaluate the effectiveness of the proposed strategy, a comprehensive economic model has been developed. This model quantifies, first, the annual cost savings achieved through reduced electricity purchases, based on the tariff structure detailed in the methodology section. Second, it estimates the additional revenue generated from the sale of surplus energy to the grid, providing a complete picture of the strategy's financial impact.

The annual cost savings and revenue from surplus energy sales serve as the primary indicators of the strategy's economic performance, directly influencing the investment's payback period. In this study, financial projections are extended over a 25-year horizon, aligned with the estimated operational lifespan of the hybrid module.

Although savings and income are treated as constant on a yearly basis, their present value must be adjusted using a discount rate to accurately reflect long-term evolution. To accommodate varying financial scenarios, the model includes a user-defined discount rate, ensuring flexibility not only in energy management but also in the economic assessment.

The economic model, which determines the financial benefits based on the selected strategy, includes the calculation of three critical parameters to assess the project's financial viability: NPV, IRR, and payback period. These metrics provide a comprehensive evaluation of the project's potential for long-term success.

NPV in (€), derived from the Equation (4.12), is a crucial indicator for assessing the profitability of an investment. It evaluates the expected future cash flows, C_t in (€), and discounts them to their present value using a specified rate, r, providing insight into whether the investment will generate a profit or incur a loss.

$$NPV = \sum_{t=0}^{n} \frac{C_t}{(1+r)^t} \tag{4.12}$$

Referring to the IRR, as defined by Equation (4.13), this metric represents the interest rate at which the NPV equals zero. In other words, it signifies the rate at which the investment would neither generate a profit nor incur a loss, indicating a break-even point.

$$0 = \sum_{t=0}^{n} \frac{C_t}{(1+IRR)^t} \tag{4.13}$$

Finally, the discounted payback period shows the time needed to recover the initial investment, considering the time value of money. It is determined by identifying the year in which the cumulative discounted cash flows exceed the initial investment.

4.2.2.2 Inter-building energy redistribution

By analysing the energy purchase prices across different periods and tariff models, as detailed in the methodology section, in conjunction with the average energy sale price estimated in Section 4.2.2.1, it has been determined that an alternative approach could potentially optimize the benefits from surplus energy management.

Considering the relatively low energy sale price and the structure of tariffs such as 3.0TD, where, during certain periods, energy purchase costs can exceed the sale price by up to threefold, an effective strategy would be to redirect surplus energy to high-demand areas within the port. This would significantly enhance economic savings by maximizing self-consumption where the cost differential is greatest. Additionally, this approach would reduce reliance on the external grid, leading to fewer transactions between the hybrid module and the network. As a result, it would not only lower emissions but also decrease grid demand for both the targeted infrastructures and other buildings subject to the 3.0TD tariff, amplifying the overall environmental and economic benefits.

Taking into account the specific modification of reallocating surplus energy, the remaining calculations from the previous strategy will remain unchanged. The same evaluation criteria and performance indicators will be applied to assess the viability of this revised approach, once all technical and economic parameters of the case study have been defined. Figure 4.2 illustrates the updated flow graphic, outlining the operational adjustment incorporated into the strategy.

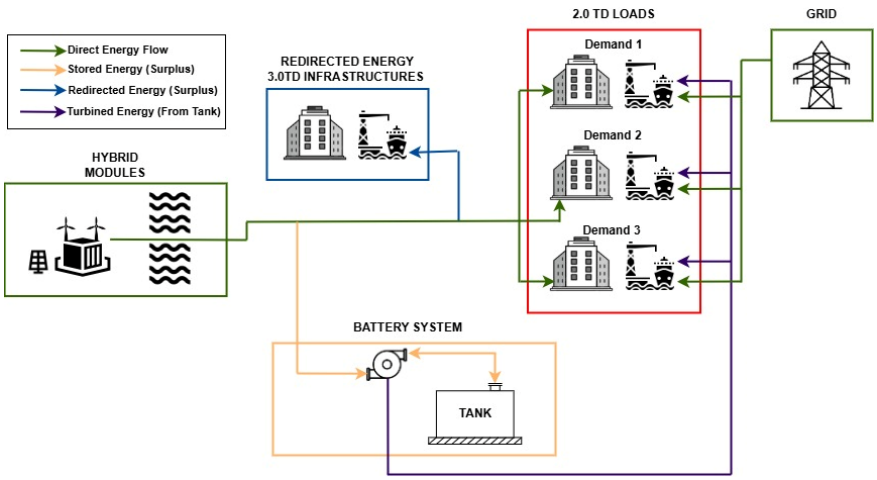

Figure 4.2. Directional energy flow for strategic redistribution under 3.0TD tariff, using PAT system.

It is important to note that these two surplus management strategies will be applied consistently across all scenarios. Therefore, from this point onward, only the economic outcomes resulting from the implementation of both strategies will be presented, with an emphasis on identifying the most advantageous option in each case.

4.2.3 Optimization process

HOPS is designed as a flexible tool for both energy and economic management and analysis, allowing users to explore a wide range of variables when evaluating the implementation of the hybrid module. This flexibility enables users to tailor the system to specific applications by identifying the most suitable configuration. However, this iterative process can often become time-consuming and labour-intensive, as relying solely on trial-and-error makes it difficult to determine whether the optimal solution has truly been achieved. To address this challenge, the tool incorporates a built-in optimization algorithm that systematically identifies the technical configuration that delivers the greatest overall benefit.

The optimization process is implemented using Microsoft Excel's integrating the Solver tool, which provides a robust framework for analytical decision-making. Solver enables users to define a clear objective function, identify the key decision variables subject to adjustment, and impose scenario-specific constraints that delineate the feasible solution space. This approach ensures that the optimal configuration is systematically determined, aligned with the technical and operational requirements of each case.

Economic viability is a fundamental requirement; therefore, HOPS is designed to maximize net return over a 25-year period, consistent with the expected operational lifespan before component replacement or decommissioning. As outlined earlier, the model incorporates a section to define total capital cost, which serves as the benchmark for investment recovery. In the present case, this cost cannot exceed 25,000 €, the maximum budget available for system development. This financial limit constitutes the first constraint, directly shaping the number and capacity of components that can be installed.

Nevertheless, the existence of a maximum budget does not guarantee that the entire amount can be

allocated in every scenario, as additional constraints may limit investment potential. A key limiting factor is the availability of usable space, which varies depending on the characteristics of each project. In some cases, ample space allows for full utilization of the allocated budget without restriction. In other situations, spatial limitations become a decisive factor, constraining the scale of the installation and, consequently, the extent of the financial investment.

While these two factors primarily define the optimization boundaries, they are not the only ones. By analysing the individual costs of each installed technology, an economic ratio expressed in euros per kilowatt-hour (€/kWh) has been derived. Equation (4.14) exemplifies how this ratio has been calculated for the solar photovoltaic section, PV_{ratio}, where $Cost_{PV}$ refers to the cost of installation in (€), Gen_{PV} to the energy generated through the PV system (kWh), and $Years$ to the applicable time period.

$$PV_{ratio} = \frac{Cost_{PV}}{Gen_{PV} \cdot Years} \tag{4.14}$$

The objective of defining this ratio is to identify the most cost-effective generation-to-investment ratio for each technology. Based on this, the system assigns a multiplier to each technology, determining the optimal allocation of each energy source to maximize returns, while ensuring adherence to both economic and spatial constraints. These multipliers are dynamic parameters within the optimization algorithm, continually adjusted in accordance with the established limits. The application of these multipliers directly influences the initial economic structure, as the cost of each component within the hybrid system is recalibrated individually, in line with these multipliers.

Up to this point, the constraints addressed have primarily related to external or economic-based limitations rather than the functional performance of the hybrid module. A central objective of the system, however, is to significantly reduce dependence on the electrical grid. To support this aim, the module must be capable of covering at least 70% of total energy demand within the scenario, either through direct renewable generation or via stored energy.

Given that the optimization algorithm is structured to prioritize long-term economic return, it is essential to define minimum contribution thresholds for both generation and storage, for example, 60% from renewable sources and 10% from the storage system. These parameters are crucial: without them, the algorithm would naturally select only the lowest-cost generation option, typically excluding storage due to its higher unit cost. This would result in considerable daytime energy surplus that cannot be utilized at night, thereby increasing grid reliance and underutilizing the storage system. Consequently, storage would have minimal impact on the system's performance, limiting any meaningful evaluation of its value, an outcome that would undermine the purpose of the hybrid design at this stage.

Another adjustable parameter, tailored to align with the defined constraints, is the storage tank capacity. Its volume is calibrated to fulfill the minimum contribution percentage specified in the system requirements. For a clear understanding, Figure 4.3 presents a comprehensive breakdown of the core parameters identified as key drivers in the scenario optimization process.

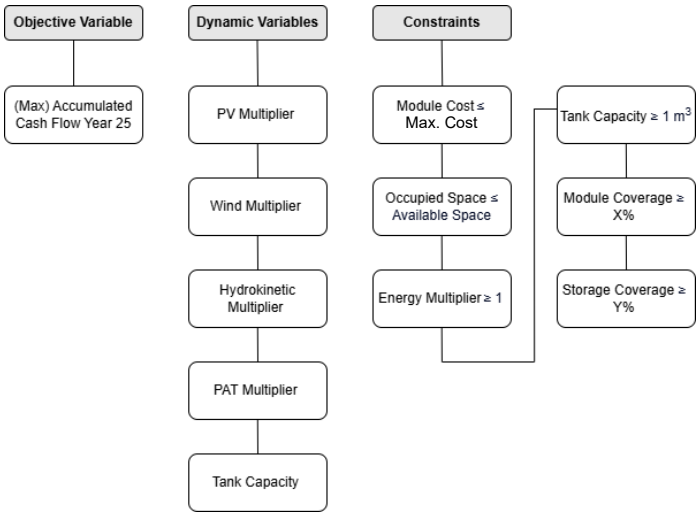

Figure 4.3. Main parameters and structural overview of the optimization system.

4.2.4 Scenario 1: Results and discussion

With the operational framework of the model for Scenario 1 fully defined, the resulting performance outcomes are now presented. To highlight the effectiveness of the system's optimization process and the influence of surplus management strategy selection, the analysis begins with an assessment of the hybrid module in its initial, non-optimized configuration. This baseline is then compared to the optimized solution identified by the tool as the most efficient and cost-effective option.

4.2.4.1 Baseline results

Establishing a reliable baseline performance is a critical step in evaluating the effectiveness of any subsequent enhancements to a technological system. In this section, the baseline scenario has been defined by setting all energy multipliers across the various generation sources to one. This configuration ensures that the system's energy performance is assessed in its original, unaltered state, providing a consistent reference point for future comparative analyses.

Since the optimal storage tank capacity for maximizing both energy coverage and economic return has not yet been established, a preliminary volume of 10 m³ was selected for this initial assessment. Under these baseline conditions, the hybrid module demonstrates encouraging performance: in the absence of storage, demand coverage reaches 56.42% (792.73 kWh), whereas total system generation amounts to 3,340.42 kWh, leaving 76.27% unallocated. Consequently, a significant portion of generated energy is not immediately used, highlighting the potential benefits of integrating storage solutions.

Subsequently, the introduction of the PAT system produces a moderate increase in demand coverage, improving it by 1.77% (24.88 kWh). Nevertheless, accounting for system inefficiencies reduces the theoretical improvement of 40.17 kWh by 15.29 kWh, underscoring the importance of considering energy losses when evaluating storage performance. Overall, the total cost of the hybrid module under these preliminary conditions is 11,922.24 €, providing a reference point for subsequent optimization of tank capacity and system configuration.

Table 4.1. Preliminary parameters and results of the hybrid module.

Tank Capacity	Module Cost	Coverage Renewable	Coverage PAT	Total Generation Capacity
10 m^3	11,922.24 €	56.42% (792.73 kWh)	1.77% (24.88 kWh)	3,340.42 kWh

To provide a comprehensive evaluation of the hybrid system's performance under varying operational conditions, two one-week periods have been selected to represent distinct seasonal contexts, referring to winter and summer. This approach enables the assessment of the storage technology's contribution to overall system efficiency, while also examining the module's adaptability to seasonal variations in energy demand profiles.

Figure 4.4 illustrates the operation of the hybrid energy system over a representative week in January, showing the contribution of each technology relative to real-time demand. As typical for winter months, photovoltaic output is substantially reduced due to lower solar irradiance, shifting the system's reliance toward wind energy, which provides the majority of renewable surplus during this period. However, the intermittent nature of wind introduces variability, and during low-generation intervals, the electrical grid must supply additional energy to consistently meet demand. These results highlight the seasonal interplay between renewable sources and the grid, emphasizing the value of diversified generation and robust grid interaction for reliable hybrid system operation. Notably, exports are minimal during this period, indicating that most generation is directed toward self-consumption.

Regarding storage operation, Figure 4.4 shows that tank volume remains at or near its minimum for a substantial portion of the week, reflecting prolonged periods when renewable generation is insufficient and frequent discharge is required to cover deficits. Nonetheless, the rapid depletion of stored energy suggests that the current tank capacity may be undersized relative to operational needs. Conversely, during periods of surplus generation, the system demonstrates an effective charging response, capturing excess energy in alignment with peak production intervals. Overall, while the control strategy functions as intended, increasing storage capacity could significantly enhance the effectiveness of the system.

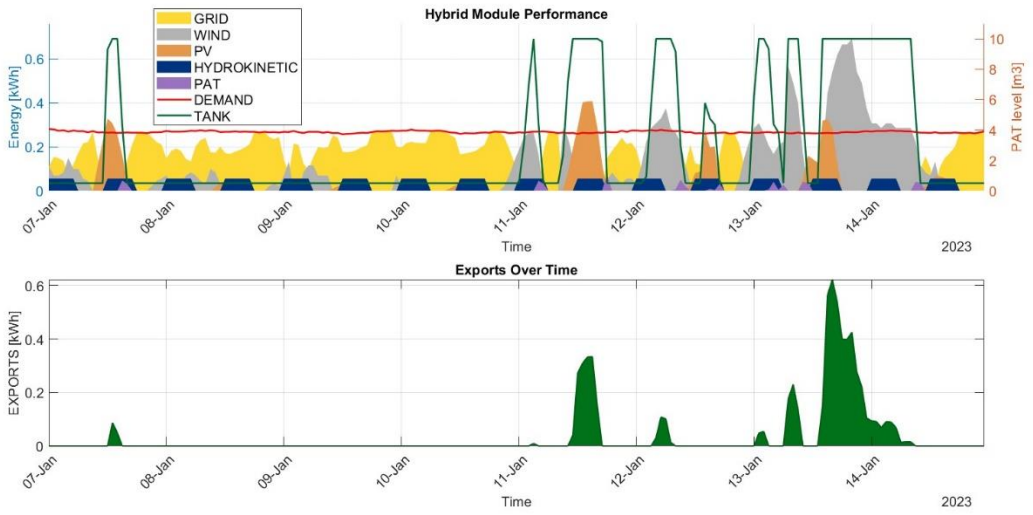

Figure 4.4. Hybrid module performance over a representative winter week (baseline configuration).

The second period analysed, corresponding to the summer season, demonstrates a markedly different operational profile compared to winter. The most notable distinction lies in the demand pattern. As illustrated in Figure 4.4, winter demand remains relatively stable throughout the day and night, showing minimal variation. In contrast, summer demand exhibits pronounced fluctuations between daytime and nighttime hours, with a significant share of consumption occurring at night, precisely when photovoltaic generation is unavailable. This shift significantly increases the system's reliance on energy storage, which becomes essential for maintaining supply during periods of low or zero solar production. In this context, the storage unit plays a vital role in meeting nighttime demand and ensuring overall system balance.

The combination of low daytime demand and high solar generation, coupled with a relatively limited storage capacity, elevates the significance of the selected surplus management strategy, particularly during the summer months, as reflected in the number of exports observed in Figure 4.5. Under these conditions, the strategy assumes a pivotal role in maintaining operational efficiency. The storage unit's charge and discharge cycles respond effectively to the dynamic interplay between generation and consumption. The abundance of daytime generation enables frequent charging, thereby reducing the duration during which the storage remains at minimum levels. However, the limited capacity of the tank imposes a constraint: deep discharges remain inevitable, underscoring the need for either increased storage capacity or complementary strategies to enhance energy availability during periods of low generation.

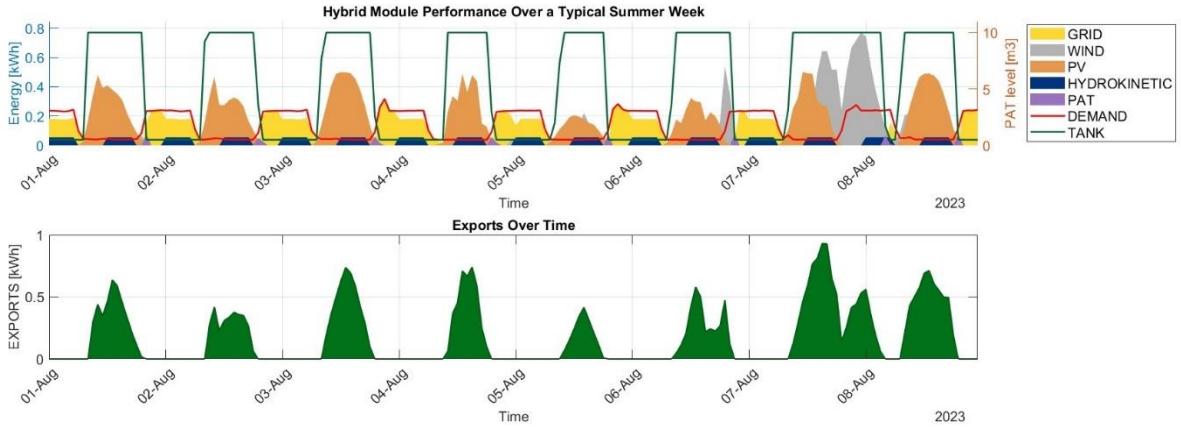

Figure 4.5. Hybrid module performance over a representative summer week (baseline configuration).

As illustrated in Figure 4.4 and Figure 4.5, the system's limited storage capacity results in the tank reaching its maximum discharge with minimal demand, underscoring the critical importance of a robust grid interconnection. Throughout much of the year, grid support remains essential to ensure uninterrupted supply. Under the current configuration, the hybrid module provides an estimated coverage of 58.19%, equivalent to approximately 5,241 hours of annual autonomy. While reliance on the grid has been substantially reduced, an annual import of 587.27 kWh is still required to fully meet the energy demands of the selected infrastructures. Figure 4.6. presents a comparative analysis of grid imports before and after the integration of the hybrid module, highlighting the effects of this initial implementation.

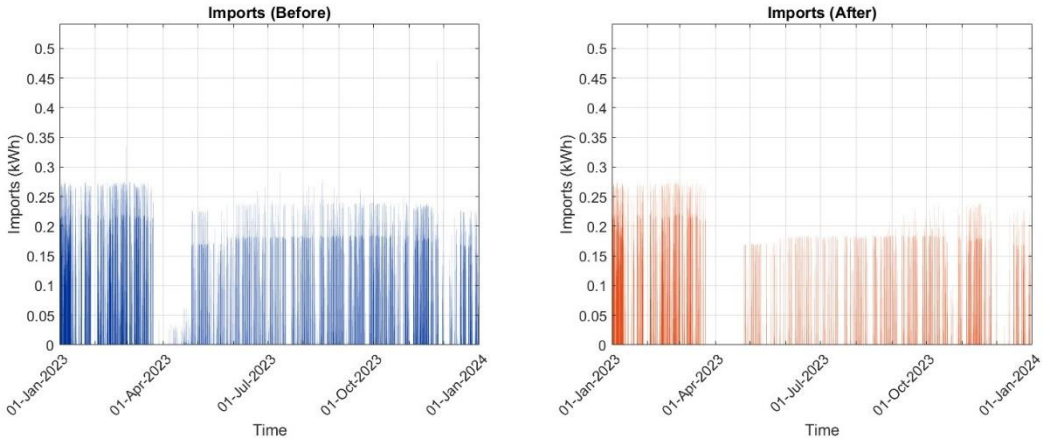

Figure 4.6. Imports comparison before and after the application of the hybrid module.

At this stage, an important question arises: why, despite the system's generation potential, has coverage of the selected demand profiles not exceeded 60%? The explanation lies in the characteristics of the energy mix and the system's restricted storage capacity. Generation relies on variable, intermittent sources with limited flexibility, while the minimal ability to store surplus energy requires immediate consumption. Whenever demand does not coincide with generation, excess electricity cannot be retained and must instead be redirected for alternative uses. In this context, the surplus management strategies discussed earlier become essential to enhance the system's overall economic performance.

From a financial perspective, the integration of the hybrid module achieves an annual direct reduction of 89.12 € in electricity costs, equivalent to approximately 59% savings under the 2.0 TD tariff. This reduction is consistent across both energy management strategies, serving as a baseline from which to assess the relative advantages of each surplus utilization approach: selling excess electricity to the grid or redirecting it to other facilities.

Selling surplus energy, at the previously defined tariff rates, generates an additional annual income of 175.44 €. When combined with the fixed savings, this results in a total yearly benefit of 264.56 €. However, extending this projection over a 25-year horizon and applying the appropriate discount rate reveals a notably low NPV, indicating that the long-term economic viability of this option remains limited.

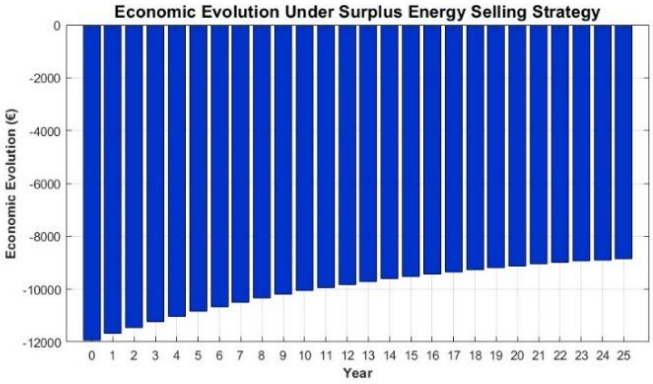

Figure 4.7. Economic evolution under the surplus energy selling strategy (baseline).

As shown in Figure 4.7, the current configuration of the hybrid module fails to recover the initial investment, resulting in a projected economic deficit of -8,839.17 € at the end of the evaluation period. To address this shortfall, additional modifications to the module will be required to develop a more optimized and financially viable solution. Given the negative financial outcomes, there is no payback period, and the internal rate of return also fails to be positive.

Upon evaluating the results of the second energy strategy, which involves redirecting energy to buildings with a 3.0 TD tariff, a notable increase in annual benefits is observed. The additional income generated nearly doubles that of the income from selling energy to the grid, rising from 175.44 € to 341.42 €. This results in a total benefit of 430.54 €, reflecting a 62.74% increase compared to the previously assessed strategy.

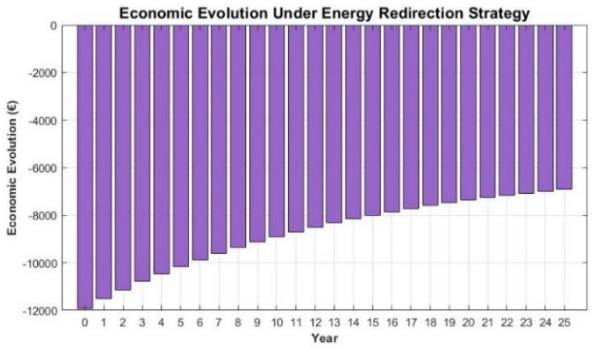

Figure 4.8. Economic evolution under the energy redirection strategy (baseline).

Despite the improved results, Figure 4.8. illustrates that these are insufficient to make the scenario economically viable, resulting in an economic deficit of -6,904.86 € and an internal rate of return of -0.77%. Given the current number of generating units and the initial investment, it is evident that there remains significant potential for further investment and optimization. The system currently occupies only 28.20 m² of the available 100 m² surface area, leaving ample space for expansion. Consequently, there is considerable scope for resource optimization. A strategic combination of increased generation capacity and a larger storage system is expected to yield more favourable and economically viable results in the long term.

4.2.4.2 Optimized results

Following the presentation of the results defining the economic and energy performance of the baseline scenario, the previously described optimization algorithm has been applied to identify the configuration that delivers the most optimal outcomes.

To achieve the optimized configuration, the model determined the optimal energy multipliers for each technology, based on the constraints detailed in Section 4.2.3. Among the energy sources available in the hybrid module, solar power stands out with the most competitive €/kWh ratio, followed by wind energy. Moreover, photovoltaic systems require the least land area per unit of assigned energy multiplier among land-based technologies. These advantages clearly steer the optimization process toward maximizing the share of solar energy in the system, while maintaining the current number of wind, hydro,

and PAT units. It is important to emphasize that this result is specific to the present case study and should not be interpreted as a universally optimal distribution, as different contexts may yield different configurations.

The optimization tool was configured to operate at the upper limits of both investment and land-use constraints to maximize potential energy surplus and economic profitability. To approach the target of 70% total energy coverage, the configuration proposed that at least 10% of coverage should be supplied by storage, while maintaining a minimum of 60% coverage from the hybrid module itself. This setup aimed to reduce reliance on the external power grid.

The analysis conducted using the HOPS framework identified the most viable solution as applying an energy multiplier of 19 to the photovoltaic unit, thereby increasing the number of installed panels from 2 to 38. Regarding the storage system, the maximum achievable coverage was 7%, below the 10% target, corresponding to a tank capacity of 43.36 m³. The spatial constraint was respected, with the total module area reaching 91.5 m² within the available 100 m². Similarly, the investment required for the implemented modifications amounted to 24,521.54 €, remaining within the allocated budget of 25,000 €.

The implementation of these modifications resulted in a substantial improvement in energy generation compared to the baseline scenario. Annual energy generation increased from 3,340.42 kWh to 17,512.55 kWh, primarily due to the expansion of the photovoltaic array. This increase significantly enhances the potential for economic returns through more effective surplus energy management.

In terms of energy coverage for the selected infrastructures, the hybrid module alone now provides 60.24% coverage, representing a 3.82 percentage point improvement over the baseline. The storage system contributes an additional 7% (98.36 kWh). However, despite the considerable increase in tank volume, the overall contribution of storage to total energy coverage remains limited. This limitation arises from the intrinsic characteristics of the storage technology, which requires energy-to-volume conversion, with each cubic meter supplying only 0.008175 kWh. Consequently, even significant expansions in storage capacity translate into modest increases in usable energy.

Moreover, the performance of the overall system is constrained by consumption patterns that peak during nighttime hours when solar generation is unavailable. As a result, the combined coverage of the module and storage reaches 67.24%, slightly below the 70% target. These findings highlight the challenges of achieving high self-sufficiency in hybrid energy systems under strict spatial and investment limitations, particularly when storage technologies exhibit low energy density and temporal mismatches with demand.

Table 4.2. Comparison of Scenario 1 under the optimized and non-optimized configurations.

	Energy Generation	**Total Coverage**	**Storage Capacity**	**Storage Contribution**	**Renewable Contribution**
S1 (Non-Optimized)	3,340.42 kWh	58.19%	10 m^3	1.77% (24.88 kWh)	56.42% (792.73 kWh)
S1 (Optimized)	17,512.55 kWh	67.24%	43.36 m^3	7% (98.36 kWh)	60.24% (846.02 kWh)

With regard to seasonal performance, the substantial increase in solar generation has introduced a significant paradigm shift, particularly during the winter months. Although solar irradiance during this period remains lower than in other seasons, the expanded photovoltaic configuration, combined with the increased storage capacity, now enables tank charging in situations where it was previously unachievable. This development has led to a transition in the system's energy dynamics, with solar energy replacing wind as the dominant source.

While this shift has resulted in moderate improvements compared to the baseline scenario, the overall impact on energy coverage remains limited. High daytime generation is offset by insufficient output during nighttime hours, when demand persists but solar availability ceases. Although the upgraded storage system offers improved performance, its capacity remains inadequate to sustain prolonged discharge cycles or ensure stable energy supply throughout the night.

Furthermore, a comparison between solar generation and actual demand reveals substantial mismatches, with frequent peaks in generation that far exceed consumption needs during certain periods of the month. This underscores the necessity of implementing effective surplus energy management strategies to optimize system performance and fully capitalize on the enhanced generation capacity of the module.

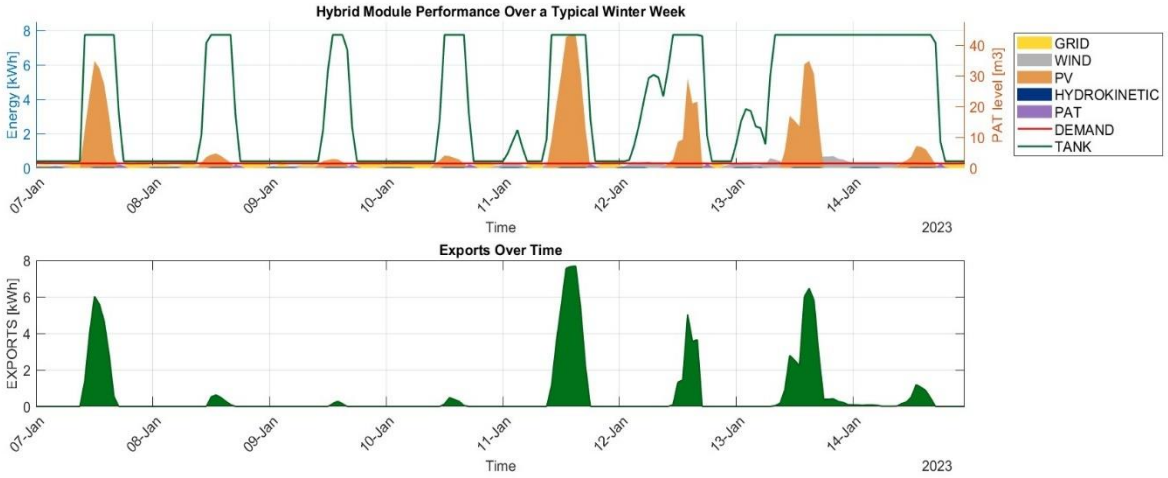

Figure 4.9. Hybrid module performance over a representative winter week, optimized configuration.

An analysis of the module's performance during a representative summer week reveals a pattern broadly consistent with that observed in winter, though characterized by higher solar generation due to increased irradiance. A key distinction between the two periods is the extended duration during which the storage tank remains at maximum capacity in summer, attributed to the longer daylight hours. While this allows for slightly greater coverage compared to the winter scenario, the contribution from the storage system remains insufficient to meet nighttime demand consistently.

Figure 4.10 illustrates the operational profile of the hybrid module over a one-week period in August, incorporating the adjustments resulting from the optimization process, together with the energy exports.

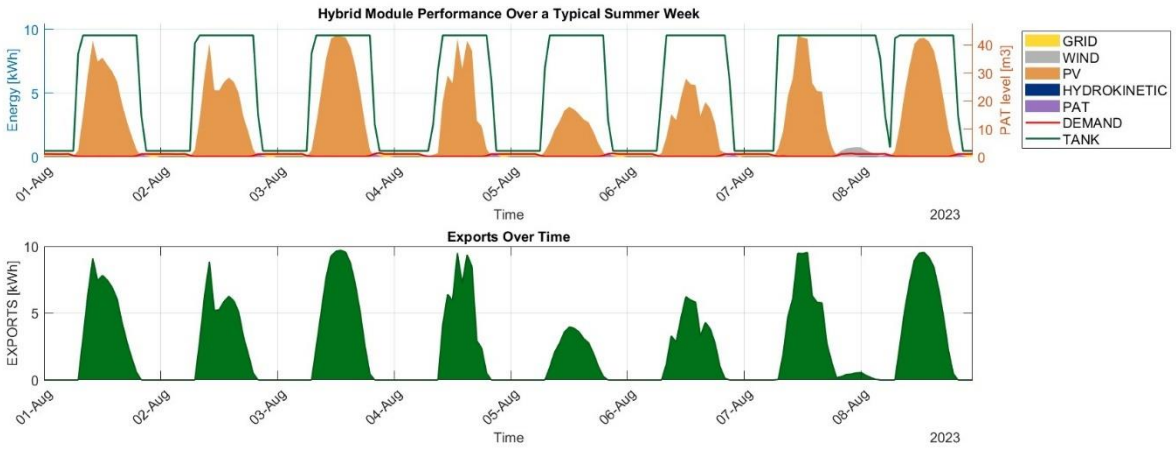

Figure 4.10. Hybrid module performance over a representative summer week, optimized configuration.

Finally, the economic performance of the system under both surplus management strategies demonstrates a marked improvement over the baseline scenario. The significant increase in excess energy generation substantially broadens the opportunities for monetization through energy sales, as well as for redirecting surplus electricity to other buildings. This enhanced flexibility contributes meaningfully to the overall economic viability of the system.

Under the strategy in which surplus energy is sold to the grid, the resulting revenue rises significantly to 1,155.20 €, representing nearly a tenfold increase compared to the baseline outcome. This is further complemented by a reduction in electricity expenses due to increased on-site demand coverage, yielding annually additional savings of 102.94 €. Combined, these gains result in a total net benefit of 1,258.14 €, underscoring the economic advantage of the optimized configuration.

When these values are projected over the system's life cycle to assess economic recovery, it becomes evident that, although the percentage of cost recovery has significantly improved, reaching 59.79%, the modifications remain insufficient to achieve full economic viability under this energy strategy. The resulting financial shortfall amounts to -9,859.73 €, despite an improvement in the internal rate of return, which has increased to 2.01%.

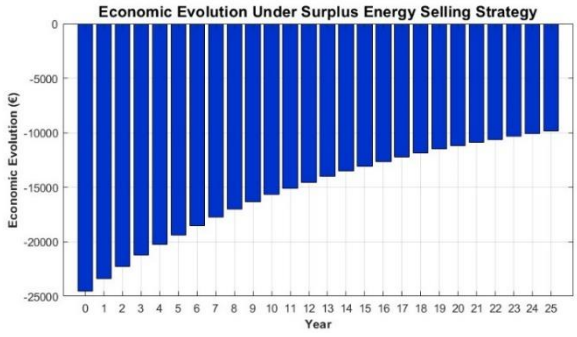

Figure 4.11. Economic evolution under the surplus energy selling strategy (optimized).

The adoption of the second surplus management strategy, marks a significant turning point, delivering the first positive net outcome among all configurations examined. This approach yields an additional profit of 2,242.99 € per year, effectively doubling the benefits achieved through energy sales to the grid.

When combined with the cost savings from reduced electricity consumption, the total economic benefit reaches 2,345.93 €. These results underscore the superior financial viability of surplus reallocation as a strategy for maximizing the system's performance and return on investment.

When applied over the evaluation period, these results indicate that the initial investment can be fully recovered within 20 years, yielding a net present value of 2,816.93 € and an internal rate of return of 8.25%. This financial trajectory is illustrated in Figure 4.12.

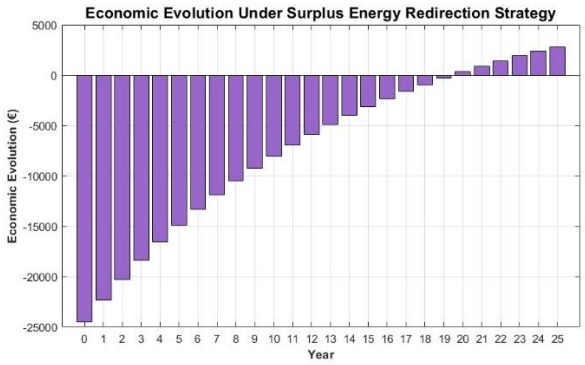

Figure 4.12. Economic evolution under the energy redirection strategy (optimized).

Despite the initial positive outcomes, further evaluation is required to determine whether alternative storage systems could yield more favourable results. Although the current configuration avoids financial losses, the returns remain relatively modest and may not be sufficiently attractive from an investment standpoint.

4.3 Scenario 2: Single hybrid module with batteries

4.3.1 Hybrid module operational strategy and energy management

In this second scenario, a significant modification is introduced by fully replacing the storage system employed in Scenario 1. The pump-as-turbine configuration is substituted with a battery-based storage system, intended to supply energy during periods when generation is insufficient. Despite the change in storage technology, the overall structure and prioritization scheme for energy distribution remain consistent. Surplus energy is first directed to charge the batteries, and any additional excess is managed using the surplus strategies previously outlined.

Operationally, this scenario presents a substantially simplified framework compared to Scenario 1. With all processes confined to the energy domain, the need for conversions between energy and volumetric units is eliminated. As a result, both the computational requirements and the energy management procedures are notably streamlined.

As with the PAT-based model, a set of initial conditions is defined to characterize system behaviour during the first hour of operation. This initial state serves as the basis for subsequent time-step analyses, using the storage state from the preceding hour as a reference point.

In the context of battery integration, two key parameters must be considered: the state of charge (SoC) and the depth of discharge (DoD), which refers to the percentage of the battery that has been discharged in comparison to the overall capacity. To ensure consistency with Scenario 1, the initial SoC is set at 50%, aligning with the initial charge level of the storage tank. However, the maximum permissible discharge is increased to 97%, reflecting the use of deep-discharge battery technology while maintaining a small buffer to prevent complete depletion. An additional critical parameter is the maximum discharge power allowable within a given time interval. This constraint, typically defined by the battery manufacturer, is directly influenced by the system's designed storage capacity and is essential for preserving battery integrity and ensuring reliable performance.

As established in Scenario 1, system operation is governed by a set of equations that model the energy flows and control mechanisms. While the previous model featured four distinct operational phases, the simplified nature of the battery-based system reduces this to three: charging, discharging, and monitoring the state of charge. This reduction underscores how the transition in storage technology leads to a more efficient and less complex energy management model.

4.3.1.1 Battery charge

The battery charging process follows the same fundamental logic applied to the tank in Scenario 1, with modifications tailored to the specific technical characteristics of battery storage systems. Charging is initiated when renewable energy generation exceeds the system's demand during a given time step, resulting in a surplus. Once this surplus is detected, the system determines whether it can be stored, subject to defined lower and upper operational limits. A maximum threshold, established by the battery's technical specifications, ensures that the system does not exceed its permissible storage capacity.

This control logic is formalized in Equations (4.15) and (4.16), which adopt a structure similar to that used in Scenario 1. As with the PAT-based model, a clear distinction between the first time step, $B_{charge,0}$ (kWh), and subsequent intervals, $B_{charge,t}$ (kWh), is maintained throughout the simulation, ensuring continuity in the system's dynamic behaviour.

$$B_{charge,0} = \begin{cases} E_{NET,0} & , \ if\ E_{NET,0} > 0\ and\ E_{NET,0} + \left(B_{max} \cdot \frac{SoC_{50\%}}{100}\right) < B_{max} \\ B_{max} \cdot \left(1 - \frac{SoC_{50\%}}{100}\right), & if\ E_{NET,0} > 0\ and\ E_{NET,0} + \left(B_{max} \cdot \frac{SoC_{50\%}}{100}\right) \geq B_{max} \\ 0 & , \ if\ E_{NET,0} < 0 \end{cases} \quad (4.15)$$

$$B_{charge,t} = \begin{cases} E_{NET,t}, & if\ E_{NET,t} > 0\ and\ SoC_{,t} + E_{NET,t} \leq B_{max} \\ B_{max} - SoC_{,t}, & if\ E_{NET,t} > 0\ and\ SoC_{,t} + E_{NET,t} > B_{max} \\ 0, & if\ E_{NET,t} \leq 0 \end{cases} \quad (4.16)$$

In these equations, B_{max} (kW), refers to the battery maximum capacity, and $SoC_{50\%}$ corresponds to the state of charge of the battery at 50% of the total capacity.

4.3.1.2 Battery discharge

Regarding battery discharge, this process is governed by Equations (4.17) and (4.18). Just as with battery charging, it is essential to define clear operational limits. In this case, the maximum allowable discharge, previously set by the user, must be strictly controlled to ensure compliance with established safety requirements.

$$B_{disch,0} = \begin{cases} \left|E_{NET,0}\right|, \ if\ E_{NET,0} \leq 0\ and\ B_{max} \cdot \left(\frac{Soc_{50\%}}{100}\right) - \left|E_{NET,0}\right| \geq B_{max} \cdot \left(\frac{100-DoD_{97\%}}{100}\right)\ and\ E_{NET,0} \leq P_{max} \\ 0, \ if E_{NET,0} < 0\ and\ B_{max} \cdot \left(\frac{Soc_{50\%}}{100}\right) - \left|E_{NET,0}\right| < B_{max} \cdot \left(\frac{100-DoD_{97\%}}{100}\right) \\ 0, \quad if\ E_{NET,0} > 0 \end{cases} \tag{4.17}$$

$$B_{disch,t} = \begin{cases} \left|E_{NET,t}\right|, \ if\ E_{NET,t} < 0\ and\ SoC_{t-1} - \left|E_{NET,t}\right| \geq B_{max} \cdot \left(\frac{100-DoD_{97\%}}{100}\right)\ and\ E_{NET,t} \leq\ P_{max} \\ SoC_{t-1} - B_{max} \cdot \left(\frac{100-DoD_{97\%}}{100}\right), \ if\ E_{NET,t} < 0\ and\ SoC_{t-1} - \left|E_{NET,t}\right| < B_{max} \cdot \left(\frac{100-DoD_{97\%}}{100}\right) \\ 0, \ if\ E_{NET,t} \geq 0 \end{cases} \tag{4.18}$$

The formulation of Equations (4.17) and (4.18), is marked by the definition of the battery discharge at the initial state, $B_{disch,0}$ (kWh), the maximum power of the battery that can be discharged in one hour, P_{max} (kW), the maximum depth of discharge allowable, $DoD_{97\%}$, the discharge of the battery in the subsequent time steps, $B_{disch,t}$ (kWh), and the state of charge from the previous time step, SoC_{t-1} (kW). The rest of the variables have been defined before.

4.3.1.3 State of charge management

Accurately determining the battery state of charge is fundamental to the proper functioning of the system, as it directly influences subsequent charging and discharging operations. Any error in estimating the SoC can compromise the performance of the hybrid module, particularly if surplus energy is not managed as intended, resulting in system behaviour that deviates from expected outcomes. As illustrated in Sections 4.3.1.1 and 4.3.1.2, the definition of the battery state of charge is considerably more straightforward compared to the PAT configuration involving a tank-based storage system. This highlights one of the key simplifications achieved in the development of the management model, enabled solely by modifying the type of storage employed. This change not only reduces system complexity but also facilitates more seamless interactions between the various operational processes, as detailed in Equations (4.19) and (4.20).

$$SoC_{,0} = \left(B_{max} \cdot \frac{SoC_{50\%}}{100}\right) + B_{charge,0} - B_{dich,0} \tag{4.19}$$

$$SoC_{,t} = SoC_{,t-1} + B_{charge,t} - B_{disch,t} \tag{4.20}$$

$SoC_{,0}$ (kW), corresponds to the state of charge at the initial time step and the $SoC_{,t}$ (kW), refers to the state of charge in the following time steps.

4.3.2 Optimization process

The optimization process for this scenario, in terms of system dynamics, closely parallels the approach previously applied in the PAT system configuration. The same optimization tool, Solver, will be used, with the primary objective remaining the identification of the system configuration that yields the highest economic return in year 25.

As in the earlier scenario, the energy multipliers of each technology involved, and the storage system capacity will serve as the key decision variables. These parameters will be adjusted to determine the optimal setup for maximizing economic performance. The main difference in this case is the absence of the reversible pump-turbine unit, which was a variable in the PAT-based system but is not present in the current configuration and thus excluded from the optimization process.

With respect to system constraints, only a minor adjustment is introduced: the analysis no longer focuses on determining the optimal storage volume (in m^3) required to achieve the desired energy coverage. Instead, the constraint is redefined to establish a minimum required battery capacity, expressed in terms of power.

4.3.3 Scenario 2: Results and discussion

Following the detailed analysis of the management model's operation with battery-based storage, along with the optimization process and the parameters defined to maximize the performance of the hybrid system, this section presents the results for both the baseline and the optimized configurations. As in the previous scenario, this allows for a clear and consistent comparison between system performances.

4.3.3.1 Baseline results with batteries.

To rigorously evaluate the self-sufficiency of the hybrid module, it is crucial to analyse its performance under baseline design conditions. This involves resetting both the generation components and the storage system to their original specifications, specifically, using energy multipliers of 1 and a storage capacity of 1 kW.

Implementing this system configuration reveals an immediate and significant improvement over the PAT approach. By avoiding the substantial inefficiencies associated with mechanical conversion and enabling direct energy storage, without the need for transformation into volumetric form, the system achieves notable gains in both efficiency and scalability. It allows for significantly higher energy density, requiring less physical space and offering a much more cost-effective solution, reducing at the same time the number of components needed to implement this new storage solution.

Talking about the energy results, the coverage provided exclusively by the generation units remains consistent with Scenario 1 at 56.42%, as the only variable altered in this case is the storage technology. The most notable improvement appears in the contribution of the storage system. While the PAT-based configuration in the baseline scenario offered only a marginal increase of 1.77%, the battery-based system raises this contribution significantly to 16.77%, equivalent to 235.72 kWh. This enhancement

enables the hybrid module to surpass the target of covering at least 70% of the selected demand, achieving a total coverage of 73.19%, without requiring any additional system optimization. Table 4.3 summarizes the energy mix and compares the performance between Scenario 1 and Scenario 2.

Table 4.3. Energy mix comparison between Scenario 1 and Scenario 2

Energy Mix PAT Configuration		**Energy Mix Battery Configuration**	
Generation Units	792.79 kWh (56.42%)	Generation Units	792.79 kWh (56.42%)
PAT System	24.88 kWh (1.77%)	Battery System	235.72 kWh (16.77%)
Grid	587.57 kWh (41.81%)	Grid	376.73 kWh (26.81%)

Building on the previous analysis, a significant reduction in grid energy imports stands out as a direct result of the improved storage system performance. Under the current configuration, only 376.73 kWh are needed to fully meet the demand, while the system delivers coverage for 6,478 hours annually. This substantial increase in operational autonomy highlights the efficiency gains achieved through the integration of the new storage solution. Figure 4.13 presents a comparative analysis of grid imports between the baseline configuration in Scenario 1 and the setup in Scenario 2.

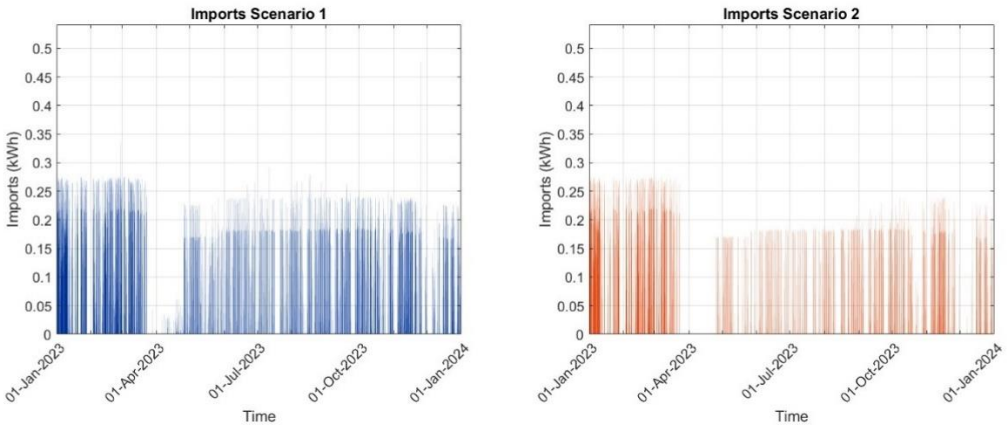

Figure 4.13. Imports comparison between S1 and S2 before optimization.

From an operational and performance standpoint, particularly when examining seasonal variability, noticeable though modest differences can be observed following the integration of the new storage technology. During a representative winter week, the system still experiences extended periods of insufficient storage capacity, with state-of-charge levels remaining near minimum for much of the week. This limitation is primarily attributable to the reduced generation potential caused by unfavourable weather conditions typical of the season. Out of the 192 hours comprising the analysed week, the system with the new storage configuration successfully covered 75 hours under baseline conditions, compared to only 58 hours covered by the PAT-based system. This represents an improvement of 8.85% over the previous scenario.

A key difference introduced by the battery-based system is its higher storage capacity compared to the previous tank solution. As a result, charging and discharging processes are no longer as immediate or abrupt; instead, they occur more gradually and are better regulated. This behaviour is advantageous, as it allows the system to cover demand over a greater number of hours. Figure 4.14 illustrates this

improved performance, showing the system's typical behaviour during winter, including the battery's state-of-charge profile.

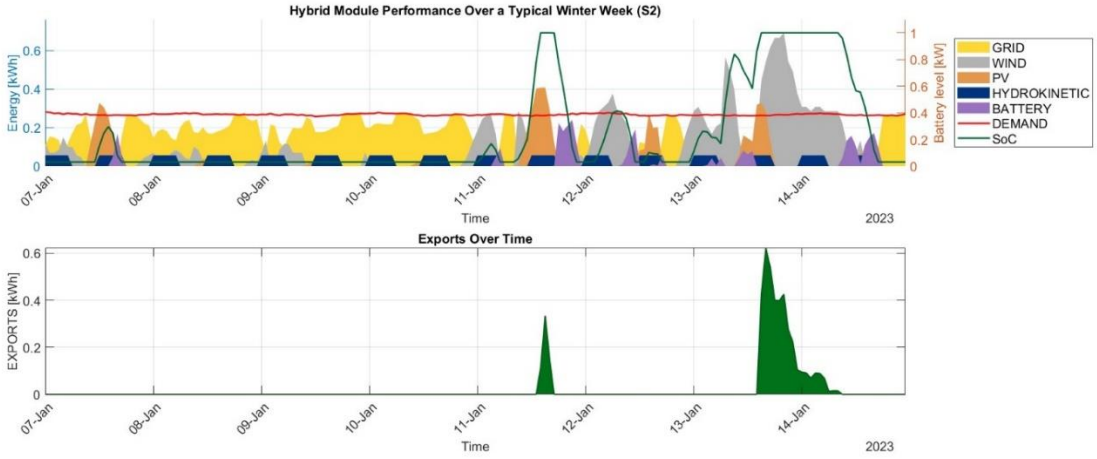

Figure 4.14. Hybrid module performance over a representative winter week (baseline S2).

During the summer period, the energy profile demonstrates a marked improvement in hourly coverage, driven by more favourable weather conditions and the resulting increase in renewable energy generation. This profile more clearly highlights the improved discharge behaviour of the battery system, which delivers a smoother and more stable energy supply compared to the previous PAT-based configuration. Despite this improvement, the battery system still does not fully satisfy nighttime demand.

Over the course of the 192-hour week analysed, the implementation of the new storage solution has extended energy coverage by 29 additional hours, from 103 hours with the PAT system to 132 hours using the battery configuration.

While these results are derived from a non-optimized energy management strategy, they already indicate a substantial performance enhancement. The weekly operational dynamics of each component within the hybrid system, including generation, storage, and consumption, are depicted in Figure 4.15, offering a comprehensive view of system behaviour under the revised setup, together with the corresponding exports of the month.

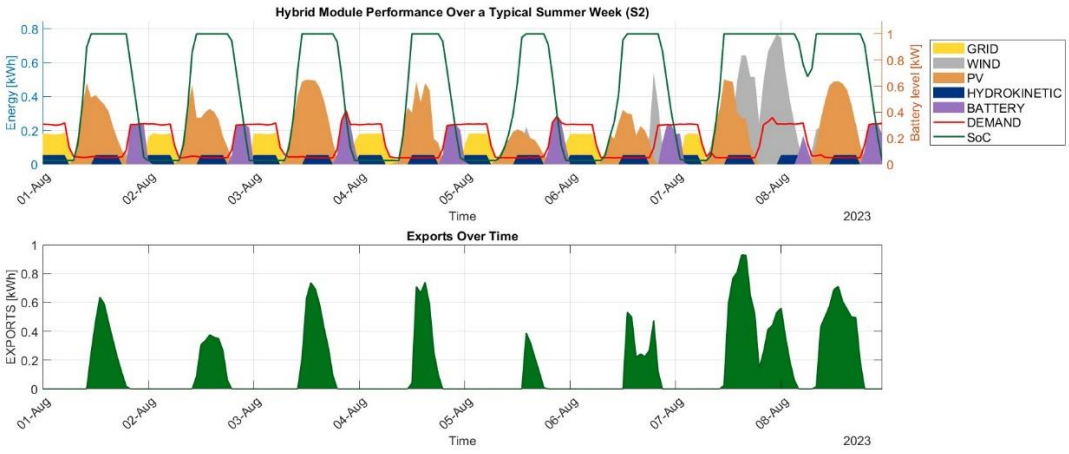

Figure 4.15. Hybrid module performance over a representative summer week (baseline S2).

After analysing the most significant results regarding energy management and system performance with the new storage solution, attention now turns to evaluating whether the investment is financially justifiable, not only through enhanced energy coverage but also through the optimized use of surplus energy.

Before analysing the results in detail, it is important to note that the selected storage technology benefits from ongoing cost reductions driven by continuous innovation. The system is also simpler, incorporating fewer components than the previous configuration. This streamlining has reduced the total cost of the hybrid module from 11,922.24 € to 8,680 €, improving the potential for a positive return on investment.

Enhanced energy coverage and higher self-consumption have substantially decreased the cost of electricity purchased from the grid, from 153.16 € to 41.06 €, generating about 15% additional savings compared to the PAT-based scenario.

However, despite these improvements and the availability of 2,312.45 kWh for grid export under the first surplus management strategy, this surplus remains insufficient to recover the initial investment. The resulting revenue of 161.87 €, combined with 112.10 € in grid cost savings, yields an annual economic gain of 273.97 €.

Although this scenario demonstrates better energy performance, the economic improvement remains modest, with a net difference of less than 10 € compared to the PAT configuration. By the end of the analysis period, the system still shows a deficit of -5,487.24 €, indicating no return on investment.

Implementing the second surplus management strategy delivers more favourable outcomes. The additional annual profit increases to 314.58 €, resulting in a total annual benefit of 426.68 €, after accounting for grid electricity costs. Over a 25-year period, discounted to present value, this performance enables partial recovery of the initial investment. Nevertheless, a deficit of -3,707.69 € remains, with an internal rate of return of 1.65%.

While full cost recovery is not yet achieved, the significantly smaller deficit compared to the previous configuration highlights strong potential for improvement. With further optimization, the system could reach profitability and deliver returns attractive to investors.

4.3.3.2 Optimized results with batteries

After establishing the baseline results, the next step is to analyse the system's behaviour following the application of the optimization algorithm, and to examine the key outcomes derived from this process.

The first step is to define the configuration of the hybrid module after recalibrating the energy multipliers for each generation source, while simultaneously determining the optimal storage capacity required to meet the specified performance targets. Given the strong baseline results, particularly in terms of demand coverage, the optimization process will focus on enhancing the system's autonomy. The new objective is for the hybrid module to supply at least 85% of the total energy demand independently, with minimal reliance on the grid. This shift is aimed at maximizing emissions reductions. To achieve this, the system must deliver a minimum of 65% of the demand through renewable generation, with the

remaining 20% met via energy storage.

Taking the current constraints into consideration, a maximum investment of 25,000 € and a maximum usable area of 100 m², the configuration identified as the most effective, while fully respecting all limitations, involves applying an energy multiplier of 21 to the photovoltaic system and of 2 to both the wind and hydrokinetic sections. This setup results in a hybrid module consisting of 42 solar panels, 6 wind turbines, and 4 hydrokinetic turbines. The battery storage capacity has also been revised to 1.28 kW to ensure adequate energy availability. With this configuration, the total cost of the system amounts to 24,712.10 € and the total occupied area is 98.89 m², remaining within both the budgetary and spatial constraints.

Before evaluating the economic viability of the proposed solution, it is essential to first analyse its energy performance. The updated design of the hybrid module allows renewable sources alone to cover 69.75% of the total energy demand, equivalent to 980.18 kWh. This already exceeds the total coverage achieved in Scenario 1, even when storage was included. By adding the battery system's contribution of 281.66 kWh, total coverage rises to 89.90%, leaving just 143.33 kWh to be supplied by the grid. As a result, grid dependency is reduced to a minimal level.

In this case, analysing system performance over two representative weeks, consistent with the methodology used so far, reveals significantly different behaviour compared to previous configurations. During the typical winter week, for the first time, there are no extended periods of unmet demand or prolonged intervals with the storage system at minimum capacity. Of the 192 hours evaluated, the system is able to meet demand for 154 hours, highlighting its enhanced ability to ensure energy supply under winter conditions. This improvement is largely due to the fact that the increase in generation capacity was not limited to the photovoltaic array but also included a modest expansion of wind and hydrokinetic units. This broader distribution of generation sources has strengthened nighttime supply, reducing the strain on the storage system and improving overall system resilience.

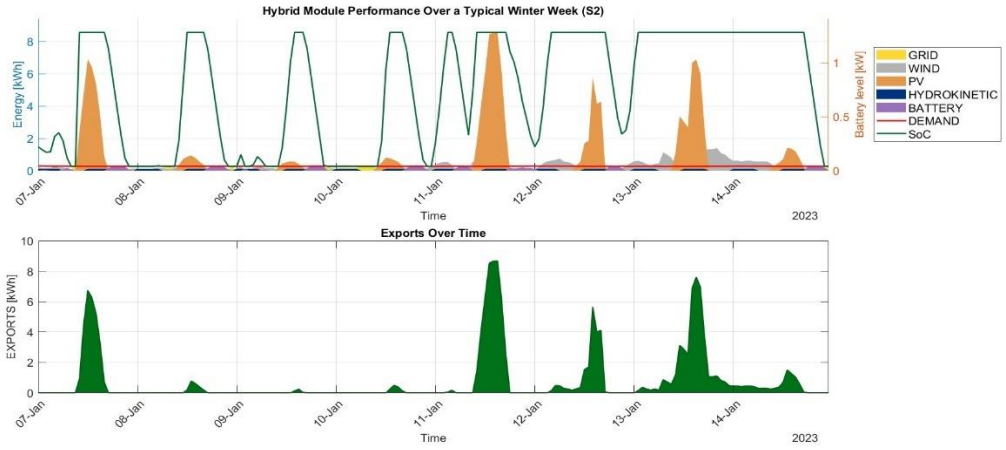

Figure 4.16. Hybrid module performance over a representative winter week (Optimized S2).

In the summer period, the system contends with a more variable and cyclical demand profile, marked by significantly higher consumption during nighttime hours. As a result, it was not entirely possible to prevent the storage system from reaching its minimum capacity during certain intervals. However, the

enhancements introduced have effectively smoothed the battery's discharge profile, limiting both the duration and frequency of periods when storage alone cannot meet demand. As illustrated in Figure 4.17, surplus energy, primarily from the solar array, frequently exceeds the energy requirements needed for full coverage throughout much of the period. To maximize the economic performance of the system, these surpluses should be strategically managed and potentially redirected for complementary uses or grid interaction.

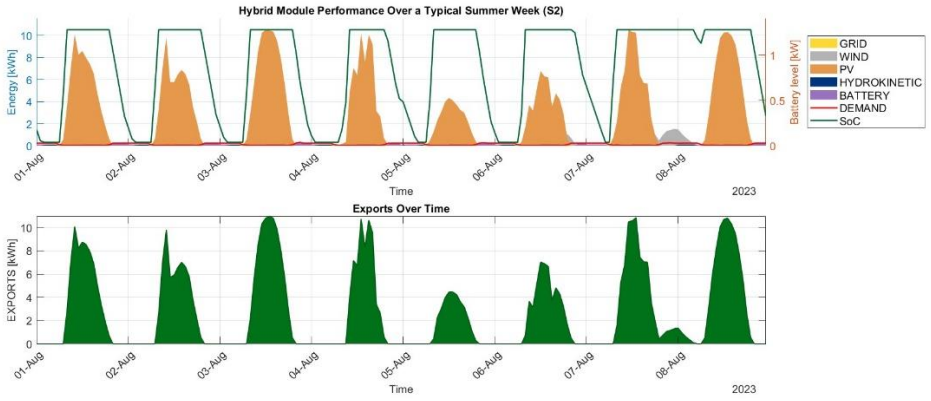

Figure 4.17. Hybrid module performance over a representative summer week (Optimized S2).

After assessing the system's energy performance improvements through optimization, it is necessary to determine whether these translate into financial benefits. The increased generation capacity resulted in a total surplus of 20,379.02 kWh, which could generate an additional annual income of 1,426.53 € if sold to the grid. Combined with electricity bill savings of 137.54 €, the total annual financial benefit amounts to 1,564.07 €.

However, financial projections at year 25 indicate that the initial investment would not be recovered, with a remaining deficit of -6,485.05 €, as represented in Figure 4.18. These results show that, under current conditions, grid export is not economically viable. Across all evaluated scenarios, this strategy fails to yield a return on investment. Consequently, future analyses will focus on alternative surplus management strategies, such as reallocating excess energy to nearby buildings, which have demonstrated and are expected to provide significantly more favourable outcomes.

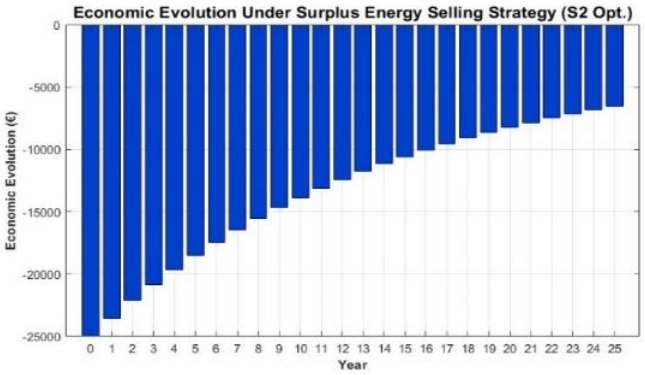

Figure 4.18. Economic evolution under the surplus energy selling strategy S2 (Optimized).

After confirming that the first surplus management strategy remains ineffective in recovering the initial investment, the alternative approach, redirecting surplus energy, as demonstrated with the application of the PAT system, yields significantly more favorable financial outcomes. Maintaining annual electricity bill savings of 137.54 € and generating an additional 2,771 € per year through energy redirection, the total annual benefit rises to 2,908.54 €, nearly double that of the grid export strategy.

When projected over the full lifecycle of the hybrid module, this scenario results in a net present value of approximately 9,182.79 €, with a payback period achieved in year 14 and an internal rate of return of 10.88%. These results assume maximum coverage conditions. Notably, if more flexible energy coverage targets were applied, such as 60% from the hybrid module and 15% from storage, the economic performance improves further, with an estimated NPV of 13,545.91 € and a shortened payback period of 11 years. The main reason why reducing the energy coverage requirement leads to improved results lies in the decreased need for storage capacity. With lower storage requirements, the 15% coverage target can be achieved with a smaller capacity. Consequently, the storage system reaches full charge more quickly, allowing a greater share of energy to be exported to other buildings with higher tariffs. At the same time, the reduced coverage target enables a decrease in module costs, further enhancing the system's overall economic performance.

Figure 4.19 illustrates the economic performance of the new solution, highlighting their greater potential to attract investment and enhance long-term profitability.

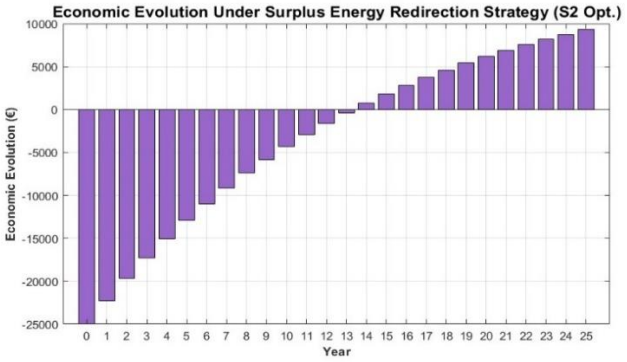

Figure 4.19. Economic evolution under the energy redirection strategy S2 (Optimized).

Chapter 5

Parallel Module Deployment – Case Study

In this second case study, the impact of configuring hybrid modules in a parallel arrangement on both energy performance and economic outcomes is analysed. To this end, two additional scenarios are evaluated, both involving three hybrid modules but differing in their interconnection and storage configuration. The first scenario features a centralized storage system, where all modules are connected to a single shared storage unit. In contrast, the second scenario adopts a decentralized approach, with each module operating independently and equipped with its own dedicated storage system.

5.1 Overview

In the previous chapter, a detailed analysis was carried out on the system's performance and operation when only a single module was available. This evaluation offered valuable insights into the most efficient operating modes across different scenarios, laying the groundwork for a more focused analysis involving the parallel deployment of multiple modules.

To improve the clarity and streamline the current simulation process, results related to the surplus management strategy, specifically, the sale of excess energy to the grid, have been intentionally omitted. The earlier case study revealed significant and growing differences in performance between energy redirection and grid export as surplus energy increases. While these findings are not elaborated upon here, they can be found in the Appendix A for further reference.

For the parallel module configuration, only results involving the most promising energy storage technology, either the PAT system or batteries, are presented. Parallel configuration aims to assess whether a shared storage system offers greater benefits compared to individual storage tailored to each module's demand. Since three optimal demand profiles were previously identified for the hybrid module, three modules were arranged in parallel, each corresponding to one of these profiles.

5.2 Scenario 3: Parallel management with shared storage system

5.2.1 Hybrid modules operational strategy and parallel energy management

The implementation of parallel configurations constitutes a key advancement in this study, enabling a comprehensive evaluation of module performance under coordinated operation. In this arrangement, each module is assigned a unique demand profile, while surplus energy is redirected to a centralized storage system rather than individual storage units. This design strategy aims to maximise resource sharing and inter-module support, thereby enhancing overall system operational synergy.

While the internal logic of the model remains based on the equations established in the initial two scenarios, several dynamic modifications have been introduced. In this configuration, surplus energy generated by any module is consistently directed to support the central storage system rather than being immediately allocated to other modules in need. The central storage then supplies the necessary energy to units unable to meet their assigned demand. This operational approach minimizes deep discharges observed in previous scenarios and prioritizes maintaining support from the generating units to the storage system whenever feasible.

It is important to highlight that this operational approach is advantageous only if the storage system does not introduce significant conversion losses that would reduce overall efficiency. Consequently, batteries

represent the most viable option, as the PAT system, with an efficiency of approximately 60%, would incur substantial energy losses when continuously prioritizing storage. Figure 5.1 illustrates the flow diagram detailing the operation and interactions among the system's primary components.

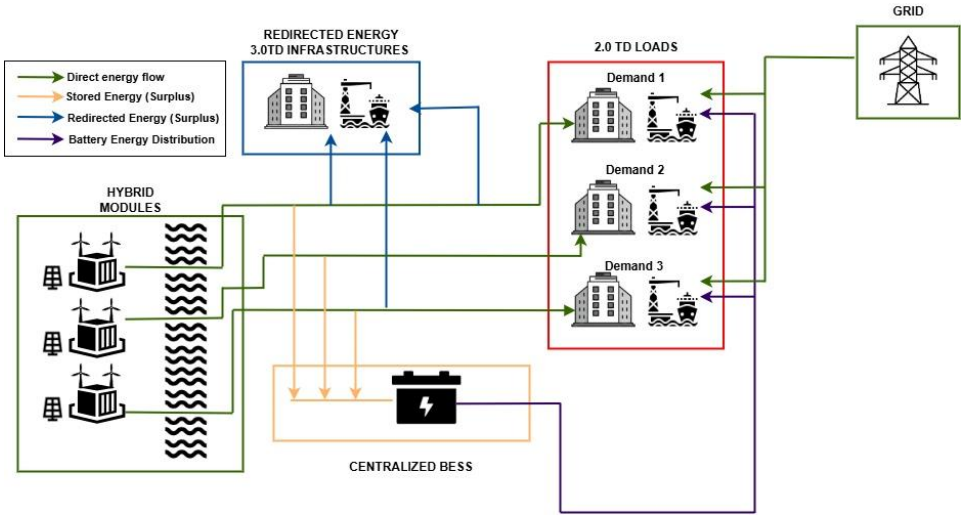

Figure 5.1. Flow diagram of parallel module distribution with centralized storage unit.

As previously noted, the fundamental equations governing the system remain largely unchanged; however, minor adjustments have been introduced in the battery loading process. The mentioned modifications are demonstrated in the Equations (5.1) to (5.3):

$$E_{surplus,t} = \begin{cases} E_{Net(M1),t}, & if\ E_{Net(M1),t} > 0 \\ 0, & otherwise \end{cases} + \begin{cases} E_{Net(M2),t}, & E_{Net(M2),t} > 0 \\ 0, & otherwise \end{cases} + \begin{cases} E_{Net,(M3),t}, & E_{Net(M3),t} > 0 \\ 0, & otherwise \end{cases} \quad (5.1)$$

$$B_{charge,0} = \begin{cases} E_{surplus,0}, & if\ E_{surplus,0} > 0\ and\ E_{surplus} + B_{max} \cdot \left(\frac{SoC_{50\%}}{100}\right) \leq B_{max} \\ 0, & if\ E_{surplus,0} \leq 0 \\ B_{max} - B_{max} \cdot \left(\frac{SoC_{50\%}}{100}\right), & if\ E_{surplus,0} > 0\ and\ E_{surplus} + B_{max} \cdot \left(\frac{SoC_{50\%}}{100}\right) \geq B_{max} \end{cases} \quad (5.2)$$

$$B_{charge,t} = \begin{cases} E_{surplus,t}, & if\ SoC_{,t} + E_{surplus,t} \leq B_{max} \\ B_{max} - SoC_{,t}, & if\ SoC_{,t} + E_{surplus,t} \geq B_{max} \\ 0, & if\ SoC_{,t} = B_{max} \end{cases} \quad (5.3)$$

Where $E_{Net(M1),t}$, $E_{Net(M2),t}$ and $E_{Net(M3),t}$ (kWh), corresponds to the net energy balance for module 1, 2 and 3 respectively, at a specific time step, and $E_{surplus,t}$ (kWh), references to the toal combined energy surplus in the parallel management configuration. The rest of the variables have been previously defined.

As presented in Equation (5.1), the system initially evaluates the energy balance across the three modules, identifying and aggregating any surplus energy. When a positive balance is detected, the system assesses the storage unit's available capacity to absorb this surplus. If sufficient capacity exists, the excess energy is promptly stored in the batteries, without considering potential deficits in other

modules. Once the storage system reaches its maximum capacity, any remaining surplus is designated as final surplus and managed according to the predefined strategy, namely, redirecting the energy to other port infrastructures at preferential rates, as previously outlined. Aside from this adjustment, the system's operational logic remains unchanged, with a distinction made between the initial hour, Equation (5.2), and the subsequent time periods, Equation (5.3).

5.2.2 Optimization process

As with the single-module operation, it is essential to implement an optimization process to identify the configuration that yields the best overall performance. In the case of three modules, both cost and land use constraints have been reassessed, since the spatial and budgetary limits defined in earlier scenarios are insufficient to maximize overall benefits. This is primarily due to the minimal additional space and limited financial margin available under the previous conditions, which restrict the installation of additional energy-generating units and consequently limit surplus generation.

The space allocation strategy prioritizes treating each module individually, recognizing that spatial requirements vary according to specific demand levels. For example, Vieja Rula's energy demand substantially exceeds that of Embarcadero, thereby justifying a larger portion of the available area to support a greater number of generating units and ensure optimal demand fulfillment. Consequently, a total area of 200 m² has been designated for the parallel installation of the three modules, providing ample flexibility to evaluate multiple configurations and identify the most profitable solution. The specific allocations are as follows: Module 1 is assigned 120 m², Module 2, 20 m², and Module 3, 60 m².

In terms of budget, the capital investment has been revised upward to accommodate the financial requirements of deploying three modules. This expanded configuration necessitates a greater number of high-cost components, such as wind turbines, hydrokinetic turbines, and containers, which represent a significantly larger investment compared to other scenarios. Consequently, a higher initial expenditure is unavoidable. Rather than applying a simple proportional increase based on the budget of the standalone hybrid module, the new financial cap considers the potential for greater efficiency through shared operation. The maximum allowable investment has been set at 50,000 €, a figure that also aligns with the spatial limitations of the installation area. To integrate cost, space, and performance into the optimization process, a new metric will be introduced: the benefit generated per square metre. This indicator serves as a valuable benchmark for assessing the spatial efficiency of different configurations and identifying the arrangement that delivers the highest return relative to available surface area.

Another key aspect of energy management in this configuration is that, due to the use of a shared storage system, energy coverage will continue to be evaluated collectively, treating all modules as a unified operational block. However, this collective assessment approach will be phased out in future scenarios, particularly those involving dedicated storage systems tailored to each module's individual characteristics. In the current setup, what is differentiated is the application of module-specific energy multipliers, introduced to accommodate the spatial constraints previously defined. This allows for a more granular and efficient allocation of generating units, ensuring each module adheres to its space limitations while maximizing overall performance.

To provide a clearer understanding of how these variables and constraints are integrated into the revised optimization algorithm, Figure 5.2 presents a schematic overview of the optimization variables.

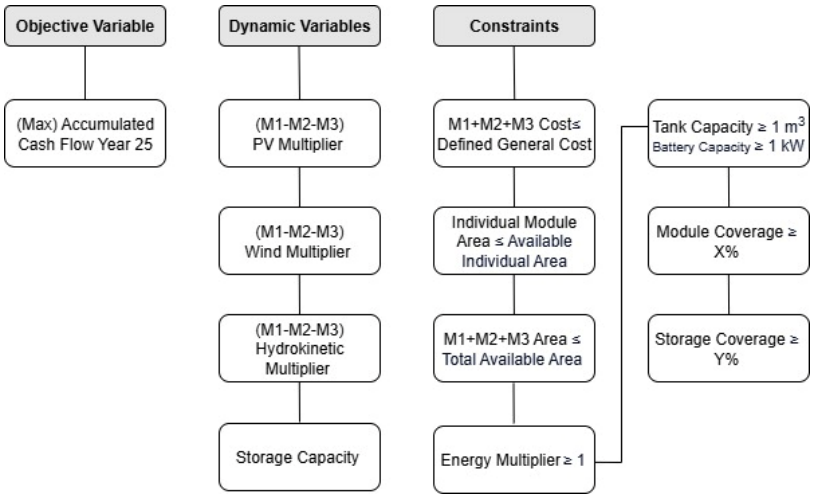

Figure 5.2. Optimization variables and constraints to evaluate the best parallel configuration.

5.2.3 Scenario 3: Results and discussion

Following the introduction of the scenario's specific characteristics and the adjustments made to both the system configuration and the optimisation process, the resulting performance of the modules under these defined conditions is now presented.

It is important to highlight that, in this analysis, no comparisons will be drawn against the baseline configuration in which all energy multipliers were set to one. This is due to the inherent expectation that such a configuration would deliver suboptimal results under the current constraints. Instead, all comparisons will reference Scenario 2, which has previously demonstrated the highest overall return and therefore serves as the benchmark for evaluation.

Prior to examining the simulation results, it is essential to detail the final configuration of each module following the optimisation process, including their respective annual energy generation figures and the overall system output. Module 1, allocated the largest surface area, accommodates the highest number of generation units: 64 solar panels, 3 wind turbines, and 2 hydrokinetic turbines. Module 2, associated with the lowest energy demand, retains its original setup as defined in the initial parameters. Module 3 comprises 26 solar panels, 3 wind turbines, and 2 hydrokinetic turbines, aligning with its intermediate demand profile and available space.

The resulting annual energy generation for Modules 1, 2, and 3 is estimated at 27,747.97 kWh, 3,340.43 kWh, and 12,788.51 kWh, respectively, contributing to a total system generation of 43,876.91 kWh per year. To support system reliability and meet demand consistently, the optimal storage capacity determined through the optimisation process is 1 kW.

A summary of the spatial allocation, energy generation, and demand assignment for each module under the current configuration is provided in Table 5.1.

Table 5.1. Designation of the available area, generation and demand to the hybrid modules.

Module	Area (m^2)	Generation (kWh)	Demand (kWh)
1	120	27,747.97	1,226.96
2	20	3,340.43	6.54
3	60	12,788.51	171.66
TOTAL	200	43,876.91	1,405.17

Based on this analysis, the annual energy performance of the modules is presented. With the current demand profiles and installed infrastructure, the system achieved a coverage rate of 90.91%, representing a 1.11% improvement over Scenario 2, which already exhibited strong performance. Achieving 100% demand coverage was not the goal, as it would likely reduce economic efficiency by requiring larger storage capacity and higher investment costs. The current configuration limits grid imports to 127.76 kWh, significantly reducing external dependence.

Regarding time-based coverage, the system supplied energy during 7,921 hours (90.42%) of the year, confirming the reliability of the configuration. Additionally, a total surplus of 42,599.97 kWh was produced. A comparison with Scenario 2 shows that a 109.01% increase in surplus energy results in only a 1.11% coverage gain, indicating that Scenario 2 was already near the theoretical coverage limit. Thus, the higher installed capacity yields marginal coverage benefits but increases total energy production. Figure 5.3 compares both the coverage levels and the capacity to generate surpluses across all previously analysed scenarios, illustrating that higher generation capacity does not necessarily result in increased coverage. Detailed hourly profiles of generation, demand, and storage behaviour are provided in Appendix A.

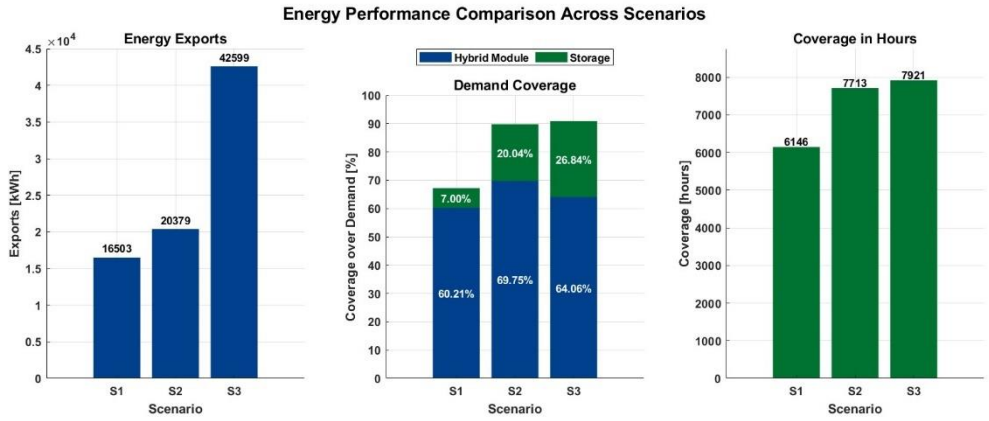

Figure 5.3. Energy performance comparison across scenarios.

Although coverage gains are limited, the increased energy generation and surplus may help shorten the payback period and enhance the project's long-term financial performance. The final investment cost of the optimized hybrid system is 48,060 €.

With the final cost of the hybrid module established, the analysis proceeds to the two main financial revenue streams: the reduction in electricity expenses and the income generated from surplus energy redirection. Starting with the cost savings, the original annual electricity bill of 153.16 € is reduced to

13.93 €, resulting in savings of 139.23 €. In addition, the redirection of surplus energy yields an annual revenue of 5,791.71 €. Together, these two streams produce a total annual financial benefit of 5,930.94 €. It is important to note that this annual profit must be discounted at a 7% rate of return to reflect its present value over time.

Considering all the factors discussed, the key financial indicators reveal a notably positive outlook, despite the substantial upfront investment required at the beginning of the evaluation period. The net present value at year 25 stands at 21,056.74 €, an increase of 11,873.95 € compared to Scenario 2, demonstrating the strong long-term financial performance of the optimized configuration.

It is important to note, however, that while the NPV reflects the total monetary gain after recovering the initial investment, it does not fully capture the efficiency of capital use. For this purpose, the internal rate of return offers a more accurate metric, as it indicates the return generated per euro invested. In this case, the IRR reaches 11.54%, exceeding the 10.88% achieved in Scenario 2. This reinforces the conclusion that the proposed configuration presents more attractive financial conditions, confirming its suitability as the more advantageous investment option; however, the relatively small differences between the scenarios leave room for further discussion regarding the final investment decision.

In addition to these two parameters, several supplementary metrics are used to evaluate the economic performance of the scenario, including the payback period and a newly introduced indicator: euros generated per square meter, which reflects the economic efficiency relative to the used area. In this scenario, the initial investment is recovered in just 13 years, one year earlier than in Scenario 2. Furthermore, it achieves an efficiency of 353.82 €/m², surpassing the 342.74 €/m² obtained in Scenario 2. To conclude the financial analysis, Figure 5.4 illustrates the economic evolution over the 25-year assessment period, confirming the scenario's financial viability and full investment recovery by year 13.

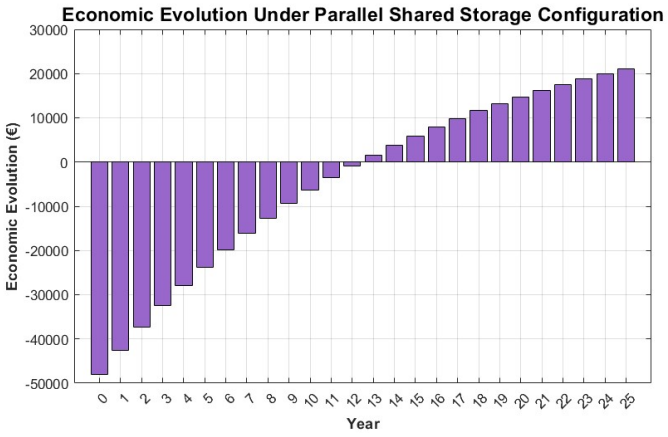

Figure 5.4. Economic evolution under a parallel shared storage configuration.

5.3 Scenario 4: Parallel management under individual storage systems

5.3.1 Hybrid modules operational strategy and parallel energy management

In the final scenario, a decentralized storage configuration is evaluated to assess whether assigning one storage unit per module, rather than relying on a centralized system, it can improve overall system performance and better align with the specific demand profiles of each module. In this setup, storage capacity is treated as an independent variable and included in the optimization process to determine the actual capacity required for each module individually.

A key characteristic of this configuration is the minimal interaction between modules. Each storage unit is designed to satisfy the respective module's demand constraints autonomously, significantly reducing the need for energy transfer between modules. As in previous scenarios, the available space remains a critical constraint, heavily influencing the choice of storage technology.

The pump-as-turbine system, while technically viable, presents substantial spatial limitations due to the need for auxiliary components, particularly a storage tank, which occupies considerable space. This makes the PAT system less compatible with the modular design constraints. In contrast, battery storage offers a more compact and space-efficient solution. Its smaller dimensions enables integration within the container itself, thereby preserving space for additional generation units.

Given these factors, the battery system has been selected as the most suitable technology for this scenario. Nonetheless, for the sake of comparison, the same configuration has also been modelled using the PAT system. Key performance indicators for both configurations are presented in the Appendix A.

Regarding the internal logic that governs the operation of this strategy, the differences between Scenario 4 and Scenario 2 are minimal. In both cases, the primary objective is to use the generated energy to meet the assigned demand as much as possible. Any surplus energy is then directed to the storage system to provide support during periods of insufficient generation. The storage system of each module is designed exclusively to meet its own energy demand and cannot be used to support other modules. Allowing one module to supply energy to another could jeopardize its ability to cover its future consumption, potentially leading to system inefficiencies or imbalances, in the way how is configured.

The main distinction lies in the allocation of demand: whereas Scenario 2 concentrated all three demand profiles in a single module, the current scenario distributes them across three separate modules. However, the same set of operational equations is applied independently to each module. Due to this new configuration and the relatively low energy demand of some of the selected infrastructures, a significant energy surplus is expected across all modules. As a result, the subsequent redistribution of this excess energy becomes a critical aspect of the system's overall performance.

For clarity, Figure 5.5 presents a flow diagram illustrating the operational logic of this strategy.

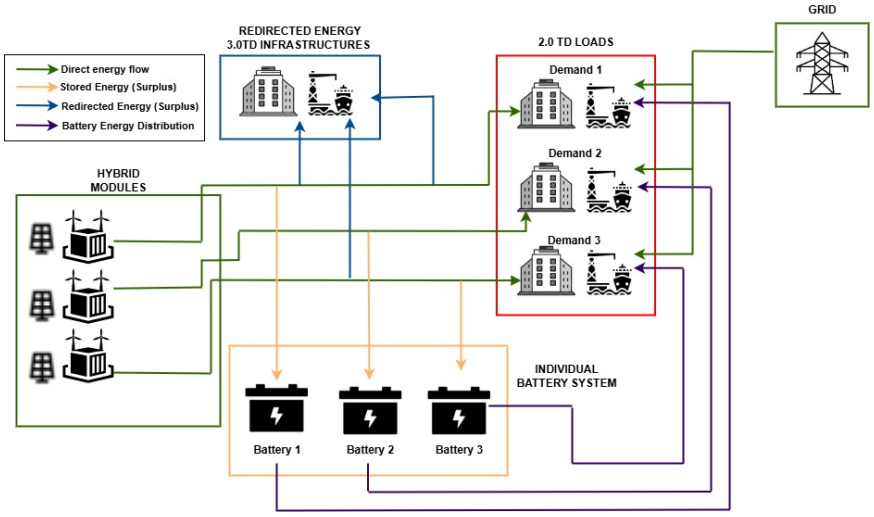

Figure 5.5. Flow diagram of parallel module distribution with individual storage systems.

5.3.2 Optimization process

As with the operation, the optimization process also follows a similar methodology to that used in Scenario 2. However, the key distinction lies in the increased complexity of the system configuration. In the case of the parallel setup, additional variables are introduced to accurately reflect the individual performance of each module. This expanded formulation ensures that the optimization maximizes the results obtention, ultimately leading to a more precise and efficient solution

Consistent with Scenario 3, energy multipliers are applied to each of the three modules based on their individual characteristics and operational constraints. To ensure a fair comparison with other scenarios that utilize a parallel management configuration, the total area used in Scenario 3 is adopted as an uniform constraint. This area is distributed according to the specific demand profiles level assigned to each module: 120 m² for Module 1, 20 m² for Module 2, and 60 m² for Module 3, resulting in a total allocated area of 200 m².

One of the most notable differences compared to Scenario 3 is the introduction of a maximum budget of 25,000 € per module, reflecting the greater level of operational independence among the modules in this configuration. This contrasts with the previous scenario, where a single, centralized budget was allocated to the entire system. The objective of this approach is to evaluate whether setting individual budget caps imposes any significant limitations when compared to a flexible budget distribution under a global maximum investment.

Finally, another key distinction lies in the need to optimize the individual storage capacities of the modules. This adds two additional variables to the optimization process, enabling a more tailored and efficient solution that aligns with the specific demand patterns of each module. The optimization is conducted in accordance with the minimum hybrid and storage coverage ratios defined for each module, ensuring that the system is both responsive and well-adapted to the operational requirements.

5.3.3 Scenario 4: Results and discussion

With both the operational and optimization processes defined, the results for this scenario are now presented and compared with those from other scenarios, particularly Scenario 3, which also features a parallel configuration.

Before analyzing the final energy outcomes, it is essential to outline the final system configuration for each module, including the optimal storage capacities assigned to their respective energy storage systems. Module 1, which has the largest available area, also hosts the highest number of generation units: 60 solar panels, 3 wind turbines, and 2 hydrokinetic turbines. For Modules 2 and 3, the number and type of generation units are identical to those used in Scenario 3.

Regarding storage requirements, the optimized storage capacities are 0.72 kW, 0.01 kW, and 0.07 kW for Modules 1, 2, and 3, respectively. As observed, the storage needs for Modules 2 and 3 are negligible, so minimal that they are practically unnecessary and fall below commercially available battery sizes. Nonetheless, for the purpose of consistency and completeness in this analysis, the results are presented assuming these storage capacities are implemented.

Starting with the key energy results, it is essential to first define the energy coverage provided by the different modules, taking into account the minimum energy constraints that need to be met. For clarity and simplicity, all results are summarized in Table 5.2.

Table 5.2. Individual storage and module contribution to the demand coverage.

	Minimum Hybrid Module Coverage	Minimum Storage Coverage	Hybrid Module Energy Coverage	Storage Energy Coverage	Energy Imports (kWh/%)
Module 1	60%	15%	745.33 kWh / 60.75%	184.88 kWh / 15.07%	296.75 kWh / 24.19%
Module 2	80%	15%	5.33 kWh / 81.45%	0.98 kWh / 15.00%	0.23 kWh / 3.55%
Module 3	80%	10%	149.07 kWh / 86.84%	17.17 kWh / 10.00%	5.42 kWh / 3.15%

The combined energy coverage of the three modules, relative to the total demand of 1,405.17 kWh, amounts to only approximately 78.48%. When compared to Scenario 3, this reflects a decrease in coverage of 12.43%. This reduction indicates that the low demand observed in modules 2 and 3, along with limited interaction between them, significantly reduces the overall system efficiency compared to Scenarios 2 and 3. As a result, energy imports increase to 302.40 kWh in this scenario, which has a direct and adverse effect on the final return on investment.

Regarding the definition of energy surplus, a reduction compared to Scenario 3 has been observed. This decrease is a direct consequence of the optimization strategy applied. As previously mentioned, instead of allocating a general budget across all three modules, individual maximum budgets have been set for each module. As a result, even though the overall system requires a lower total investment than in Scenario 3, the budget cap for Module 1 was reached. This constraint prevented the installation of the same number, or more, solar panels as in Scenario 3. Consequently, four fewer solar panels were

installed in Module 1, leading to a reduction in surplus energy of 1,400.17 kWh.

Despite having significantly higher energy generation capacity and consequently, a much larger surplus, compared to Scenario 2, the overall energy performance of the system could not be improved. This outcome highlights the critical importance of effective interaction between generation, demand, and storage. It also reinforces the notion that oversizing the generation system does not necessarily lead to better energy coverage.

There is a threshold beyond which additional generation, whether from PV panels, wind turbines, or hydrokinetic turbines, contributes primarily to surplus energy. This is particularly relevant given that all generation sources considered are intermittent, producing energy within limited time windows. For instance, increasing solar capacity will only improve coverage if the demand is concentrated during daylight hours. In cases like the selected demand profiles, where demand does not align with solar generation peaks, the storage system quickly reaches its maximum capacity, and any additional energy produced is simply used as surplus, without enhancing coverage. For all these reasons, this operating model has proven suboptimal from an energy standpoint, with significantly more effective and attractive alternatives available for implementation.

Following the assessment of all energy-related modifications, it is essential to examine their economic impact. A key consideration is the final investment required for the installation of the parallel hybrid module system. In this configuration, the use of fewer generating units, particularly in Module 1, has reduced the initial investment from 48,060.00 € in Scenario 3 to 46,730.93 € in Scenario 4. Despite this reduction, the cost remains significantly higher than those estimated for Scenarios 1 and 2.

Moreover, the lower energy coverage achieved, as previously noted, limits the potential for offsetting electricity import costs. In this scenario, the maximum achievable reduction amounts to 120.20 €, less favorable than the savings observed in Scenarios 2 and 3. However, the difference is relatively minor, approximately 20 €, and is unlikely to materially influence the overall economic outcome.

In terms of surplus energy redirection, this configuration has made 41,199.80 kWh available for allocation to other buildings, generating additional annual revenue of 5,599.02 €. As observed in all other scenarios, the return on investment is primarily driven by surplus utilization, largely due to the absence of intermediate consumption profiles better aligned with current generation levels.

These two economic streams have led to strong financial performance, with a full payback achieved in 13 years and a NPV of 19,918.45 €. Although the payback period matches Scenario 3, the lower volume of surplus energy results in a slightly reduced NPV, still clearly positive. The IRR is 11.42%, marginally lower than in Scenario 3 and only slightly higher than in Scenario 2.

The economic efficiency per unit area is also comparable to Scenario 3, at 352.26 €/m². Overall, while this configuration may not be the most energy-efficient, it offers a solid economic return, confirming its viability. The financial evolution over the 25-year lifespan of the hybrid modules is illustrated in Figure 5.6, together with a comparison of the economic efficiency with the rest of scenarios.

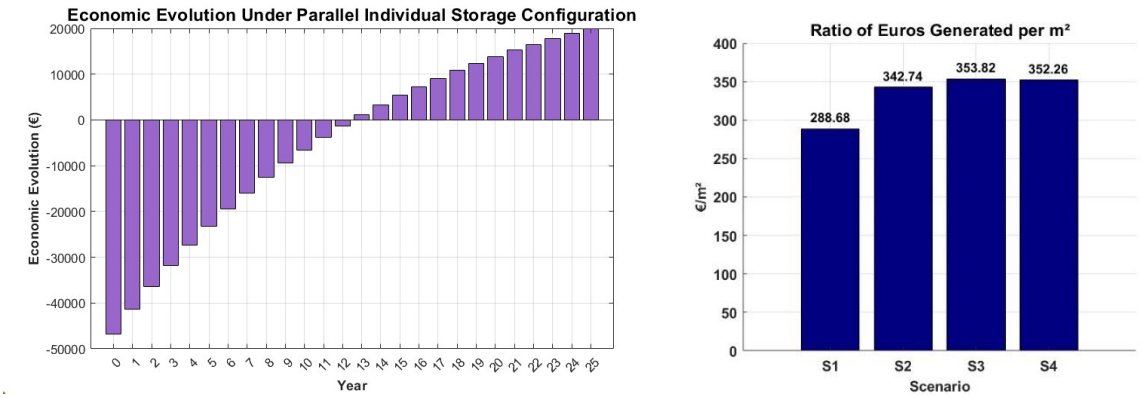

Figure 5.6. Economic evolution under a parallel individual storage configuration.

Chapter 6

Conclusions and Future Work

This chapter represents the conclusion of the thesis, presenting the key findings derived from the case studies and analysed scenarios. Additionally, it outlines proposals for future work aimed at further improving the current concept and exploring its potential applications across a variety of different contexts.

6.1 Conclusions

Following the implementation of the energy management model on the designed hybrid module and the evaluation of the previously analysed scenarios, a set of conclusions and key observations have been drawn, which are presented in detail as follows.

I. The objectives set at the beginning of the project have been fully achieved, with the results demonstrating a strong positive impact, not only by confirming the hybrid module's ability to effectively meet most of the assigned demand profiles, but also by significantly improving generation forecasts compared to the preliminary design. Through the methodology adopted and the use of more advanced techniques for estimating energy output, overall energy production has been increased by 253%. This result is particularly significant, as it confirms that relying solely on predefined generation ratios to estimate the output of a renewable technology is unreliable, mainly due to the inherent intermittency of weather-dependent sources. Therefore, it is essential not only to use robust and comprehensive datasets, but also to analyse the underlying patterns, whether solar irradiance, wind speed, or marine currents, to accurately estimate not just how much energy can be produced, but also when it will be available and to what extent it can be matched to demand.

II. Given that the hybrid system is designed to operate on a small scale, selecting demand profiles that align well with the module's generation capacity becomes critically important, particularly for optimizing the use and sizing of storage systems. In the current case study, identifying suitable demand profiles proved challenging, as only three fell within the generation range of the hybrid system. Furthermore, these profiles were characterized by energy consumption concentrated predominantly during nighttime hours, placing even greater emphasis on the role and impact of energy storage technologies.

III. In order to ensure maximum stability and coverage of the selected demand profiles, the application of two different storage systems has been analyzed: initially, the PAT system, as the original technology proposed in the preliminary design, and subsequently, the use of batteries as an alternative solution. The evaluation of both technologies has revealed that, under current conditions, the PAT system proves to be less advantageous. Due to its lower energy density and reduced efficiency compared to batteries, it underperforms in both economic return and demand coverage. When comparing Scenario 1 (PAT), which includes a 300 W PAT system with a storage tank of 43.36 m^3 with Scenario 2 (batteries) containing a total of 1.28 kW installed, the coverage of demand profiles was 67.71% and 89.90% respectively, clearly highlighting the superior performance of battery storage technology.

    An additional drawback of the PAT system is its spatial requirement. While batteries can be integrated directly within the container, occupying no additional external space, the PAT system requires components such as a storage tank, which, depending on its size, can take up considerable space. Given that the system's effectiveness heavily relies on surplus energy

availability, every additional square meter becomes increasingly valuable in enhancing investment returns, further supporting the conclusion that batteries are the optimal technology for the designed hybrid module.

IV. When the assessment is limited to scenarios utilizing batteries as the sole storage technology, identified as the optimal option, all configurations yield favorable results from both economic and energy performance perspectives. In every case, the coverage ratio exceeds 78% of the total demand, and the NPV surpasses 9,000 €. An interesting consideration that arises is whether, under the current consumption profiles, deploying multiple modules in parallel or consolidating the entire demand within a single module offers a more advantageous outcome.

In terms of energy performance, both Scenario 2 (single module) and Scenario 3 (parallel shared storage) demonstrate similar coverage levels, each reaching approximately 90%. In contrast, Scenario 4 (parallel individual storage) exhibits a notable decline, with coverage dropping to 78.48%. As previously discussed, the limited interconnection in Scenario 4 restricts the capacity of modules with surplus energy to offset deficits in others, thereby reducing overall system performance.

From an economic perspective, Scenario 4 presents stronger financial performance than Scenario 2, achieving an IRR of 11.42% and an NPV of 19,918.45 €, compared to an IRR of 10.88% and an NPV of 9,182.79 € for Scenario 2. However, the substantially higher initial investment (46,730.93 € in Scenario 4 versus 24,712.10 € in Scenario 2) and the increased spatial requirements of an additional 90.31 m², stemming from the need to install three independent modules, one for each demand profile, render Scenario 2 the more practical and cost-effective alternative overall.

As previously noted, the model is highly sensitive to the management of energy surpluses, which represent the primary mechanism for recovering the initial investment. The additional space allocated in Scenarios 3 and 4 (three modules operating in parallel), 200 m² compared to 100 m² in Scenario 2 (single module), is therefore not primarily aimed at increasing demand coverage, but at generating larger surpluses to enhance investment recovery. This underscores the superior resource efficiency of Scenario 2 under the current demand profiles. Despite producing smaller surpluses, Scenario 2 achieves an IRR of 10.88%, nearly matching those of Scenarios 3 and 4 (11.54% and 11.42%, respectively), with a payback period of 14 years, virtually equivalent to the 13 years observed in Scenarios 3 and 4.

Additionally, it is important to note that the economic results obtained in Scenario 2 still present room for improvement. If slightly higher returns are desired, one possible approach would be to reduce the demand coverage target and deliver a greater share of energy as surplus. When applying this operational strategy, it is found that, even with a higher demand coverage than in Scenario 4, reaching 80.45% of total demand, it is possible to achieve a payback period of only 11 years, a NPV of 13,419.64 €, and an IRR of 12.97%, thereby surpassing all previously presented economic outcomes.

Based on all the findings, it becomes clear that when dealing with low-demand profiles, consolidating them under a single module is a far more viable approach. This configuration naturally promotes interaction between the demand profiles, resulting in near-complete coverage. At the same time, it maximizes space efficiency and requires only half the capital investment compared to Scenarios 3 and 4. Moreover, it achieves economic viability with significantly lower surplus levels, further reinforcing its suitability for implementation.

V. Another important aspect considered in the study is that selling surplus energy back to the grid is not recommended across all proposed scenarios. Recovering the initial investment through this strategy would require an excessively high volume of surplus energy, primarily due to the low selling price. Therefore, unless there is a significant increase in the feed-in tariff, redirecting the surplus to other infrastructures proves to be a much more beneficial approach. This is especially true given that the electricity prices under tariff 3.0TD are considerably higher than the current selling rates to the grid.

VI. Last but not least, it is also essential to underscore the development process of the hybrid model, which served as the foundation for all the results presented. The choice of MS Excel-Solver as the primary development platform proved to be highly beneficial. Its widespread global use enhances the model's accessibility, enabling not only experts but also non-specialist users to engage with HOPS through an intuitive and user-friendly interface.

One of the key advantages of using Excel lies in its clear and structured optimization environment, which has significantly facilitated the identification and resolution of potential issues within the optimization process, something that can be more complex when using code-based tools. Furthermore, the integration of Macros within Excel allowed for the creation of interactive dashboards that improve the clarity and interpretability of results across different scenarios. This capability has been instrumental in identifying anomalies and swiftly correcting inconsistencies during the model's development, thereby reinforcing the effectiveness and practicality of this modelling tool.

Despite offering numerous advantages, MS Excel model also presents a set of limitations that have impacted the development of the energy management model. One of the main challenges lies in data handling, particularly when managing large volumes of information. While MS Excel’s visual structure can be helpful, the software struggles with performance when multiple interconnected sheets are involved. This becomes especially evident when working with dashboards and other interactive elements, as MS Excel is not inherently designed to process such high data loads efficiently.

Moreover, although optimization may be more straightforward than with code-based environments, the implementation of priority equations that govern the behaviour of each scenario can become considerably more cumbersome. Since these formulas often require interaction across multiple sheets, they must be implemented with great care, as errors can be introduced easily. When complex conditional statements are used to define the behaviour of a

specific cell, they can become so extensive that, in the event of a malfunction, identifying the specific variable causing the issue becomes particularly difficult. Therefore, careful review and validation of logic structures is essential throughout the model development process.

6.2 Future work

The study conducted has laid the foundation for the application of optimization methods and energy management strategies to the designed hybrid module, yielding a highly positive impact and generating valuable insights and results for its implementation in the Port of Avilés. Nevertheless, further work remains to be done to refine the model and assess whether the extrapolation of HOPS to other locations, where the hybrid module could be implemented, would deliver similarly positive outcomes.

Firstly, for future studies, it is important to identify infrastructures with demand profiles more closely aligned with the base generation capacity of the hybrid module prior to optimization. This would allow for a more accurate assessment of the module's baseline impact in a more favourable operational environment. When multiple modules are deployed in parallel, it would be interesting to evaluate their performance under slightly higher demand conditions than those tested. The main purpose of incorporating additional generation capacity is to accommodate greater demand; however, this could not be assessed in the present study, as the remaining demand profiles were too high relative to the generation capacity of each module.

Secondly, with the rapid development of energy storage technologies, it becomes essential to evaluate how the integration of new storage systems could influence the performance of the hybrid module. An interesting approach would be to use the hybrid system as a testing platform for emerging technologies, particularly given its clear illustration of how energy storage density affects demand profiles coverage, especially in scenarios where consumption is predominantly concentrated during nighttime hours.

Regarding the optimization model, the logical next step would be to transition it into a more professional environment that offers greater flexibility. Currently, the model operates with a maximum of three simultaneous demand profiles and supports up to three modules in a parallel configuration. Therefore, it would be highly valuable to develop a dedicated professional software solution, beyond the current MS Excel Solver based framework, which could enable commercialization and facilitate the application of hybrid modules across a wider range of use cases and contexts.

Finally, as part of future research, it would be worthwhile to explore the deployment of hybrid modules in alternative scenarios, such as remote areas with limited access to the electrical grid. This would allow underserved communities to benefit from clean energy, particularly in disadvantaged regions of the world with scarce resources.

Appendix A

Extended Energy Profiles and Results

This first section of the appendix presents the energy profiles and key results for the full study period, to facilitate a quick and straightforward comparison between the different scenarios. In addition to the four main scenarios analysed throughout the thesis, two additional cases are included. These represent the outcomes for a parallel configuration using PAT technology, considering both shared and individual storage systems.

A.1 Extended energy profiles and results of the hybrid system under single module PAT deployment (S1)

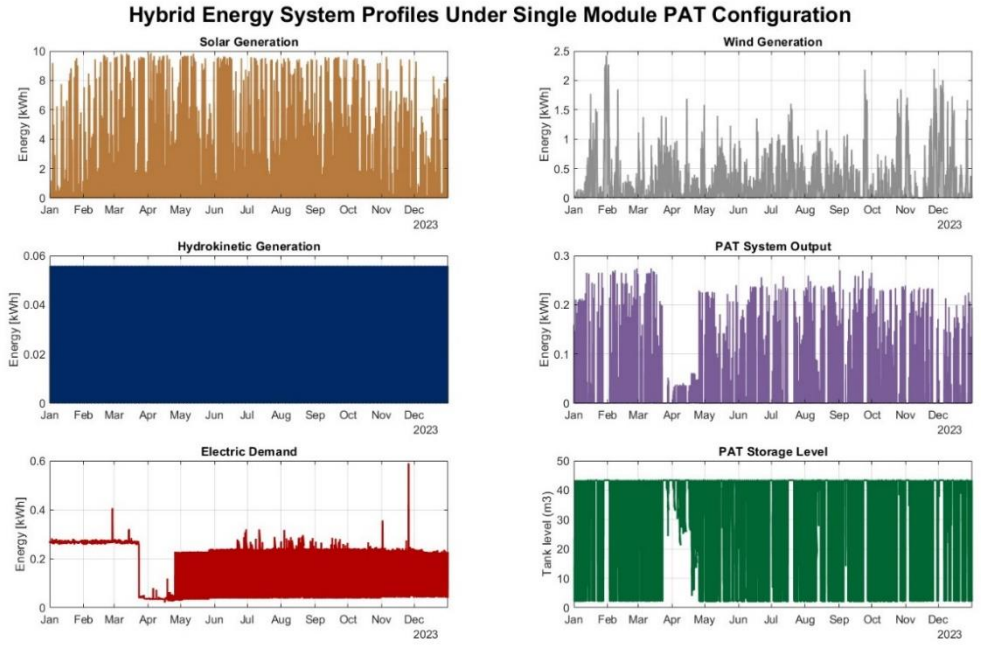

Figure A.1. Single module with PAT energy profiles across the complete study timeline.

Table A.1. Single hybrid module with PAT (design and composition).

SINGLE HYBRID MODULE WITH PAT SYSTEM		
DEMAND		
Number	Name	Demand
1	Vieja Rula	1,226.96 kWh
2	Luz Roja	6.55 kWh
3	Embarcadero	171,66 kWh
	TOTAL DEMAND:	1,405.17 kWh
FINAL COMPOSITION OF THE MODULE		
Technology	Energy multiplier (Number of units)	Power Installed
PV Panels	19 (38 PV Panels)	15.39 kW
Wind Turbines	1 (3 Wind Turbines)	2.40 kW
Hydrokinetic Turb.	1 (2 Hydrokinetic Turbines)	0.075 KW
PAT	1 (1 PAT System)	0.3 kW
FINAL TANK DESIGN		
Tank Capacity	43.36	m^3
Tank Area	10.46	m^2
TOTAL AREA		
Final Area	94.70	m^2

Table A.2. Single hybrid module with PAT (energy and financial performance).

OPERATIONAL PERFORMANCE				
Energy performance			Time performance	
Hybrid module coverage	846.02 kWh	60.21%	Time Coverage	6146 hours
PAT system coverage	98.35 kWh	7.00%		
Deficit	460.81 kWh	32.79%	Time Deficit	2614 hours
Total	1,405.17 kWh	100.00%	Total	8760 hours
FINANCIAL PERFORMANCE				
Selling Energy			Redirecting Energy	
Energy Surplus	16,502.88 kWh		Energy Surplus	16,502.88 kWh
Module cost	24,521.54 €		Module cost	24,521.54 €
Cost reduction	102.94 €		Cost reduction	102.94 €
Selling profits	1,155.20 €		Selling profits	2,242.99 €
Rate of return	7%		Rate of return	7%
Selling price	0,07 €/kWh		Selling price	3.0 TD
NPV	-9,859.73 €		**NPV**	**2,816.93 €**
IRR	2.01%		**IRR**	**8.25%**
Payback	#N/D		**Payback**	**20**
€/kWh Ratio	0.036 €		€/kWh Ratio	0.066 €
€/m² Ratio	154.825 €		**€/m² Ratio**	**288.687 €**

A.2 Extended energy profiles and results of the hybrid system under single module battery deployment (S2)

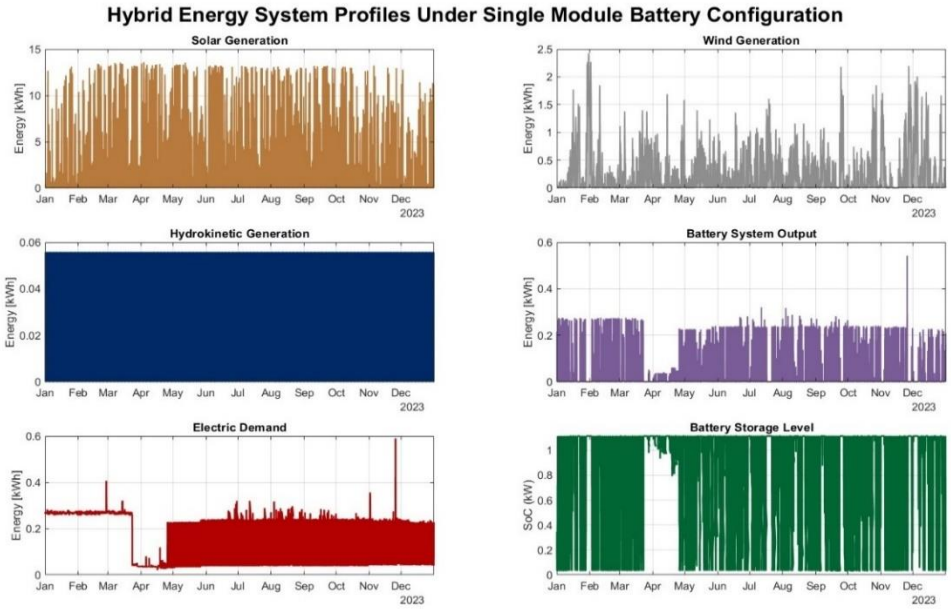

Figure A.2. Single module with battery energy profiles across the complete study timeline.

Table A.3. Single hybrid module with battery (design and composition).

SINGLE HYBRID MODULE WITH BATTERY SYSTEM		
DEMAND		
Number	Name	Demand
1	Vieja Rula	1,226.96 kWh
2	Luz Roja	6.55 kWh
3	Embarcadero	171,66 kWh
	TOTAL DEMAND:	1,405.17 kWh
FINAL COMPOSITION OF THE MODULE		
Technology	Energy multiplier	Power Installed
PV Panels	21 (42 PV Panels)	17.01 kW
Wind Turbines	2 (6 Wind Turbines)	4.80 kW
Hydrokinetic Turb.	2 (4 Hydrokinetic Turbines)	0.150 kW
FINAL BATTERY DESIGN		
Battery Capacity	1.28	kW
Battery Area	0	m^2
TOTAL AREA		
Final Area	98.89	m^2

Table A.4. Single hybrid module with battery (energy and financial performance).

OPERATIONAL PERFORMANCE				
Energy performance			Time performance	
Hybrid module coverage	980.18 kWh	69.75%	Time Coverage	7713 hours
Battery system coverage	281.67 kWh	20.04%		
Deficit	143.33 kWh	10.20%	Time Deficit	1047 hours
Total	1,405.17 kWh	100.00%	Total	8760 hours
FINANCIAL PERFORMANCE				
Selling Energy			Redirecting Energy	
Energy Surplus	20,379.02 kWh		Energy Surplus	20,379.02 kWh
Module cost	24,712.10 €		Module cost	24,712.10 €
Cost reduction	137.54 €		Cost reduction	137.54 €
Selling profits	1,426.53 €		Selling profits	2,771.00 €
Rate of return	7%		Rate of return	7%
Selling price	0.07 €/kWh		Selling price	3.0 TD
NPV	-6,485.05 €		**NPV**	**9,182.79 €**
IRR	3.89%		**IRR**	**10.88%**
Payback	#N/D		**Payback**	**14**
€/kWh Ratio	0.036 €		€/kWh Ratio	0.067 €
€/m2 Ratio	184.311 €		**€/m2 Ratio**	**342.74 €**

A.3 Extended energy profiles and results of the hybrid system under parallel configuration (S3.1)

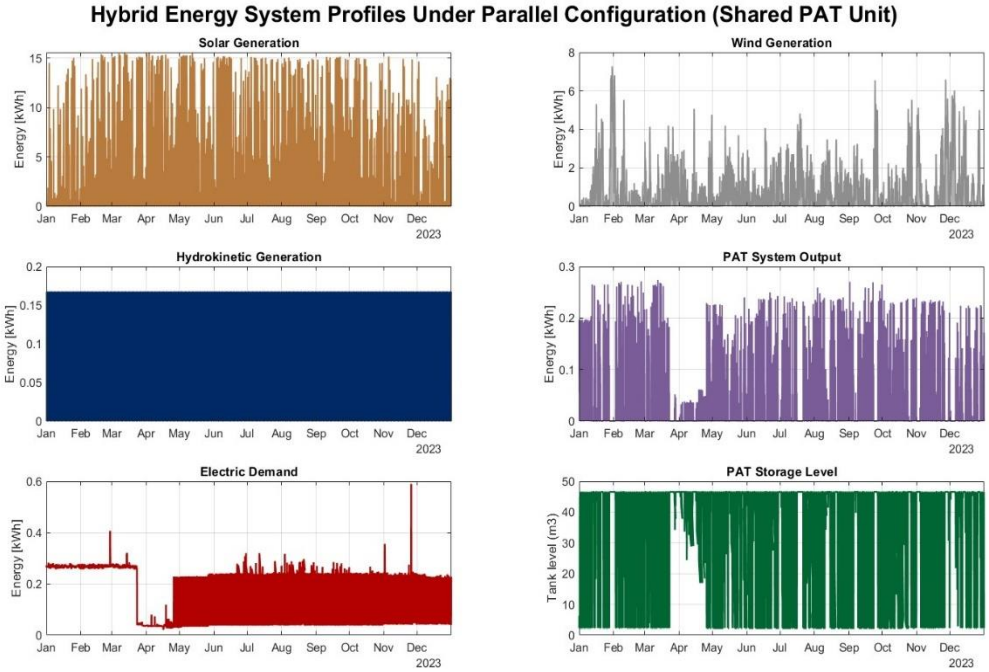

Figure A.3. Parallel configuration (shared PAT) profiles across the complete study timeline.

Table A.5. Parallel configuration with shared PAT (design and composition).

PARALLEL MANAGEMENT SHARED PAT UNIT		
DEMAND		
Number	Name	Demand
1	Vieja Rula	1,226.96 kWh
2	Luz Roja	6.55 kWh
3	Embarcadero	171,66 kWh
	TOTAL DEMAND:	1,405.17 kWh
FINAL COMPOSITION OF THE MODULES		
MODULE 1		
Technology	Energy multiplier (Number of units)	Power Installed
PV Panels	10 (20 PV Panels)	8.10 kW
Wind Turbines	1 (3 Wind Turbines)	2.40 kW
Hydrokinetic Turb.	1 (2 Hydrokinetic Turbines)	0.075 KW
MODULE 2		
PV Panels	10 (PV Panels)	8.10 kW
Wind Turbines	1 (3 Wind Turbines)	2.40 kW
Hydrokinetic Turb.	1 (2 Hydrokinetic Turbines)	0.075 KW

MODULE 3		
PV Panels	10 (20 PV Panels)	8.10 kW
Wind Turbines	1 (3 Wind Turbines)	2.40 kW
Hydrokinetic Turb.	1 (2 Hydrokinetic Turbines)	0.075 KW
FINAL TANK DESIGN		
Tank Capacity	46.55	m^3
Tank Area	11.24	m^2
PAT	0.3	kW
TOTAL AREA		
Final Area	157.97	m^2

Table A.6. Parallel configuration with shared PAT (energy and financial performance).

OPERATIONAL PERFORMANCE				
Energy performance			Time performance	
Hybrid module coverage	889.65 kWh	63.31%	Time Coverage	6672 hours
PAT system coverage	211.00 kWh	15.02%		
Deficit	304.53 kWh	21.67%	Time Deficit	2088 hours
Total	1,405.17 kWh	100.00%	Total	8760 hours
FINANCIAL PERFORMANCE				
Selling Energy			Redirecting Energy	
Energy Surplus	30,038.45 kWh		Energy Surplus	30,038.45 kWh
Module cost	44,802.93 €		Module cost	44,802.93 €
Cost reduction	119.97 €		Cost reduction	119.97 €
Selling profits	2,102.69 €		Selling profits	4,084.76 €
Rate of return	7%		Rate of return	7%
Selling price	0.07 €/kWh		Selling price	3.0 TD
NPV	-18,900.96 €		**NPV**	**4,197.29 €**
IRR	1.73%		**IRR**	**8.02%**
Payback	#N/D		**Payback**	**21**
€/kWh Ratio	0.034 €		€/kWh Ratio	0.065 €
€/m^2 Ratio	163.966 €		**€/m^2 Ratio**	**310.183 €**

A.4 Extended energy profiles and results of the hybrid system under parallel configuration (S3.2)

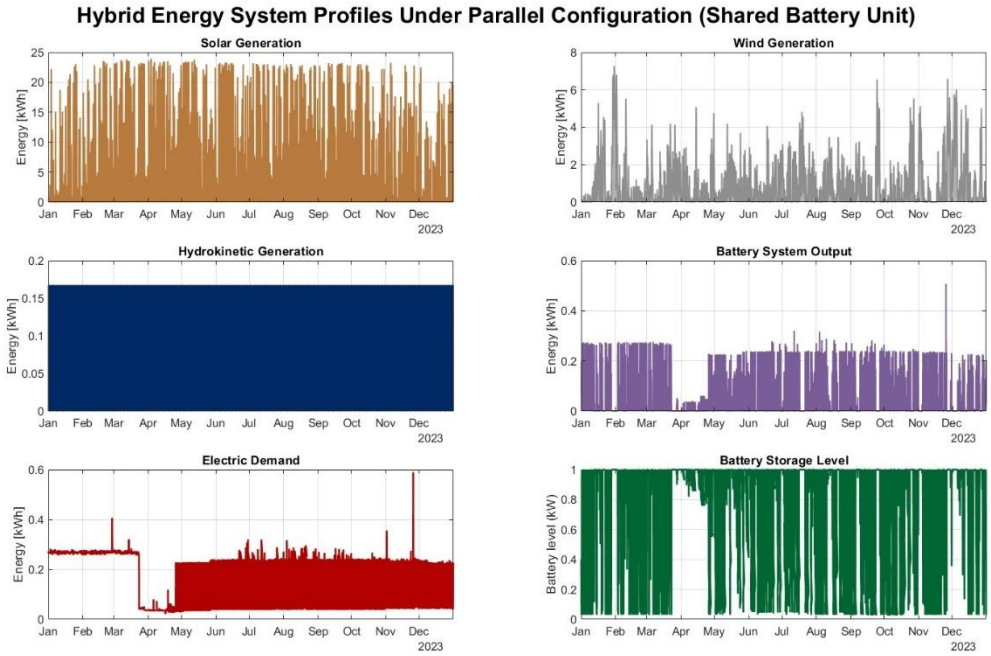

Figure A.4. Parallel configuration (shared battery) profiles across the complete study timeline.

Table A.7. Parallel configuration with shared battery (design and composition).

PARALLEL MANAGEMENT SHARED BATTERY UNIT		
DEMAND		
Number	Name	Demand
1	Vieja Rula	1,226.96 kWh
2	Luz Roja	6.55 kWh
3	Embarcadero	171,66 kWh
	TOTAL DEMAND:	1,405.17 kWh
FINAL COMPOSITION OF THE MODULES		
MODULE 1		
Technology	Energy multiplier (Number of units)	Power Installed
PV Panels	32 (64 PV Panels)	25.92 kW
Wind Turbines	1 (3 Wind Turbines)	2.40 kW
Hydrokinetic Turb.	1 (2 Hydrokinetic Turbines)	0.075 KW
MODULE 2		
PV Panels	1 (2 PV Panels)	0.81 kW
Wind Turbines	1 (3 Wind Turbines)	2.40 kW
Hydrokinetic Turb.	1 (2 Hydrokinetic Turbines)	0.075 KW

MODULE 3		
PV Panels	13 (26 PV Panels)	10.53 kW
Wind Turbines	1 (3 Wind Turbines)	2.40 kW
Hydrokinetic Turb.	1 (2 Hydrokinetic Turb)	0.075 KW
FINAL BATTERY DESIGN		
Battery Capacity	1	kW
Battery Area	0 (Included in the container)	m2
TOTAL AREA		
Final Area	195.34	m^2

Table A.8. Parallel configuration with shared battery (energy and financial performance).

OPERATIONAL PERFORMANCE				
Energy performance			Time performance	
Hybrid module coverage	900.17 kWh	64.06%	Time Coverage	7921 hours
Battery system coverage	377.24 kWh	26.84%		
Deficit	127.76 kWh	9.09%	Time Deficit	839 hours
Total	1,405.17 kWh	100.00%	Total	8760 hours
FINANCIAL PERFORMANCE				
Selling Energy			Redirecting Energy	
Energy Surplus	42,599.97 kWh		Energy Surplus	42,599.97 €/kWh
Module cost	48,060.00 €		Module cost	48,060.00 €
Cost reduction	139.24 €		Cost reduction	139.24 €
Selling profits	2,982.00 €		Selling profits	5,791.71 €
Rate of return	7%		Rate of return	7%
Selling price	0.07 €/kWh		Selling price	3.0 TD
NPV	-11,686.42 €		**NPV**	**21,056.74 €**
IRR	4.14%		**IRR**	**11.54%**
Payback	#N/D		**Payback**	**13**
€/kWh Ratio	0.034 €		€/kWh Ratio	0.065 €
€/m^2 Ratio	186.204 €		**€/m^2 Ratio**	**353.823 €**

A.5 Extended energy profiles and results of the hybrid system under parallel configuration (S4.1)

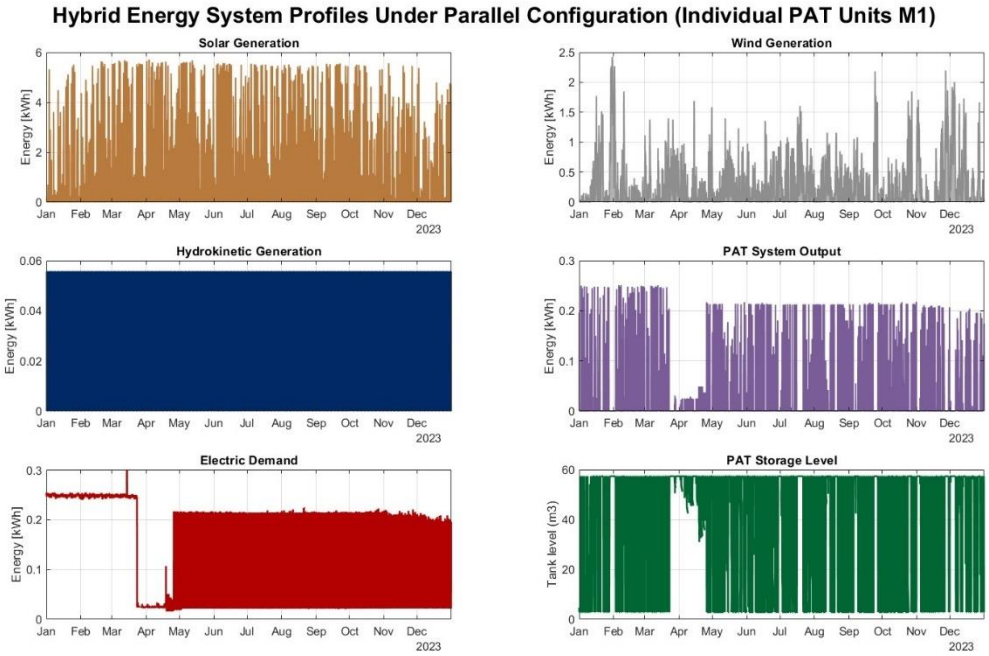

Figure A.5. Parallel configuration (individual PAT Mod. 1) profiles across the complete study timeline.

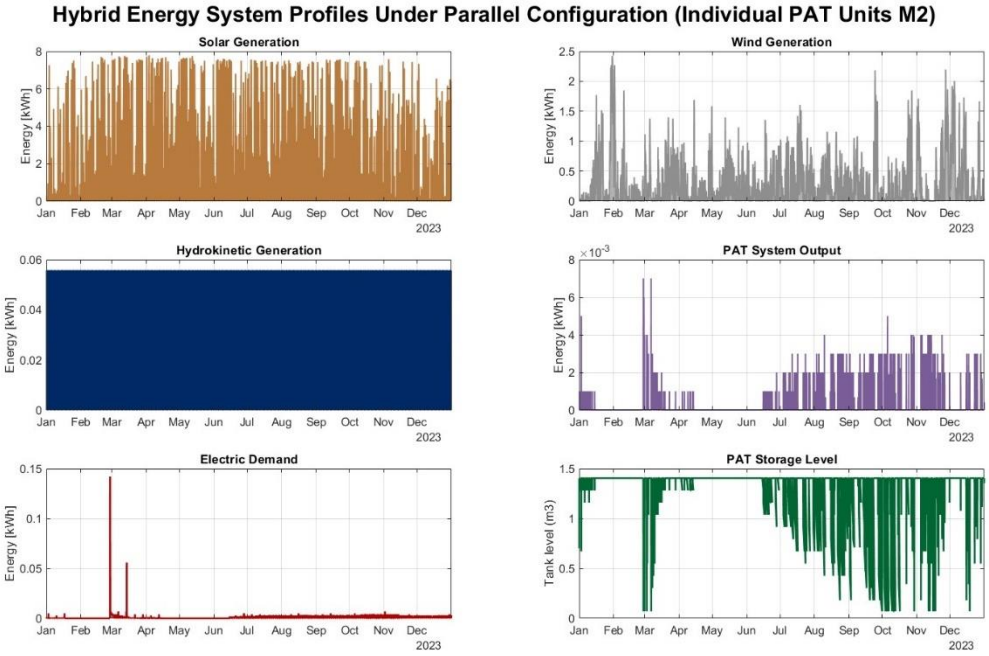

Figure A.6. Parallel configuration (individual PAT Mod. 2) profiles across the complete study timeline.

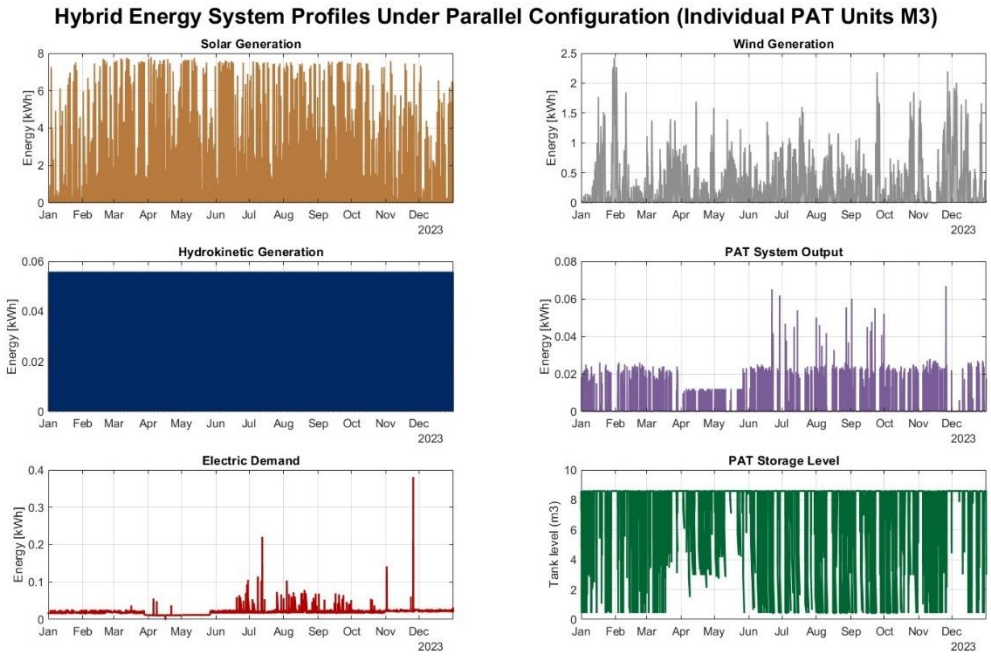

Figure A.7. Parallel configuration (individual PAT Mod. 3) profiles across the complete study timeline.

Table A.9. Parallel configuration with individual PAT units (design and composition).

PARALLEL MANAGEMENT INDIVIDUAL PAT UNITS		
DEMAND		
Number	Name	Demand
1	Vieja Rula	1,226.96 kWh
2	Luz Roja	6.55 kWh
3	Embarcadero	171,66 kWh
	TOTAL DEMAND:	1,405.17 kWh
FINAL COMPOSITION OF THE MODULES		
MODULE 1 (With 0.3 kW PAT system)		
Technology	Energy multiplier (Number of units)	Power Installed
PV Panels	11 (22 PV Panels)	8.91 kW
Wind Turbines	1 (3 Wind Turbines)	2.40 kW
Hydrokinetic Turb.	1 (2 Hydrokinetic Turbines)	0.075 KW
MODULE 2 (With 0.1 kW PAT system)		
PV Panels	15 (30 PV Panels)	12.15 kW
Wind Turbines	1 (3 Wind Turbines)	2.4 kW
Hydrokinetic Turb.	1 (2 Hydrokinetic Turbines)	0.075 KW
MODULE 3 (With 0.1 kW PAT system)		
PV Panels	15 (30 PV Panels)	12.15 kW
Wind Turbines	1 (3 Wind Turbines)	2.40 kW
Hydrokinetic Turb.	1 (2 Hydrokinetic Turbines)	0.075 KW

FINAL TANK DESIGN		
MODULE 1		
Tank Capacity	57.37	m^3
Tank Area	13.85	m^2
MODULE 2		
Tank Capacity	1.40	m^3
Tank Area	0.34	m^2
MODULE 3		
Tank Capacity	8.59	m^3
Tank Area	2.07	m^2
TOTAL AREA		
Final Area	198.76	m^2

Table A.10. Parallel configuration with individual PAT units (energy and financial performance).

GENERAL OPERATIONAL PERFORMANCE				
MODULE 1				
Energy performance			Time performance	
Hybrid module coverage	736.12 kWh	60.00%	Time Coverage	6413 hours
PAT system coverage	122.63 kWh	9.99%		
Deficit	368.21 kWh	30.01%	Time Deficit	2347 hours
Total	1,226.96 kWh	100.00%	Total	8760 hours
MODULE 2				
Hybrid module coverage	5.49 kWh	83.88%	Time Coverage	8726 hours
PAT system coverage	0.98 kWh	15.00%		
Deficit	0.07 kWh	1.12%	Time Deficit	34 hours
Total	6.55 kWh	100.00%	Total	8760 hours
MODULE 3				
Hybrid module coverage	149.10 kWh	86.86%	Time Coverage	8478 hours
PAT system coverage	17.17 kWh	10.00%		
Deficit	5.39 kWh	3.14%	Time Deficit	282 hours
Total	171.66 kWh	100.00%	Total	8760 hours
FINANCIAL PERFORMANCE				
Selling Energy			Redirecting Energy	
Energy Surplus	38,815.25 kWh		Energy Surplus	38,815.25 kWh
Module cost	59,869.08 €		Module cost	59,869.08 €
Cost reduction	112.43 €		Cost reduction	112.43 €
Selling profits	2,717.07 €		Selling profits	5,275.03 €
Rate of return	7%		Rate of return	7%
Selling price	0.07 €/kWh		Selling price	3.0 TD
NPV	-26,895.25 €		**NPV**	**2,914.18 €**
IRR	1.33%		**IRR**	**7.54%**
Payback	#N/D		**Payback**	**23**
€/kWh Ratio	0.034 €		€/kWh Ratio	0.065 €
€/m^2 Ratio	160.256 €		**€/m^2 Ratio**	**305.133 €**

A.6 Extended energy profiles and results of the hybrid system under parallel configuration (S4.2)

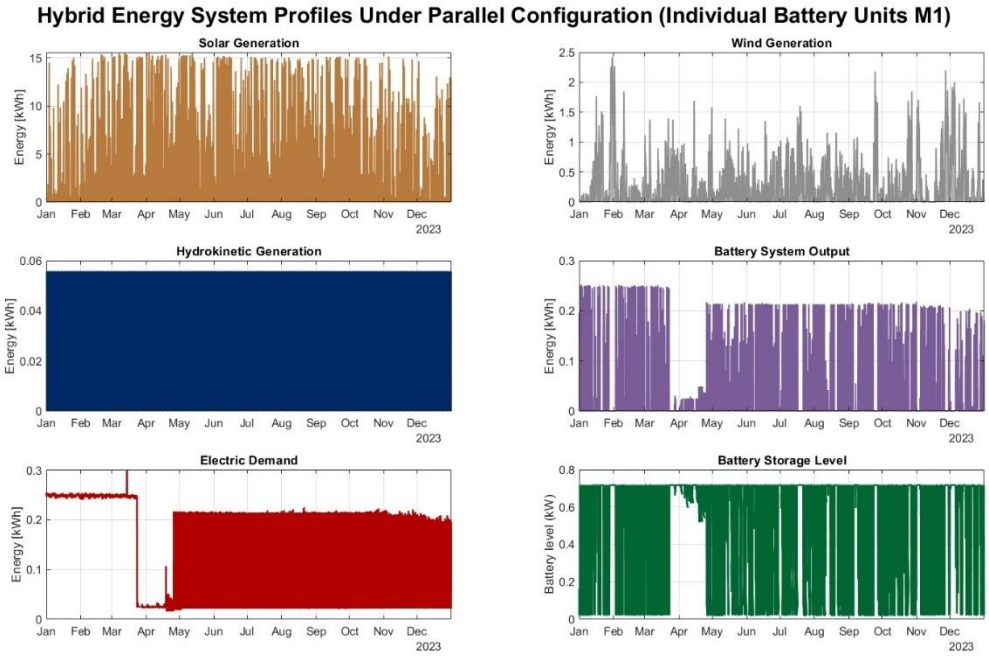

Figure A.8. Parallel configuration (individual bat. Mod. 1) profiles across the complete study timeline.

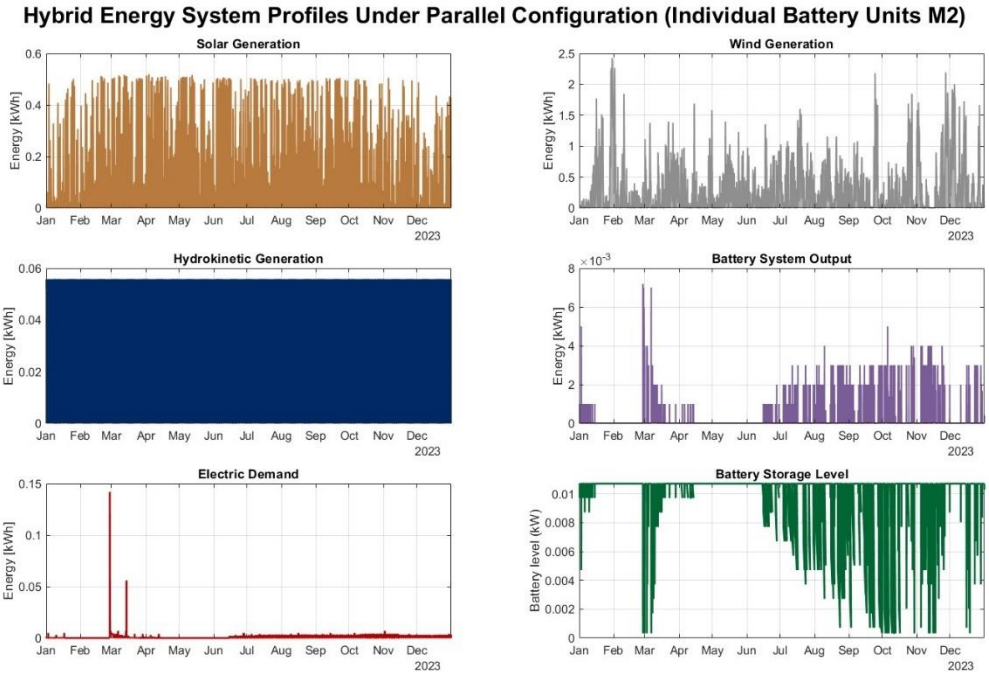

Figure A.9. Parallel configuration (individual bat. Mod. 2) profiles across the complete study timeline.

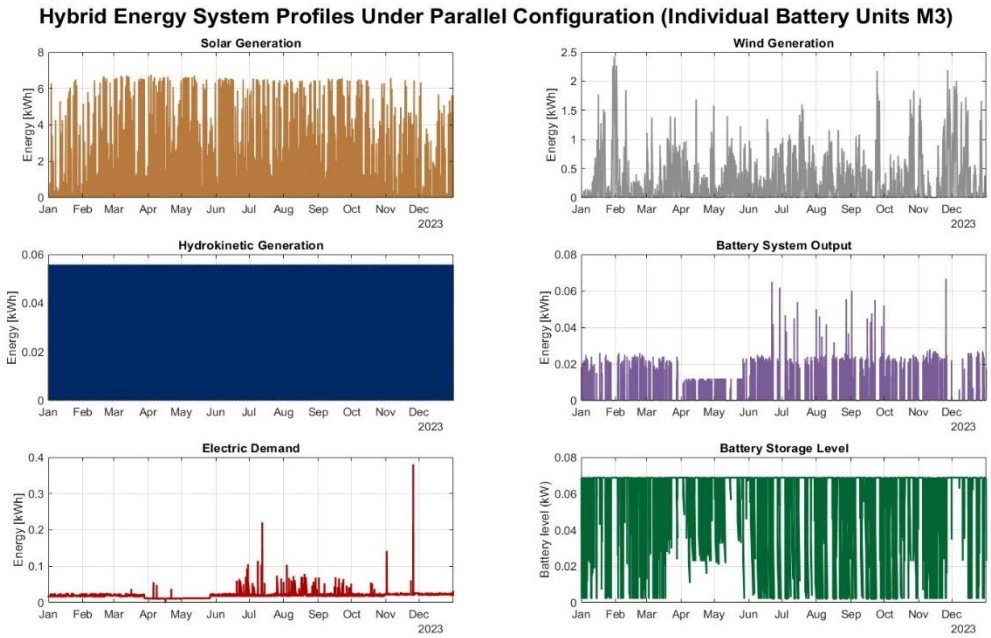

Figure A.10. Parallel configuration (individual bat. Mod. 3) profiles across the complete study timeline.

Table A.11. Parallel configuration with individual battery units (design and composition).

PARALLEL MANAGEMENT INDIVIDUAL BATTERY UNITS		
DEMAND		
Number	Name	Demand
1	Vieja Rula	1,226.96 kWh
2	Luz Roja	6.55 kWh
3	Embarcadero	171,66 kWh
	TOTAL DEMAND:	1,405.17 kWh
FINAL COMPOSITION OF THE MODULES		
MODULE 1		
Technology	Energy multiplier (Number of units)	Power Installed
PV Panels	30 (60 PV Panels)	24.30 kW
Wind Turbines	1 (3 Wind Turbines)	2.4 kW
Hydrokinetic Turb.	1 (2 Hydrokinetic Turbines)	0.075 KW
MODULE 2		
PV Panels	1 (2 PV Panels)	**0.81 kW**
Wind Turbines	1 (3 Wind Turbines)	2.4 kW
Hydrokinetic Turb.	1 (2 Hydrokinetic Turbines)	0.075 KW
MODULE 3		
PV Panels	13 (26 PV Panels)	5.27 KW
Wind Turbines	1 (3 Wind Turbines)	2.4 kW
Hydrokinetic Turb.	1 (2 Hydrokinetic Turbines)	0.075 KW

FINAL BATTERY DESIGN		
MODULE 1		
Battery Capacity	0.72	kW
Battery Area	0 (Included in the container)	m2
MODULE 2		
Battery Capacity	0.01	kW
Battery Area	0 (Included in the container)	m2
MODULE 3		
Battery Capacity	0.07	kW
Battery Area	0 (Included in the container)	m2
TOTAL AREA		
Final Area	189.20	m^2

Table A.12. Parallel configuration with individual battery units (energy and financial performance).

GENERAL OPERATIONAL PERFORMANCE				
MODULE 1				
Energy performance			Time performance	
Hybrid module coverage	745,33 kWh	60,75%	Time Coverage	6828 hours
Battery system coverage	184,88 kWh	15,07%		
Deficit	296,7518074	24,19%	Time Deficit	1932 hours
Total	1226,96 kWh	100,00%	Total	8760 hours
MODULE 2				
Hybrid module coverage	5,33 kWh	81,45%	Time Coverage	8724 hours
Battery system coverage	0,98 kWh	15,00%		
Deficit	0,23 kWh	3,55%	Time Deficit	36 hours
Total	6,55 kWh	100,00%	Total	8760 hours
MODULE 3				
Hybrid module coverage	149,07 kWh	86,84%	Time Coverage	8474 hours
Battery system coverage	17,17 kWh	10,00%		
Deficit	5,42 kWh	3,15%	Time Deficit	286 hours
Total	171,66 kWh	100,00%	Total	8760 hours
FINANCIAL PERFORMANCE				
Selling Energy			Redirecting Energy	
Energy Surplus	41,199.80 kWh		Energy Surplus	41,199.80 kWh
Module cost	46,730.93 €		Module cost	46,730.93 €
Cost reduction	120.20 €		Cost reduction	120.20 €
Selling profits	2,883.99 €		Selling profits	5,599.02 €
Rate of return	7%		Rate of return	7%
Selling price	0.07 €/kWh		Selling price	3.0 TD
NPV	-11,721.38 €		**NPV**	**19,918.45 €**
IRR	4.04%		**IRR**	**11.42%**
Payback	#N/D		**Payback**	**13**
€/kWh Ratio	0.034 €		€/kWh Ratio	0.065 €
€/m^2 Ratio	185.03 €		**€/m^2 Ratio**	**352.26 €**

Appendix B

Datasheets

This section of the appendix includes the datasheets of the main commercial components considered in the project, such as solar panels, inverters, and the selected wind turbines. It is intended to serve as a reference for the key specifications of these components, supporting a better understanding of the methodology section.

JA SOLAR

JAM54S30 395-420/MR Series

MECHANICAL DIAGRAMS

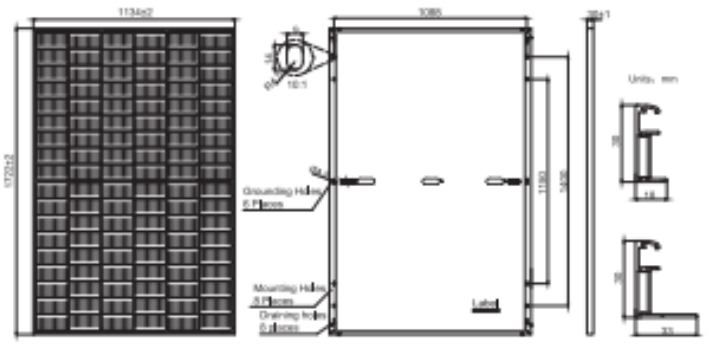

Remark: customized frame color and cable length available upon request

SPECIFICATIONS

Cell	Mono
Weight	21.5kg
Dimensions	1722±2mm×1134±2mm×30±1mm
Cable Cross Section Size	4mm² (IEC), 12 AWG(UL)
No. of cells	108(6x18)
Junction Box	IP68, 3 diodes
Connector	MC4-EVO2/ QC 4.10-35
Cable Length (Including Connector)	Portrait: 300mm(+)/400mm(-); Landscape: 1200mm(+)/1200mm(-)
Packaging Configuration	36pcs/Pallet 936pcs/40HQ Container

ELECTRICAL PARAMETERS AT STC

TYPE	JAM54S30 -395/MR	JAM54S30 -400/MR	JAM54S30 -405/MR	JAM54S30 -410/MR	JAM54S30 -415/MR	JAM54S30 -420/MR
Rated Maximum Power(Pmax) [W]	395	400	405	410	415	420
Open Circuit Voltage(Voc) [V]	36.98	37.07	37.23	37.32	37.45	37.58
Maximum Power Voltage(Vmp) [V]	30.84	31.01	31.21	31.45	31.61	31.80
Short Circuit Current(Isc) [A]	13.70	13.79	13.87	13.95	14.02	14.10
Maximum Power Current(Imp) [A]	12.81	12.90	12.98	13.04	13.13	13.21
Module Efficiency [%]	20.2	20.5	20.7	21.0	21.3	21.5
Power Tolerance	0~+5W					
Temperature Coefficient of Isc(α_Isc)	+0.045%/°C					
Temperature Coefficient of Voc(β_Voc)	-0.275%/°C					
Temperature Coefficient of Pmax(γ_Pmp)	-0.350%/°C					
STC	Irradiance 1000W/m², cell temperature 25°C, AM1.5G					

Remark: Electrical data in this catalog do not refer to a single module and they are not part of the offer.They only serve for comparison among different module types.

ELECTRICAL PARAMETERS AT NOCT

TYPE	JAM54S30 -395/MR	JAM54S30 -400/MR	JAM54S30 -405/MR	JAM54S30 -410/MR	JAM54S30 -415/MR	JAM54S30 -420/MR
Rated Max Power(Pmax) [W]	296	302	306	310	314	318
Open Circuit Voltage(Voc) [V]	34.75	34.88	35.12	35.23	35.37	35.50
Max Power Voltage(Vmp) [V]	29.08	29.26	29.47	29.72	29.89	30.09
Short Circuit Current(Isc) [A]	10.96	11.03	11.10	11.16	11.22	11.29
Max Power Current(Imp) [A]	10.25	10.32	10.38	10.43	10.50	10.57
NOCT	Irradiance 800W/m², ambient temperature 20°C,wind speed 1m/s, AM1.5G					

OPERATING CONDITIONS

Maximum System Voltage	1000V/1500V DC
Operating Temperature	-40°C~+85°C
Maximum Series Fuse Rating	25A
Maximum Static Load,Front Maximum Static Load,Back	5400Pa(112lb/ft²) 2400Pa(50lb/ft²)
NOCT	45±2°C
Safety Class	Class II
Fire Performance	UL Type 1

CHARACTERISTICS

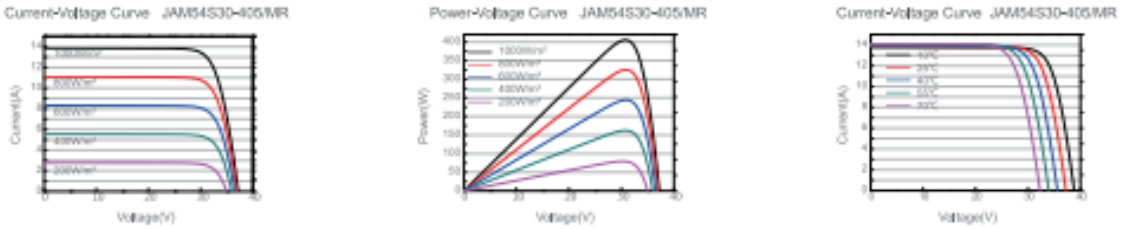

Figure B.1. Solar panel datasheet.

Datos técnicos	GW700-XS-11	GW1000-XS-11	GW1500-XS-11	GW2000-XS-11	GW2500-XS-11	GW3000-XS-11
Entrada						
Máx. voltaje de entrada (V)	500	500	500	500	600	600
MPPT Rango de voltaje de funcionamiento (V)	40 ~ 450	40 ~ 450	50 ~ 450	50 ~ 450	50 ~ 550	50 ~ 550
Voltaje de arranque (V)	40	40	50	50	50	50
Voltaje nominal de entrada (V)	360					
Máx. corriente de entrada por MPPT (A)	15					
Máx. corriente de cortocircuito por MPPT (A)	18.75					
Número de MPPT	1					
Número de cadenas por MPPT	1					
Salida						
Potencia nominal de salida (W)	700	1000	1500	2000	2500	3000
Potencia nominal aparente de salida (VA)	700	1000	1500	2000	2500	3000
Máx. Potencia Activa CA (W)	800[*1]	1100[*1]	1650[*1]	2200[*1]	2750[*1]	3300[*1]
Máx. Potencia Aparente CA (VA)	800[*1]	1100[*1]	1650[*1]	2200[*1]	2750[*1]	3300[*1]
Voltaje nominal de salida (V)	230	230	230	230	220 / 230	220 / 230
Frecuencia nominal de red CA (Hz)	50 / 60					
Máx. corriente de salida (A)	3.5	4.8	7.2	9.6	12.0	14.3
Factor potencia de salida	~1 (Ajustable, desde 0.8 capacitivo a 0.8 inductivo)					
Máx. distorsión armónica total	<3%					
Eficiencia						
Máx. eficiencia	97.2%	97.2%	97.3%	97.5%	97.6%	97.6%
Eficiencia europea	96.0%	96.4%	96.6%	97.0%	97.2%	97.2%
Protección						
Detección aislamiento de resistencia fotovoltaica	Integrado					
Monitor de corriente residual	Integrado					
Protección anti-isla	Integrado					
Protección sobrecorriente CA	Integrado					
Protección cortocircuito CA	Integrado					
Protección alto voltaje CA	Integrado					
Interruptor CC	Integrado					
Protección contra sobretensiones CC	Tipo III (Opcional Tipo II)					
Protección contra sobretensiones CA	Tipo III					
Interruptor de circuito por falla de arco (AFCI)	Opcional					
Apagado remoto	Integrado					
Datos generales						
Temperatura de Operación (°C)	-25 ~ +60					
Humedad relativa	0 ~ 100%					
Altura Máx. de Operación (m)	3000					
Método de enfriamiento	Convección natural					
Interface	LED, LCD, WLAN + APP					
Comunicación	WiFi o LAN o RS485 (Opcional)					
Peso (kg)	5.8					
Medidas (Ancho x Alto x Profundo mm)	295 x 230 x 113					
Emisión de ruido (dB)	<25	<25	<25	<25	<30	<30
Topología	No aislado					
Consumo corriente nocturna (W)	<1					
Grado de protección	IP65					
Conector CC	MC4 (2.5 ~ 4mm²)					
Conector CA	Conector "Plug & Play"					

*1: Para Bélgica Máx. corriente activa CA (W) y Máx. corriente aparente CA (VA): GW700-XS-11 es 700, GW1000-XS-11 es 1000, GW1500-XS-11 es 1500, GW2000-XS-11 es 2000, GW2500-XS-11 es 2500, GW3000-XS-11 es 3000.
*: Visite el sitio web de GoodWe para ver los últimos certificados.

Figure B.2. Inverter datasheet.

Nominaal vermogen	800w	plaats van herkomst	Jiangsu, China
naam van het merk	SMARRAD	modelnummer	SR-800
Uitvoervoltage	12v 24v	Rotor Diameter	0.9m
Maximaal vermogen	800w	Nominale spanning	12v/24v
Nominale windsnelheid	11 m/s	Opstart windsnelheid	2 m/s
Veilige windsnelheid	45 m/s	Generator type	3 fase ac pmg
Mes nummer	5 bladen	Mes materiaal	Nylon vezel
Materiaal	Zeldzame aarde ndfeb	Kleur	Rood

Verpakking en levering

Packaging Details	Carton	Selling Eenheden	Single item
enkele pakket maat	62X49X32 cm	enkele brutogewicht	12.000 KG
Voorbeelden van verpakkingen			

Figure B.3. Wind turbine datasheet.

Appendix C

Site pictures

This appendix presents images of the hybrid module installation at the Port of Avilés, carried out during the current year.

Figure C.1. Installation of the hybrid module at the Port of Avilés (1).

Figure C.2. Installation of the hybrid module at the Port of Avilés (2).

References

[1] Hy4res. (2023). Hy4res. [online] Available at: https://hy4res.eu/ [Accessed 8 Jul. 2025].

[2] UN Trade and Development (UNCTAD). (2024). Review of Maritime Transport 2024 | Navigating maritime chokepoints. [online] Available at: https://unctad.org/publication/review-maritime-transport-2024?utm_source.

[3] Wan, Z., Nie, A., Chen, J., Pang, C. and Zhou, Y. (2025). Transforming ports for a low-carbon future: Innovations, challenges, and opportunities. Ocean & Coastal Management, [online] 264, p.107636. doi: https://doi.org/10.1016/j.ocecoaman.2025.107636.

[4] European Commission (2023). Decarbonising maritime transport – FuelEU Maritime. [online] Mobility and Transport. Available at: https://transport.ec.europa.eu/transport-modes/maritime/decarbonising-maritime-transport-fueleu-maritime_en.

[5] EU, in (2025). Sustainable Ships. [online] Sustainable Ships. Available at: https://www.sustainable-ships.org/stories/2025/eu-shore-power-demand-2030.

[6] Buonomano, A., Giuzio, G.F., Maka, R., Palombo, A. and Russo, G. (2024). Empowering sea ports with renewable energy under the enabling framework of the energy communities. Energy Conversion and Management, 314, pp.118693–118693. doi: https://doi.org/10.1016/j.enconman.2024.118693.

[7] Dimitrios Cholidis, Nikolaos Sifakis, Nikolaos Savvakis, Tsinarakis, G., Avraam Kartalidis and Arampatzis, G. (2025). Enhancing Port Energy Autonomy Through Hybrid Renewables and Optimized Energy Storage Management. Energies, [online] 18(8), pp.1941–1941. doi: https://doi.org/10.3390/en18081941.

[8] Elsayed, I., Kanaan, H. and Mehanna, M. (2024). Feasibility and optimal sizing analysis of hybrid PV/Wind powered seawater desalination system: A case study of four locations, Egypt. Heliyon, [online] 10(22), pp.e40313–e40313. doi: https://doi.org/10.1016/j.heliyon.2024.e40313.

[9] Tang, D., Zheng, Z. and Guerrero, J.M. (2024). A hybrid multi-criteria dynamic sustainability assessment framework for integrated multi-energy systems incorporating hydrogen at ports. International Journal of Hydrogen Energy, [online] 99, pp.540–552. doi: https://doi.org/10.1016/j.ijhydene.2024.12.075.

[10] Micallef, A., Apap, M., Licari, J., Spiteri Staines, C. and Xiao, Z. (2025). Renewable energy systems in offshore platforms for sustainable maritime operations. Ocean Engineering, 319, p.120209. doi: https://doi.org/10.1016/j.oceaneng.2024.120209.

[11] Elalfy, D.A., Gouda, E., Kotb, M.F., Bureš, V. and Sedhom, B.E. (2024). Comprehensive review of energy storage systems technologies, objectives, challenges, and future trends. Energy Strategy Reviews, 54, pp.101482–101482. doi: https://doi.org/10.1016/j.esr.2024.101482.

[12] Koholé, Y.W., Wankouo Ngouleu, C.A., Fohagui, F.C.V. and Tchuen, G. (2024). A comprehensive comparison of battery, hydrogen, pumped-hydro and thermal energy storage technologies for hybrid renewable energy systems integration. Journal of Energy Storage, [online] 93, p.112299. doi: https://doi.org/10.1016/j.est.2024.112299.

[13] Pare, S. (2025). Walvis Bay saltworks: The monster refinery in Namibia with colorful ponds that cover the land like patchwork. [online] Live Science. Available at: https://www.livescience.com/planet-earth/walvis-bay-saltworks-the-monster-refinery-in-namibia-with-colorful-ponds-that-cover-the-land-like-patchwork?utm_source [Accessed 8 Jul. 2025].

[14] Khalili, Y., Yasemi, S., Bagheri, M. and Sanati, A. (2025). Advancements in hydrogen storage technologies: Integrating with renewable energy and innovative solutions for a sustainable future. Energy Geoscience, p.100408. doi: https://doi.org/10.1016/j.engeos.2025.100408.

[15] Olatomiwa, L., Mekhilef, S., Ismail, M.S. and Moghavvemi, M. (2016). Energy management strategies in hybrid renewable energy systems: A review. Renewable and Sustainable Energy Reviews, 62, pp.821–835. doi: https://doi.org/10.1016/j.rser.2016.05.040.

[16] Zheng, Y., Zhou, X., Yu, J., Xue, X., Wang, X. and Tu, X. (2025). Predictive analytics for sustainable energy: An in-depth assessment of novel Stacking Regressor model in the off-grid hybrid renewable energy systems. Energy, [online] 324, p.135916. doi: https://doi.org/10.1016/j.energy.2025.135916.

[17] Tahir, K.A. (2025). A Systematic Review and Evolutionary Analysis of the Optimization Techniques and Software Tools in Hybrid Microgrid Systems. Energies, [online] 18(7), p.1770. doi: https://doi.org/10.3390/en18071770.

[18] Maghami, M.R. and Mutambara, A.G.O. (2023). Challenges associated with Hybrid Energy Systems: An artificial intelligence solution. Energy Reports, 9, pp.924–940. doi: https://doi.org/10.1016/j.egyr.2022.11.195.

[19] Kim, S., Heo, S., Nam, K., Woo, T. and Yoo, C. (2023). Flexible renewable energy planning based on multi-step forecasting of interregional electricity supply and demand: Graph-enhanced AI approach. Energy, 282, pp.128858–128858. doi: https://doi.org/10.1016/j.energy.2023.128858.

[20] Hwang, J., Kim, J. and Yoon, S. (2025). DT-BEMS: Digital twin-enabled building energy management system for information fusion and energy efficiency. Energy, p.136162. doi: https://doi.org/10.1016/j.energy.2025.136162.

[21] Renewable Technology Innovation Indicators: Mapping Progress in Costs, Patents and Standards. Internation Renewable Energy Agency, (2022).

[22] Fernández-Jiménez, A., (2024). HY4RES Project Report: Pilot Site Mapping (Port of Avilés). Version 2, September 2024. University of Oviedo (UNIOVI), prepared for VertigoLAB.

[23] Calabrò, Emanuele. “An Algorithm to Determine the Optimum Tilt Angle of a Solar Panel from Global Horizontal Solar Radiation.” *Journal of Renewable Energy*, vol. 2013, 2013, pp. 1–12, https://doi.org/10.1155/2013/307547.

[24] Ayuntamiento de Avilés, (2022). Memoria para la consulta pública previa de la Ordenanza Municipal reguladora de la instalación de paneles fotovoltaicos o solares en Avilés. Avilés: Ayuntamiento de Avilés.

[25] Khudri Johari, Muhd, et al. “Comparison of Horizontal Axis Wind Turbine (HAWT) and Vertical Axis Wind Turbine (VAWT).” International Journal of Engineering & Technology, vol. 7, no. 4.13, 9 Oct. 2018, p. 74, https://doi.org/10.14419/ijet.v7i4.13.21333. Accessed 9 Apr. 2025.

[26] Al-Rawajfeh, Mohammad A., and Mohamed R. Gomaa. “Comparison between Horizontal and Vertical Axis Wind Turbine.” *International Journal of Applied Power Engineering (IJAPE)*, vol. 12, no. 1, 1 Mar. 2023, p. 13, https://doi.org/10.11591/ijape.v12.i1.pp13-23. Accessed 9 Apr. 2025.

[27] Puertos del Estado. “PORTUS (Puertos Del Estado).” *Puertos.es*, 2024, portus.puertos.es/#/.

[28] Ferraiuolo, R., Gharib-Yosry, A., Fernández-Jiménez, A., Espina-Valdés, R., Álvarez-Álvarez, E., Del Giudice, G. and Giugni, M. (2022). Design and Experimental Performance Characterization of a Three-Blade Horizontal-Axis Hydrokinetic Water Turbine in a Low-Velocity Channel. EWaS5 International Conference: ‘Water Security and Safety Management: Emerging Threats or New Challenges? Moving from Therapy and Restoration to Prognosis and Prevention’, [online] p.62. doi: https://doi.org/10.3390/environsciproc2022021062 .

[29] Mena Palacios, M.F. (2018). Aplicación del modelo de simulación IBER para determinar el potencial energético de ríos y estuarios: caso ría de avilés.

[30] Bantelay, D.T., Gebresenbet, G., Admasu, B.T., Tigabu, M.T. and Getie, M.Z. (2024). Performance prediction of a pump as a turbine using energy loss analysis. Energy Reports, [online] 12, pp.210–225. doi: https://doi.org/10.1016/j.egyr.2024.06.023.

[31] Nasir, A., Dribssa, E., Girma, M. and Madessa, H.B. (2023). Selection and Performance Prediction of a Pump as a Turbine for Power Generation Applications. Energies, [online] 16(13), p.5036. doi: https://doi.org/10.3390/en16135036.